Die approbierte Originalversion dieser Dissertation ist an der Hauptbibliothek der Technischen Universität Wien aufgestellt (http://www.ub.tuwien.ac.at).

The approved original version of this thesis is available at the main library of the Vienna University of Technology (http://www.ub.tuwien.ac.at/englweb/).

DISSERTATION

Development of a model system for the study of spontaneous mutagenesis in glucose-limited stationary yeast cells

Ausgeführt zum Zwecke der Erlangung des akademischen Grades eines
Doktors der Naturwissenschaften
unter der Leitung von

Univ. Prof. DI Dr. techn. Christian P. Kubicek
Institut 166
Institut für Verfahrenstechnik, Umwelttechnik und Technische Biowissenschaften

Eingereicht an der Technischen Universität Wien
Fakultät für Technische Chemie

von
Petra Dorninger
0106987
Wurmserg. 15/33, 1150 Wien

Wien, Aug. 2011

Kurzfassung

Das Auftreten spontaner Mutationen kann zur Entstehung von Krebs beitragen, besonders wenn eine Zelle einer definierten Anzahl an genetischen Veränderungen ausgesetzt ist. Dies wiederum kann in den verschiedenen Krebsarten unterschiedlich sein. Die ermittelten Mutationsraten in proliferierenden Zellen sind jedoch nicht ausreichend hoch, um die häufigen multiplen Mutationen zu erklären. Aus diesem Grund nimmt man an, dass eine bedeutende Anzahl an Mutationen aus sich nicht teilenden Zellen entsteht.

Adaptive Mutationen im Modellorganismus *Saccharomyces cerevisiae* sind besonders gut geeignet, um spontane Mutagenese in ruhenden Zellen zu untersuchen. Aminosäurehungerung findet häufig eine Anwendung, um einen Zellzyklusarrest herbeizuführen. Besonders das *lys2ΔBgl* System ist gut untersucht, indem Hefezellen für die essentielle Aminosäure Lysin gehungert werden. Diese Art der Hungerung birgt jedoch einige Nachteile in Betracht auf Stringenz des Zellzyklusarrests, der Anwesenheit von Glukose im Versuchsaufbau sowie das Nachahmen von natürlichen Gegebenheiten. Darum wurde in dieser Studie den beschriebenen Grenzen entgegengewirkt, indem die Aminosäurehungerung durch eine Kohlenhydrathungerung ersetzt wurde. Die beiden Zielgene *FBP1*, kodierend für Fruktose-1,6-bisphosphatase, und *PCK1*, kodierend für Phosphoenolpyruvat Carboxykinase, sind an der Glukoneogenese beteiligt und wurden disruptiert, um den Syntheseweg zu blockieren. Die Studie zeigt, dass das Unterbinden der Glukoneogenese auf nicht zuckerhaltigen Kohlenstoffquellen zu einem strikten Zellzyklusarrest ohne Restwachstum führt – und zwar von Beginn der Selektion an. Drei alternative Nährstoffe (Laktat, Pyruvat und Glyzerin) wurden für die Kohlenhydrathungerung getestet, wobei sich Laktat als die geeignetste Quelle herausstellte. In weiterer Folge wurde ein Hefestamm mit einer revertierbaren Frameshift-Mutation im *FBP1*-Gen konstruiert, um adaptive Mutationsversuche durchzuführen. Revertanten konnten mit dem neuen *fbp1FS-128* System über einen Zeitraum von 22 Tagen ohne Artefakte detektiert werden. Das System konnte somit erfolgreich etabliert werden und wurde weiters für die Untersuchung einer *rad27Δ* Reparaturmutante herangezogen, was bisher mit Lysinhungerung nicht möglich war. Des Weiteren wurde ein Stamm mit einer Fusion des humanen Tumorsuppressorgens TP53 und *FBP1* konstruiert, um die Mutationsfrequenz zu erhöhen.

Abstract

The occurrence of spontaneous mutations can lead to cancer especially if a cell undergoes a certain amount of genetic changes, which differs from type to type of cancers. However, mutation rates determined in proliferating cells are not sufficient to explain the observed frequencies of multiple mutations. Consequently, it is assumed that a nameable fraction of mutations also arises from non-proliferating cells.

Adaptive mutations in the model organism *Saccharomyces cerevisiae* are particularly suitable to study spontaneous mutagenesis in quiescent cells. Common systems use amino acid starvation to provoke cell cycle arrest. In particular the *lys2ΔBgl* system is well-studied, where yeast cells are starved for the essential amino acid lysine. However, some disadvantages arise from this type of starvation, with regard to stringency of cell cycle arrest, mimicking of natural circumstances and presence of glucose in the experimental setup. Therefore, in this study those limits were antagonized by replacing amino acid starvation with starvation for carbohydrates. Two target genes, *FBP1* encoding the enzyme fructose-1,6-bisphosphatase and *PCK1* encoding phosphoenolpyruvate carboxykinase, involved in gluconeogenesis were impaired to block the pathway. The study showed that a block in gluconeogenesis leads to a strict cell cycle arrest without residual growth from the beginning of selection on non-sugar carbon sources. Three alternative nutrients (lactate, pyruvate and glycerol) were tested in carbohydrate starvation, revealing lactate to be the most suitable one. Furthermore, a frameshift strain with a revertible mutation in the FBP1 gene was constructed to perform adaptive mutation assays. Revertant colonies could be detected with the new *fbp1FS-128* system over a time course of 22 days without artifacts. The system was established successfully and was also used to study *rad27Δ* repair gene mutant, which was not feasible with previously used lysine starvation. Moreover, a fusion of the tumor suppressor gene *TP53* and *FBP1* was constructed to increase mutation frequency.

To Jasmin

Acknowledgements

I would like to thank my supervisor Dr. Erich Heidenreich, who gave me the possibility to do my research work at the Institute of Cancer Research. I also thank him for the scientific input throughout my thesis.

Further, I would like to thank my supervisor from the University of Technology, Dr. Kubicek, for the freedom of my topic and good cooperation throughout my thesis.

Special thanks to Resi Lengheimer and Sandra Weinzettl for excellent teamwork in the lab and the good laughs we shared in breaks.

Furthermore, I would like to thank my family and my friends for their support and understanding through my thesis, especially their patience at the end of my thesis. Thanks to Christof Lemberger for his support, especially in the beginning of my time as a PhD student. Special thanks to David Schmidinger for his caring support as well as his computer support when I was in the final phase of writing my thesis.

List of Abbreviations

A	adenine
aa	amino acid
AMP	adenosine monophosphate
ARS	autonomous replication sequence
ATP	adenosine triphosphate
BER	base excision repair
bp	base pairs
C	cytosine
cAMP	cyclic adenosine monophosphate
CEN	centromer
CSRE	carbon source responsive element
dNTP	desoxyribonucleotid triphosphate
FASAY	functional analysis of separated alleles in yeast
FBP1	fructose-1,6-bisphosphatase gene
FBPase-1	fructose-1,6-bisphosphatase
FS	frameshift
G	guanine
GOI	gene of interest
HK	hexokinase
HR	homologous recombination
IPTG	isopropyl-Beta-D-thiogalactopyranoside
K.l.	*Kluyveromyces lactis*
MMS	methylmethane sulfonate

MMR	mismatch repair
NADH	nicotinamide adenine dinucleotide
NER	nucleotide excision repair
NHEJ	non-homologous end-joining
nt	nucleotide
ORF	open reading frame
PCK1	phosphoenolpyruvate carboxykinase gene
PCR	polymerase chain reaction
PEPCK	phosphoenolpyruvate carboxykinase
PFK-1	phosphofructokinase-1
P_i	inorganic phosphate
PK	pyruvate kinase
PKA	protein kinase A
RE	restriction enzyme
rpm	rounds per minute
ss	single stranded
SSA	single strand annealing
T	thymine
TOR	target of rapamycin
TP53	tumor suppressor protein p53
UAS	upstream activating sequence
URS	upstream repressing sequence
YNB	yeast nitrogen base

Table of Contents

1. INTRODUCTION 1

1.1. Mutations and Cancer 1

1.2. Research on Adaptive Mutagenesis in budding yeast 3

1.3. *Saccharomyces cerevisiae* as a model organism 7

1.4. Glycolysis and Gluconeogenesis 8

- 1.4.1. Basics 8
- 1.4.2. Fermentative and non-fermentative metabolism in yeast 10
- 1.4.3. Insights on FBP1 and PCK1 10

1.5. Aim of the study 11

2. MATERIALS AND METHODS 13

2.1. Materials 13

- 2.1.1. Media 13
  - 2.1.1.1. Media for yeast cultivation 13
  - 2.1.1.2. Media for *E. coli* cultivation 15
- 2.1.2. Yeast strains and yeast plasmids 15
- 2.1.3. *E. coli* strains and plasmids 16
  - 2.1.3.1. *E. coli* strains 16
  - 2.1.3.2. Bacterial plasmids 16
- 2.1.4. Buffers and stock solutions 16
  - 2.1.4.1. Further reagents: 18
- 2.1.5. List of primers 19

2.2. Methods 21

- 2.2.1. Molecular biological Methods 21
  - 2.2.1.1. Construction of yeast strains 21
  - 2.2.1.2. Yeast Transformation 24
  - 2.2.1.3. *E. coli* transformation 26
  - 2.2.1.4. Genomic DNA preparation from yeast 27
  - 2.2.1.5. Plasmid Preparation of *E. coli* 28
  - 2.2.1.6. Ligation 29

2.2.1.7. Restriction digest of DNA 30
2.2.1.8. Polymerase Chain Reaction (PCR) 30
2.2.1.9. Site directed mutagenesis 33
2.2.1.10. Gel electrophoresis 34
2.2.1.11. DNA precipitation 35
2.2.1.12. DNA purification 36
2.2.1.13. Sequence analysis 36
2.2.2. Microbiological Methods 36
2.2.2.1. Cultivation of yeast strains 36
2.2.2.2. Cultivation of *E. coli* 36
2.2.2.3. Marker test 36
2.2.2.4. Adaptive mutation assay 37
2.2.2.5. Reconstruction Assay 38

3. RESULTS 40

3.1. *PCK1* deletion 40
3.1.1. Construction of deletion strain YΔPCK1 40
3.1.2. Cell cycle arrest and survival on different carbon sources 44

3.2. *FBP1* deletion 47
3.2.1. Construction of the deletion strain YΔF1 47
3.2.2. Cell cycle arrest and survival on different carbon sources 51
3.2.3. YΔF1 in a Reconstruction Assay 52

3.3. *FBP1* +1 Frameshift 53
3.3.1. Construction of URA$^+$ precursor strain YUF 53
3.3.2. Frameshift insertion strategy in *FBP1* 56
3.3.2.1. One step gene replacement. 58
3.3.2.2. Modified one-step gene replacement 60
3.3.2.3. Two step gene replacement („loop-in/loop-out“) 61
3.3.3. Adaptive mutation assay with YFAM 76
3.3.4. Reconstruction Assay with YFAM revertants 80
3.3.5. Implementation of the new assay for DNA repair studies 83
3.3.5.1. Construction of YFA27 83
3.3.5.2. Adaptive mutation assay with YFA27 87

3.4. *hTP53-FBP1* Fusiongene 88
3.4.1. Construction of fusion strain *hTP53-FBP1* (YPF63) 89
3.4.2. Reconstruction Assay with YPF63 94

3.5. *hTP53* +1 Frameshift 95
3.5.1. Frameshift insertion strategy in *hTP53-FBP1* 95
3.5.2. Construction of YPFA 97
3.5.3. Adaptive mutation assay with YPFA 104
3.5.4. Endeavors to optimize *hTP53-FBP1* fusion strain 107
3.5.4.1. Construction of improved URA$^+$ strain without loxP sites (YUFΔlP) 108
3.5.4.2. Optimal Kozak sequence 112
3.5.5. Complications encountered with YPFA 113
3.5.5.1. Reconstruction Assays 113
3.5.5.2. Sequence analysis 118

4. DISCUSSION 120

4.1. Cell cycle arrest mediated by a block in gluconeogenesis 120
4.2. Homology-driven gene replacements 122
4.3. *FBP1* +1 frameshift strain 124
4.3.1. Strain construction 124
4.3.2. Adaptive mutation assay 125
4.3.3. Reconstruction assay 128
4.3.4. Sequence analysis 128

4.4. *hTP53-FBP1* +1 frameshift fusion strain 129

4.4.1. Adaptive mutation assay 131
4.4.2. Reconstruction assay 133
4.4.3. Sequence analysis 134
4.4.4. Concluding remarks on the *hTP53/FBP1* fusion 134

5. REFERENCES 136

1. Introduction

1.1. Mutations and Cancer

Mutations are one or more alterations in the DNA sequence or in the genome. Both DNA strands however, consist of chemically intact structure. There are different types of mutations, such as point mutations within a gene (base substitutions, frameshifts) or mutations affecting a chromosome (i.e. chromosome rearrangements, translocations, duplications, inversions). In a third type, the mutation affects the whole genome, altering the chromosome count (aneuploidy or polyploidy). Furthermore, mutations occur in the germ line as well as in the soma. Germ line mutations are inhereditable in contrast to mutations affecting somatic cells. The latter ones are only passed on to a limited clone through rounds of cell growth and division.

Mutagenesis plays an important role in evolution and is responsible for the genetic variety we know today. Due to mutations organisms were able to sustain selective pressure and gain an advantage over their competitors. However, in most cases, the majority of mutations leads to a reduced fitness of the organism and furthermore can proceed to cancer.

In the year 2000, Hanahan and Weinberg proposed six hallmarks of cancer. They suggested that a tumor has to fulfill following criteria: self-sufficiency in growth signals, insensitivity to anti-growth signals, evading apoptosis, limitless replicative potential, sustaining angiogenesis and tissue invasion and metastasis (Hanahan and Weinberg, 2000) as shown in Fig. 1A). Eleven years later they amended the six checkpoints for full malignancy with two further emerging criteria (Fig. 1B). Those include deregulation of cellular energetics, meaning that in tumorigenesis a metabolic switch takes place in order to favor growth and proliferation of tumor tissue. The different metabolism in malignant tissue was first observed by Otto Warburg (Warburg, 1956a, b) and is referred to as the Warburg-effect nowadays. It postulates that cancer cells reprogram their cell metabolism to perform glycolysis in the presence of oxygen and decrease respiration in mitochondria. The second emerging hallmark “avoiding immune destruction” enables cancer cells to avoid attack and elimination by immune cells (Hanahan and Weinberg, 2011).

Furthermore, two enabling characteristics for multistep tumorigenesis, which can be responsible for the onset of hallmark capabilities, were proposed. Inflammation produces a constant surplus of reactive oxygen species that also attack and damage nucleic acids. Additionally, the development of genome instability and mutation in cancer cells can generate random mutations.

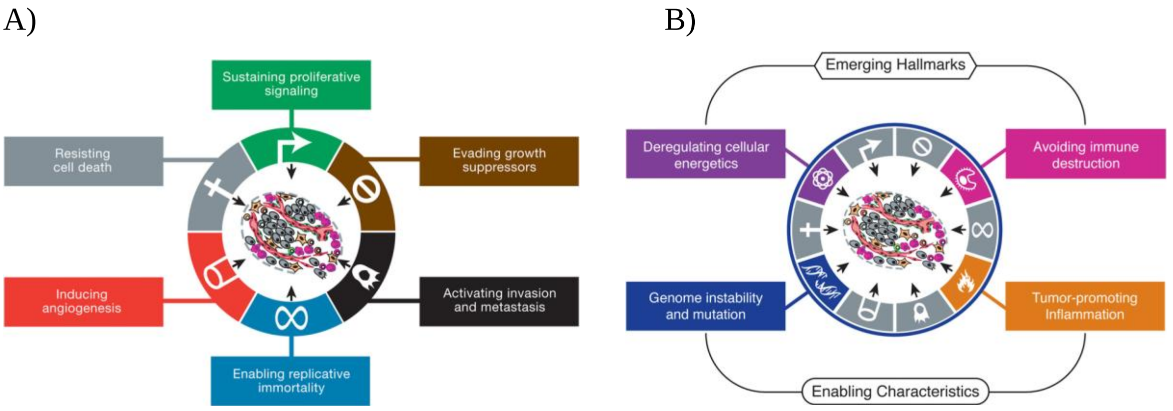
A)
Sustaining proliferative signaling
Resisting cell death
Evading growth suppressors
Inducing angiogenesis
Activating invasion and metastasis
Enabling replicative immortality
B)
Emerging Hallmarks
Deregulating cellular energetics
Avoiding immune destruction
Genome instability and mutation
Tumor-promoting Inflammation
Enabling Characteristics

Fig. 1. A) The six hallmarks of cancer (Hanahan and Weinberg, Cell 2000) and B) The recently expanded hallmarks (Hanahan and Weinberg, Cell 2011)

Mutation can be triggered by exogenous influence, like chemicals or irradiation but every cell also undergoes spontaneous mutations. One problem in cancer research is the mutation rate determined in proliferating cells. When mutation rates from different studies in human cells are compared, a rate of 1 x 10^{-6} to 1x 10^{-7} is found to account for the inactivation of a gene, depending on its size. Those rates are not sufficient to explain the high mutation rate in tumors (Loeb, 1991; Strauss, 1992). In cancer multiple mutations as well as elevated mutation rates are observed. At least 9 mutations are required for the development of colon cancer in humans in 25-50% of all examined cases (Fearon and Vogelstein, 1990). One model to explain the described discrepancy is the mutator phenotype postulated by Loeb (1991). He argues that in early tumorigenesis one step induces multiple mutations and therefore leads to an increased mutation rate. This would produce a hypermutability state in progressed tumors. Originally, he thought that these mutations would be restricted to genes which control replication and repair mechanisms. However, later the hypothesis was expanded to include genes involved in cellular responses, chromosome segregation or damage surveillance (Loeb et al., 2003).

One year after the postulation of the mutator phenotype, Strauss postulated another hypothesis why the determined mutation rates in somatic cells were insufficient for human cancers (Strauss, 1992). He thought to see a connection between the occurrence of reported point mutations in cancer and the studies of Cairns (Cairns et al., 1988) and Hall (1990) in bacteria. Both researchers put their cells under selective pressure, which permits survival but not growth. Herewith, a new class of mutation was declared – to be specific, spontaneous mutations in non-dividing cells. They observed mutations as a function of time instead of generation.

1.2. Research on Adaptive Mutagenesis in budding yeast

For a long time the theory that mutations are a result of replication and polymerase errors was unquestioned. The observations of mutations arising in non-replicating cells by Ryan (1955) was mostly ignored by other researcher or argued to be artifacts. It was not until 1988 when Cairns and his colleagues took on Ryan's hypothesis and found corresponding results (Cairns et al., 1988). Their publication caught attention and was the onset of research in the field of adaptive mutations.

When adaptive mutations were first observed, researchers gave the phenomenon various names, e.g. "directed mutation", "stressful-lifestyle associated mutation", "starvation-associated mutation" or "stationary phase mutation" (Foster, 1999). However, all names bore some misunderstanding in describing the process the correct way. The name "adaptive mutation" took over, when first used by Cairns and Foster (1991). At that time the name seemed most appropriate to describe the process in non-dividing cells that produce beneficial mutations specific to the selective pressure (Foster, 1993). The selection has to occur under non-lethal conditions, otherwise no adaptive mutations are produced. Under strict considerations, the term "adaptivity" is not correct, since also increased mutation frequencies in other genes, which are not under selective pressure, occur (Foster, 1999; Torkelson et al., 1997). However, since this detail was not known at that time, the name adaptive mutation is persistent and commonly used in bacteria as well as in yeast.

Four years after the first reports of adaptive mutations in bacteria, Steel and Jinks-Robertson (1992) observed the same phenomenon in *S. cerevisiae*. They used a yeast strain auxotrophic for lysine due to a defined +4 frameshift mutation and plated cells on lysine-free selective medium. Only cells that reversed the mutation could become prototroph for lysine and were able to grow on the selective medium. Over the time course of 8 days they monitored the appearance of colonies and further characterized them to find out if these colonies were random mutants or if they were the consequence of adaptive mutations. They observed that during the first 4 days post-plating, colonies appeared in a Luria-

Delbrück distribution (Luria and Delbruck, 1943), whereas after day 4 a Poisson distribution was given.

The distribution was first described by Luria and Delbrück (1943) when they studied mutations in *E. coli* making them resistant to the bacteriophage T1. In their experiment, they used a fluctuation assay setup, which contains multiple subcultures under the same conditions. They assumed that the cells gained the mutation in the preculture phase prior plating to phage infected plates. If the mutation developed early in preculture, the mutant will produce many identical cells and therefore form more colonies on plates, whereas a late mutation in preculture phase would only give rise to a low number of resistant clones on plates. Consequently, Luria and Delbrück observed random mutations with a high variance in parallel cultures. This variance was later declared the Luria-Delbrück distribution.

Jinks and Steel-Robertson observed exactly this high variance on day three when applying the statistics. Sometimes a high number of colonies might be present on day 3 compared to other subcultures. In this case, many mutations were obtained during the relatively early preculture phase, which enables colony formation on selective plates at day 3. If the number of colonies is much higher compared to the other subcultures, it is referred to as "jackpot". These mutations derive from replication-dependent events and are no adaptive mutations and still follow a Luria-Delbrück distribution. Colonies after day 4 resemble a Poisson distribution and are mutations derived from replication-independent events and therefore are adaptive mutations.

To further characterize revertant colonies Steel and Jinks-Robertson performed reconstruction assays to rule out, that late arising colonies are slowly growing clones. Moreover, they performed yeast transformation with *LYS2* plasmids to rule out that phenotypic lag occurred. This would be the case when cells undergoing a revertible mutation might take some time to actually build the *LYS2* gene product to start cellular division with a delay and consequently also colony formation on selective plates. In a next step they performed canavanine assays to confirm that residual growth was not responsible for the formation of colonies on the selective plates. Canavanine is an analog to arginin and is toxic to replicating cells. The last verification of having produced adaptive mutations in their assay was accomplished by the fact that no unselective neutral mutations arise when plating cells on SC-trp. All these data gave evidence to adaptive mutation in yeast.

In the same year, Hall (1992) reported of adaptive mutation in yeast when using a base substitution mutation in the initiation codon of the *HIS4* gene. Whereas the studies of Steel and Jinks-Robertson and Hall “merely” proved that there is the phenomenon of adaptive mutation in yeast, later research focused on the mechanism behind.

Since obviously also in non-proliferating cells some kind of DNA processing has to take place in order to gain beneficial mutations, a special interest was developed for DNA repair pathways.

The connection of replicative polymerases and adaptive mutagenesis was studied with a temperature sensitive polymerase δ subunit. The study suggests that adaptive mutation frequencies are higher when polymerase δ is impaired (Baranowska et al., 1995). Another report proved with a frameshift allele that a deficiency in the proofreading activity of both replicative polymerases δ and ε results in considerable increase in mutation rate and also frequency (Babudri et al., 2001).

Mismatch repair (MMR) was analyzed by Halas et al. (2002) by impairing all basic MutS and MutL-homologs, resulting in increased accumulation of adaptive revertants.

Deficiency in nucleotide excision repair (NER) due to disruptions of the genes *RAD14*, *RAD16* and *RAD26* increased mutation frequency, however there was a dependency on the functional subunit *REV3* of the translesion synthesis polymerase ζ (Heidenreich et al., 2004).

For double strand break repair Rad52, which is involved in single strand annealing (SSA) and homologous recombination (HR), as well as Rad54, only playing a role in homologous recombination, were analyzed with the *lys2ΔBgl* assay in haploid and diploid cells. Interestingly, similar results were obtained with diploid and haploid cells, suggesting, that neither HR nor SSA produces adaptive mutations, given the fact that in haploid cells no homology is given (Heidenreich et al., 2003). When experiments were performed with *dnl4* and *yku70* mutants, which encode important proteins for non-homologous end-joining (NHEJ), a decrease in mutation frequency was shown for the first time. With this study it was evident that NHEJ accounts for 50% of all adaptive frameshift mutations (Heidenreich et al., 2003). It showed that NHEJ is the only one of three double strand break repair ways producing adaptive mutations. Moreover, sequence analysis revealed that NHEJ-dependent reversion events are simple deletions in mononucleotide runs. This is comparable to the sequence analysis of revertants form a NHEJ proficient strain (Heidenreich and Wintersberger, 2001). Furthermore, it was shown that γ-irradiation induces adaptive mutations dependent on functional NHEJ (Heidenreich and Eisler, 2004). The finding that NHEJ accounts for 50% of adaptive frameshift mutations is in union with the findings of

Halas et al. (2009). They also investigated the NHEJ pathway with base substitutions and found the pathway responsible for 40% of the mutations.

The Rad6 epistasis group consists of many genes and can be divided in at least three sub-pathways. Many studies involve the key gene *RAD6* itself (Cejka et al., 2001; Rojas Gil and Vondrejs, 1999; Storchova et al., 1998) and a knock out of the gene yielded elevated adaptive mutations analyzed with base substitution assays.

Translesion synthesis enzymes can bypass noncoding lesions. When studying the polymerase η, knock out strains of *RAD30* and the subunits Rev1 were used. Deficiency of polymerase η (Rad30) had only slight effects on adaptive mutability, however, Rev1 was required for increased adaptive mutagenesis in a NER-deficient strain. Furthermore, UV-induced adaptive mutations are dependent on *REV1* and *REV3* (subunit of Pol ζ), suggesting a relationship between these two subunits (Heidenreich et al., 2006).

Summarizing, studies showed that NER, MMR, replicative polymerases such as Pol δ and Pol ε, homology-driven double strand break repair (HR and SSA) and the Rad6 epistasis group have antagonizing effects on adaptive mutagenesis; whereas NHEJ and translesion synthesis enzymes play a promotive role for adaptive mutations (Babudri et al., 2006; Heidenreich, 2007).

In these studies different alleles with auxotrophies in histidine, lysine, tryptophan and adenine were used. Most research work has been done with the *lys2ΔBgl* system, which consists of a +4 frameshift. Besides frameshift mutations, also missense and nonsense mutations were used (Cejka et al., 2001; Marini et al., 1999). However, missense mutations should not be favored since they do not lead to a truncated gene product and might have remaining function, which could be a danger with regard to leakiness. Frameshift mutations and nonsense mutation both produce a strictly non-functional gene product and are therefore considered to be more convenient for the purpose of studying adaptive mutations. However, nonsense mutations can also revert by extragenic suppression leading to two subpopulations on selective plates. Therefore, frameshift mutations are clearly favored and commonly used. Particularly the *lys2ΔBgl* allele was used for many studies, reviewed in (Heidenreich, 2007).

All systems used here for investigating adaptive mutations in yeast are based on amino acid starvation. It was shown that under these stress conditions, cells start accumulating increased ROS levels within the first days of starvation (Eisler et al., 2004; Steinboeck et al., 2010). Furthermore, lysine starvation seems to trigger apoptosis (Eisler et al., 2004).

Thus, it might be worthwhile finding another system to study adaptive mutations in yeast other than based on amino acid starvation.

1.3. *Saccharomyces cerevisiae* as a model organism

The yeast *Saccharomyces cerevisiae* is a multi functional organism, thus also given many names like baker's yeast, brewer's yeast or budding yeast. It is one of the oldest microorganisms used in biotechnological applications, e.g. food production or wine and beer production.

In the last decades, this yeast also gained importance as a model organism. It was the first eukaryote to be fully sequenced in 1996. Chromosome 3 was the beginning of the sequencing project and was completed within two years (Oliver et al., 1992). The other 15 chromosomes followed and the whole genome was sequenced within six years, mostly with shotgun sequencing (Dujon, 1996; Goffeau, 2000; Thomas, 1996).

S. cerevisiae shares some of the advantages of a prokaryote, e.g. fast growth with a generation time of 90 minutes, easy transformation, life cycle in diploid and haploid growth phase. Especially the variety of marker genes, i.e. *LYS*, *HIS*, *URA3*, *TRP*, *ADE* and vectors, such as YIp (Yeast Integrating Vector) and YEp (Yeast Episomal vector) make easy and time-efficient microbiological work possible. Another big advantage is the easy genetic approach. Target genes can be disrupted in one step to study their functionality or be replaced by another gene, which serves as marker for a selection system (Rothstein, 1991).

Even though *Saccharomyces cerevisiae* is a unicellular eukaryote, many basic processes are conserved in higher eukaryotes, therefore, the budding yeast is used as a model organism for a variety of studies, like ageing, neurodegeneration, cancer and many more. New insights about cellular function and defects are given and can be associated with human disease.

In 2001, the Nobel Prize was granted to the US researcher Hartwell and his British colleagues Hunt and Nurse, who elucidated the mechanisms of cell cycle, which was approached in the model organism *S. cerevisiae* (Hartwell, 2002).

1.4. Glycolysis and Gluconeogenesis

1.4.1. Basics

Glycolysis is the enzymatic pathway to metabolize glucose over 9 steps to pyruvate. It is a universal pathway with the highest metabolic rate of carbon turnover. The pathway is anaerob and the metabolism of glucose is also referred to as fermentation. One reason why this pathway is conserved in organisms is because it is an efficient pathway to generate energy. One molecule glucose (6 carbon atoms) is converted to two molecules pyruvate (3 carbon atoms). This metabolism sets energy free, which is stored as ATP (adensosine triphosphate) and NADH (nicotinamide adenine dinucleotide).

Glycolysis is a reversible pathway with the exception of three steps. The reversed pathway is referred to as gluconeogenesis and synthesizes carbohydrates from non-carbohydrate precursors. The three steps that cannot be catalyzed in the reverse direction by the same enzyme in gluconeogenesis are i) conversion of glucose to glucose-6-phosphate by the enzyme hexokinase (HK), ii) phosphorylation of fructose-6-phosphate to fructose-1,6-bisphosphate by phosphofructokinase-1 (PFK-1) and iii) phosphoenolpyruvate to pyruvate by pyruvate-kinase (PK). Therefore, the alternative enzymes used in gluconeogenesis are glucose-6-phosphatase instead of hexokinase; the two enzymes fructose-1,6-bisphosphatase (FBPase-1) and phosphoenolpyruvate carboxykinase (PEPCK) replace phosphofructokinase-1 and pyruvate kinase, respectively and propose a key function of gluconeogenesis.

Since both directions of the pathway are possible it requires strict regulation to avoid a futile cycle, where glucose would be metabolized and synthesized at the same time. Regulation takes place at enzymes catalyzing the irreversible steps and forming products specific for glycolysis. The enzyme hexokinase (HK) does not pose a site for key regulation, since its product glucose-6-phosphate is a universal metabolite and not specific for glycolysis. Hence, key regulation takes place at phosphofructokinase-1 (PFK-1) and pyruvate kinase (PK).

PFK-1 is allosterically inhibited by ATP and citrate and activated by fructose-2,6-bisphosphate as well as AMP (adenosine monophosphate) and ADP (adenosine diphosphate). The last step of glycolysis is catalyzed by pyruvate kinase, which is allosterically inhibited by ATP.

In short, fructose-2,6-bisphosphate and AMP activate PFK-1 (glycolysis) and inhibit fructose-1,6-bisphosphatase (gluconeogenesis).

Individual steps of glycolysis and gluconeogenesis are shown in Fig. 2.

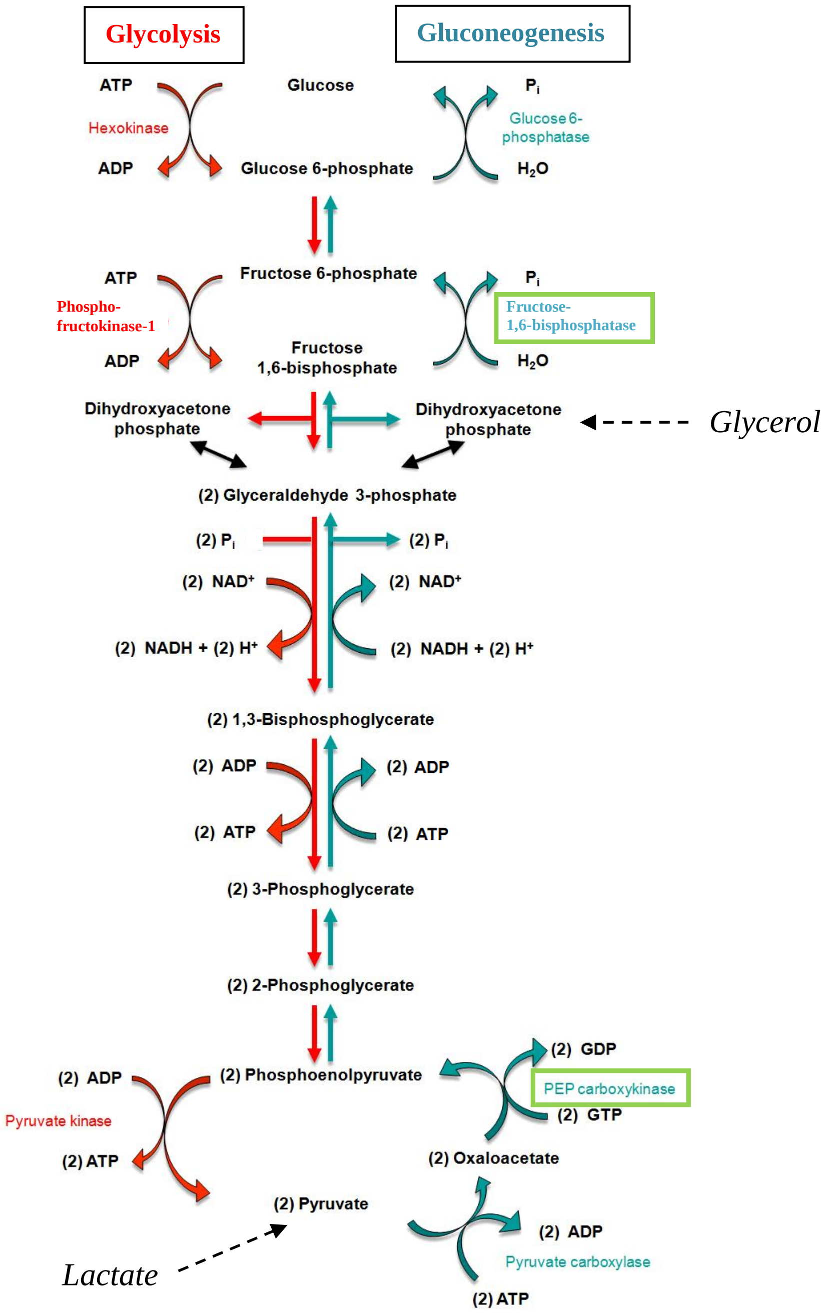
Glycolysis
Gluconeogenesis
ATP
Hexokinase
ADP
Glucose
Glucose 6-phosphate
P_i
Glucose 6-phosphatase
H_2O
ATP
Phospho-fructokinase-1
ADP
Fructose 6-phosphate
Fructose 1,6-bisphosphate
P_i
Fructose-1,6-bisphosphatase
H_2O
Dihydroxyacetone phosphate
Dihydroxyacetone phosphate
Glycerol
(2) Glyceraldehyde 3-phosphate
(2) P_i
(2) P_i
(2) NAD^+
(2) NADH + (2) H^+
(2) NAD^+
(2) NADH + (2) H^+
(2) 1,3-Bisphosphoglycerate
(2) ADP
(2) ATP
(2) ADP
(2) ATP
(2) 3-Phosphoglycerate
(2) 2-Phosphoglycerate
(2) ADP
Pyruvate kinase
(2) ATP
(2) Phosphoenolpyruvate
(2) GDP
PEP carboxykinase
(2) GTP
(2) Oxaloacetate
(2) Pyruvate
(2) ADP
Pyruvate carboxylase
(2) ATP
Lactate

Fig. 2. Steps of glycolysis on the left and gluconeogenesis on the right. The two key enzymes functioning in gluconeogenesis are marked with green boxes, which are fructose-1,6-bisphosphatase responsible for the dephosphorylation of fructose-1,6-bisphosphate generating fructose-6-phosphate and phosphoenolpyruvate carboykinase catalyzing the conversion from oxalacetate to phosphoenolpyruvate. Positions where the precursors lactate and glycerol are fed into the pathway are indicated. Figure was adapted from http://qualityinvention.com/QIlibraryArticle.php?id=194

Lactate, pyruvate and glycerol function as important precursor substrates for gluconeogenesis and can be utilized by cells as alternative carbon sources to synthesize glucose. Lactate is oxidized by the enzyme lactate dehydrogenase to pyruvate, and thus may enter the gluconeogenetic pathway. Glycerol has to be converted to glycerol-3-phosphate by the glycerol kinase and oxidized to dihydroxyacetone by a dehydrogenase to finally enter the pathway.

1.4.2. Fermentative and non-fermentative metabolism in yeast

In yeast, glucose is the preferred fermentable monosaccharide and is used as carbon source for cultivation in rich medium. When sufficient glucose is present cells grow with a generation time of 90 minutes, which is referred to as exponential phase. During glucose fermentation ethanol production takes place (Haurie et al., 2001). Once glucose is exhausted, cells switch to the diauxic shift and grow in ethanol. The metabolism is switched from glycolysis to aerobic ethanol utilization and the growth rate is drastically reduced. When ethanol stock is depleted cells enter stationary phase.

As long as sufficient glucose is offered, enzymes required for the utilization of alternative carbon sources are not synthesized at all or only at very low level, known as carbon catabolite repression or glucose repression (Gancedo, 1998). Already during the diauxic shift, transcription of genes accounting for a quarter of the whole yeast genome is reprogrammed (DeRisi et al., 1997). Furthermore, interaction of many pathways takes place. The Snf1 pathway is activated during diauxic shift and when ATP/AMP ratio drops and consequently derepresses genes required for use of alternative carbon sources and metabolic pathways that generate ATP. The TOR (target of rapamycin) pathway regulates cell growth and transition from exponential growth to diauxic shift. During diauxic shift the function of TOR is downregulated and furthermore inhibited, resulting in induced expression of carbon discrimination pathway genes. Ras/cAMP signalling plays a negative role for entry into stationary phase. Elevated levels of cyclic AMP (cAMP)-dependent protein kinase activity in cells does not allow proper diauxic shift (Pedruzzi et al., 2000). Another important regulation is promoted by the protein kinase A (PKA) pathway, which controls cell cycle progression and cell growth. It proposes a negative regulator since cells do not survive with increased PKA activity when entering stationary phase (Galdieri et al., 2010).

1.4.3. Insights on FBP1 and PCK1

The genes *FBP1* coding for fructose-1,6-bisphosphatase and *PCK1* coding for phosphoenolpyruvate carboxykinase are well characterized since they play an essential role in gluconeogenesis. Early studies showed that yeast strains with a non-functional *FBP1* gene are not able to grow on gluconeogenic carbon sources (Entian et al., 1988; Gancedo and Delgado, 1984). In the presence of glucose *FBP1* and *PCK1* are repressed. Once glucose becomes limited the gene is derepressed and expressed. Studies show that the activity of both enzymes is reduced immediately after addition of glucose (Muller et al., 1981). In the case of Fbp1p it was shown that the enzyme was degraded 5 minutes later (Entian et al., 1988). Addition of glucose to long-term starved cells leads to Fbp1p degradation by a vacuolar pathway (Cui et al., 2004; Hung et al., 2004) and addition after short-term starvation results in degradation of the enzyme by proteolytic pathway (Horak et al., 2002; Hung et al., 2004).

The promoter sequences of both genes were characterized to define regulatory regions (Mercado and Gancedo, 1992; Mercado et al., 1991). In *FBP1* two UAS were found, which are CSRE (carbon source responsive element) and one URS element, which binds the repressor Mig1 (Mercado et al., 1991). In *PCK1* two CSRE, functioning as UAS were found and two URS elements (Gancedo, 1998; Mercado and Gancedo, 1992; Schuller, 2003). In both genes, the CSRE binds the derepressing zinc finger protein Cat8 and Sip4.

1.5. Aim of the study

The purpose of this study is to develop a new selection system for stationary yeast cells to be able to study mutation frequencies. The well established *lys2ΔBgl* system, where cells are starved for the single amino acid lysine, should be replaced by an improved system. Lack of a single amino acid results in a one sided starvation, which does not reflect natural circumstances. Therefore this method is not satisfying and should be replaced by a better selection type. A promising option is carbohydrate starvation, which is supposed to result in a more relevant state of stationary phase. Carbon source starvation leads to a regulated cell cycle arrest via signalling pathways. The pathway of choice will be gluconeogenesis. Target genes should be involved only in gluconeogenesis and not in glycolysis, which reduces the possibilities down to the genes *FBP1* and *PCK1*.

First, yeast strains with gene disruptions of target genes involved in the carbon source utilization pathways will be constructed to achieve a more natural stationary phase. Different non-carbohydrate precursors, which function as substrate for gluconeogenesis should be tested. Optimal conditions will have to be determined with regard to target gene, carbon source, quality of stationary phase, residual growth and viability of arrested cells.

Moreover, it should be tested if the strain with the non-functional target gene, when used as a background strain, has an effect on the growth of a strain with the functional gene on non-carbohydrate sources.

Once the cell cycle arrest by carbohydrate starvation is optimized, a frameshift mutation will be introduced into the target gene to serve as a selection system to study mutation rates. Furthermore, adaptive mutation assays will be performed. Adaptive mutations will occasionally give rise to certain cells with the ability to re-enter the active cell cycle and to start proliferating again.

The new selection system with carbohydrate starvation should be compared with the *lys2ΔBgl*- mediated adaptive mutation assay.

2. Materials and Methods

2.1. Materials

2.1.1. Media

2.1.1.1. Media for yeast cultivation

All specifications refer to 1 l medium.

YPD	20g glucose (2%) + 20g peptone + 10g yeast extract
YPG	30g glycerol (3%) + 20g peptone + 10g yeast extract
YPAD	YPD + 30mg adenine
YPGal	20g galactose (2%) + 20g peptone + 10g yeast extract
SM	20g glucose (2%) + 6.7g YNB w/o aa
SC	SM + amino acids/bases (see list below)
SC-Lactate*	3% lactate instead of glucose
SC-Pyruvate	2% pyruvate instead of glucose
SC-Glycerol	2% glycerol instead of glucose
SC-Lactate/Pyruvate	3% lactate + 2% pyruvate instead of glucose
SC-Lactate/Glycerol	3% lactate + 2% glycerol instead of glucose
MMS gradient plate	YPD + 0,05% methyl methansulfonate
2%	SM + 2% YPD

Table 1. Composition of yeast media

* DL-Lactate 60% (w/w) from Sigma

For plates 2% agar (Oxoid, LabM) was added in all cases.

Amino acids (aa) and bases for synthetic complete (SC) media:

aa	Stock Solution per 400 ml	Stock Solution per 1 l	Concentration [mg/l]	Stock-Concentration [mg/ml]
ade*	24.0 ml	60.0 ml	30	0.5
arg	6.0 ml	15.0 ml	30	2.0
his	8.0 ml	20.0 ml	20	1.0
ileu	4.0 ml	10.0 ml	60	6.0
leu	12.0 ml	30.0 ml	60	2.0
lys	8.0 ml	20.0 ml	40	2.0
met	4.0 ml	10.0 ml	20	2.0
trp	6.0 ml	15.0 ml	30	2.0
val	0.8 ml	2.0 ml	30	15.0
ura*	8.0 ml	20.0 ml	20	1.0
thr	1.2 ml	3.0 ml	30	10.0
phe	20.0 ml	50.0 ml	50	1.0
tyr	48.0 ml	120.0 ml	30	0.25

Table 2. Amino acids and bases for synthetic complete medium

* Bases adenin und uracil were added due to a deletion in the ade and ura gene.

Drop out media were prepared as SC minus one or more amino acids.

All types of media were autoclaved for 12 minutes.

Special selection plates:

5-FOA plates	20g glucose + 6.7g YNB w/o aa + 1g FOA + 50 mg uracil + essential aa/bases for strain + 2% agar

For 400 ml 8g glucose, 8g agar and 20 ml uracil stock (see list aa above) as well as essential amino acids for the strain of interest were mixed in 300 ml ddH_2O and autoclaved for 12 minutes. Meanwhile 0.4g 5-Fluoro orotic acid (Apollo Scientific) and 2.7g YNB were dissolved on a heater in 100 ml water and filter sterilized. The solution was added to the mixture of warm agar and glucose before pouring the plates.

G418-sulphate plates	YPD + 200 µg/ml G-418

Geneticin (PAA) stock (50 mg/ml) was prepared freshly in all cases, filter sterilized and added to the autoclaved YPD after cooling to approximately 60°C.

2.1.1.2. Media for *E. coli* cultivation

All specifications refer to 1 liter medium.

LB	10g peptone + 5g yeast extract + 5g NaCl
LB$_{amp}$	LB + 100 µg/ml Amp or 200 µg/ml Amp in plates + 2% agar
X-Gal plates	LB + 800 µl X-Gal (50mg/ml stock) + 30 µl IPTG (400mM stock) + 6 ml Amp (50mg/ml stock) + 2% agar

Table 3. Composition of *E. coli* medium

Ampicillin, X-Gal and IPTG respectively were filter sterilized and added to the media after autoclaving for 12 minutes.

2.1.2. Yeast strains and yeast plasmids

YLBM	a *trp1-Δ his3-Δ200 ura3-52 lys2ΔBgl ade2-1o gal mal CUP*^{r} (Heidenreich and Wintersberger, 1998)
S288C	*MATα SUC2 gal2 mal mel flo1 flo8-1 hap1 ho bio1 bio6*
YLB27	*MATa trp1-Δ his3-200 ura3-52 lys2ΔBgl ade2-1o rad27-Δ::HIS3 gal mal CUPr*

pBY011-FBP1 (Gateway Vector PlasmID Harvard)

Amp, URA3 (S.c.,) Coli ori, ARS, CEN, pGal1-10- FBP1

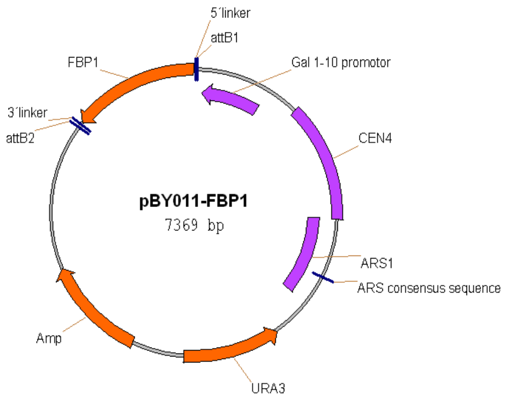

Fig. 3. Plasmid map of Gateway vector pBY011-FBP1

2.1.3. *E. coli* strains and plasmids

2.1.3.1. *E. coli* strains

DH5α

JM110 (dam deficient strain)

2.1.3.2. Bacterial plasmids

pUG6 (Gueldener et al., 2002)

pUG72 (Gueldener et al., 2002)

pUC19

pDR27H

pCN53-SN3 (Baker et al., 1990)

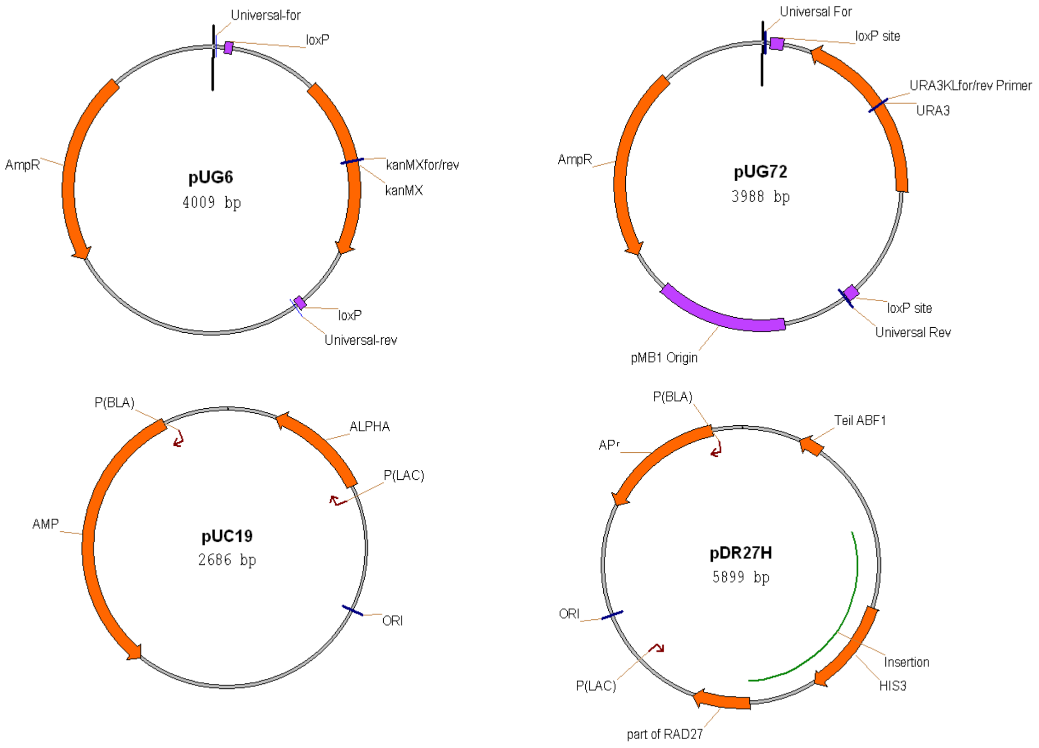
Universal-for
loxP
AmpR
pUG6
4009 bp
kanMXfor/rev
kanMX
loxP
Universal-rev
Universal For
loxP site
URA3KLfor/rev Primer
URA3
AmpR
pUG72
3988 bp
loxP site
Universal Rev
pMB1 Origin
P(BLA)
ALPHA
P(LAC)
AMP
pUC19
2686 bp
ORI
P(BLA)
Teil ABF1
APʳ
pDR27H
5899 bp
ORI
Insertion
HIS3
P(LAC)
part of RAD27

Fig. 4. Plasmid maps of pUG6, pUG72, pUC19 and pDR27H

2.1.4. Buffers and stock solutions

CM1 solution (do not autoclave)

10 mM NaOAc

50 mM $MnCl_2$

5 mM NaCl pH 5,6

CM2 solution

10 mM NaOAc

5% glycerol

70 mM $CaCl_2$

5 mM $MnCl_2$ pH 5.6

Lysis buffer for *E. coli*

0.14 M NaOH; 1% SDS; 25 mM EDTA

Lysis buffer for yeast

50 mM Tris-Cl, 20 mM Na_2-EDTA, pH 7.4

Proteinase K (1mg/ml), Sigma

dissolved in storage buffer: 2.5ml glycerol + 0.05ml 1M Tris-HCL pH 7.5 + 0.0145g $CaCl_2$ + ddH_2O to 5mL

RNaseA (10mg/ml), Roche

10mg RNaseA, 10μL 1M Tris-Cl pH7.5, 15μL 1M NaCl, 975μL H_2O, boil 15 minutes

Sorbitol buffer

1M sorbitol, 0.1M Na_2-EDTA, pH 7.5

TAE buffer (50x)

242 g/l (=2 mol/l) Tris

57.1 ml/l glacial acetic acid

100 ml/l 0.5 M EDTA, pH 8.0

TE buffer

10mM Tris-HCL pH 8; 1mM EDTA

$T_{10}E_{0,1}$ buffer

10mM Tris-HCL pH 8; 0.1mM EDTA

10x loading dye (loading buffer III) (Sambrook J., 1989)

0.42% bromophenolblue

0.42% xylene cyanol FF

66% saccharose in water

2.1.4.1. Further reagents:

Polymerases used for PCR:

company	polymerase	buffer
Qiagen	Taq kit	10x buffer
Roche	Taq	10x buffer
NEB	Taq	10x buffer
Finnzymes	Phusion (proof-reading)	5x HF buffer
Solis Biodyne	FirePol	10x buffer

Table 4. Polymerases and their corresponding buffers

Used enzymes and their reaction buffer:

enzyme	company	reactionbuffer
BamHI	Promega	buffer E
Bsu36I	NEB	NEB3
ClaI	Promega	buffer C
DrdI	NEB	NEB4
HpaI	Promega	buffer J
NarI	Promega	buffer C
SgrAI	NEB	NEB4
SspI	Promega	buffer E
StuI	Promega	buffer B
T4 ligase	Promega	10x ligasebuffer
XhoI	Promega	buffer D

Table 5. Enzymes and their reaction buffers

Fermentas FastDigest Restriction Enzymes:

HindIII	HpaI	SalI	ScaI	SspI	PvuI	XhoI

All FastDigest enzymes were combined with the 10x FD buffer.

2.1.5. List of primers

General primers	**Sequence**	**Tm**	**Length (nt)**
fbp1for	5’CCAACGCAAGGCAGCAATAGC 3’	59.4°C	21
fbp1rev	5’CAACCTGGCACCTCCTTAACGC 3’	59.5°C	22
fbp1intrev	5’CGCCTGCTAACCCAACCAAG 3’	57.0°C	20
fbp1prof	5’GGAGCAACAAGTAGTGCAATTACAGACG 3’	60.3°C	28
fbp1for2	5’GATAGGCCTAAGAATAACAGTGCGAACATATAAGAAACATCCCTCATACTACCACACATATGCCAACTCTAGTAAATGG 3’	79.7°C	79
fbp1ins1	5’TTTGAACGCGAATTGCAAGGCATTCAGTACTACATGTGAAATCACCAGTAGCGTTCTTAAATTGCTTCTGGTGCTCGAGTATGAATCTA 3’	86.1°C	89
fbp1intr2	5’ CCCATCAACTCCATCACCCAATG 3’	59.8°C	23
fbp1rev2	5’CGCTTTTCCCCCTGCTTGTTCC 3’	62.6°C	22
pck1for	5’GCGCCTCGCTTTACACTACATGG 3’	59.7°C	23
pck1rev	5’ CAGGCGATGAAGAACTGTCAGGC 3’	59.7°C	23
psy3rev	5’ GTCTGAGTCAGGCCCTTCTGTC 3’	60.5°C	22
sec61for	5’ TTTCGGCGGTGCTACCATCGG 3’	63.5°C	21
p53for	5’ATGGAGGAGCCGCAGTCAG 3’	54.9°C	19
p53rev	5’GTCTGAGTCAGGCCCTTCTGTC 3’	54.3°C	22
p53intfor	5’GCCATCTACAAGCAGTCACAGCAC 3’	57.7°C	24
p53intrev	5’GTGCTGTGACTGCTTGTAGATGGC 3’	57.7°C	24
p53UTRrev	5’ GGCAGGGGAGGGAGAGATGG 3’	59.3°C	20
pUCPD	5’ GAGCGAGGAAGCGGAAGAGCG 3’	62.2°C	21
kanMXfor	5’ CGGTTGCATTCGATTCCTGTTTGT 3’	60.9°C	24
kanMXrev	5’ ACAAACAGGAATCGAATGCAACCG 3’	60.9°C	24
uraKLfor	5’ TGTTGCTGGCTTGAAACAAGGTGC 3’	62.0°C	24
uraKLrev	5’ GCACCTTGTTTCAAGCCAGCAACA 3’	62.0°C	24
r27up	5’GAGGATGCAGCATTGCCAGC 3’	59.7°C	20
r27down	5’GGCAAACGAATTACAGCCAGTG 3’	56.2°C	22
His3for	5’TCTTTCGAACAGGCCGTACGCAGTTGTCGA3’	71.3°C	30
His3rev	5’TCGACAACTGCGTACGGCCTGTTCGAAAGA3’	71.3°C	30

Table 6. Sequence, melting temperature and length of general primers

Melting temperature for general primers was calculated with Vector NTI Suite 5.5.

Megaprimers	**Sequence**	**Tm**	**Length (nt)**
MPfbp1for	5’TATGGAGCAACAAGTAGTGCAATTACAGACGTGTATTTTGTCTTGATCTTGCTTTTTGTA*GCATAGGCCACTAGTGGATCTG* 3’	53.0°C	82
MPfbp1rev	5’GAAAGGCTTGTTGTTGTTGTCTGCTTGGGGTTGTTTGACTTTCTCAATAAATGTTCTTAT*CAGCTGAAGCTTCGTACGC* 3’	63.7°C	79
MPpck1for	5’TCTTAAATATACAGAAGTAAGACAGATAACCAACAGCCTTTCCCAGATATACATATA*GCATAGGCCACTAGTGGATCTG* 3’	53.0°C	79
MPpck1rev	5’CCAGTCCAGCCGGTGTTGATTAAGTACGCATTAGCTTTATGTTGAGACATCTTTGTAGCT*CAGCTGAAGCTTCGTACGC* 3’	63.7°C	79
MPp53for	5’TGATAGGCCTAAGAATAACAGTGCGAACATATAAGAAACATCCCTCATACTACCACACAT*ATGGAGGAGCCGCAGTCAG*3’	63.3°C	79
MPp53rev	5’ATCGGTATCAAACCCTTCGGTAGAGTCTCTTCTTGGTCCATTTACTAGAGTTGGCAT*GTCTGAGTCAGGCCCTTCTGTC*3’	66.8°C	79
MPura3for	5’TGATAGGCCTAAGAATAACAGTGCGAACATATAAGAAACATCCCTCATACTACCACACAT*CAGCTGAAGCTTCGTACGC* 3’	64.3°C	79
MPura3rev	5’ATCGGTATCAAACCCTTCGGTAGAGTCTCTTCTTGGTCCATTTACTAGAGTTGGCAT*GCATAGGCCACTAGTGGATCTG* 3’	65.0°C	79
MPura-loxPf	5’TGATAGGCCTAAGAATAACAGTGCGAACATATAAGAAACATCCCTCATACTACCACACAT*GAAGTGAGTGTTGCACCGTGCC* 3’	71.4°C	82
MPura-loxPr	5’ATCGGTATCAAACCCTTCGGTAGAGTCTCTTCTTGGTCCATTTACTAGAGTTGGCAT*CTCCTCAGAAGCTCATCGAACTGTC* 3’	71.8°C	82
MPp53rev2	5’ATCGGTATCAAACCCTTCGGTAGAGTCTCTTCTTGGTCCATTTACTAGAGTTGGCAT*GTGCTGTGACTGCTTGTAGATGGC* 3’	69.3°C	81
MPp53R3	5’CTTCTGGTGCTCGATTATGAATCTAGGAAGAGTGATGATATCGGTATCAAACCCTTCGGTAGAGTCTCTTCTTGGTCCATTTACTAGAGTTGGCAT*GTGCTGTGACTGCTTGTAGATGGC* 3’	69.3°C	120
MPp53Kozfor	5’TTTGTATGATAGGCCTAAGAATAACAGTGCGAACATATAAGAAACATCCCTCATACTACCAAAAAAATGTCTGAGCCGCAGTCAGATCCTA3’	71.1°C	91
MPp53KozF2	5’CAGACGTGTATTTTGTCTTGATCTTGCTTTTTGTATGATAGGCCTAAGAATAACAGTGCGAACATATAAGAAACATCCCTCATACTACCAAAAAAATGTCTGAGCCGCAGTCAGATCCTA 3’	71.1°C	120

Table 7. Sequence, melting temperature and length of megaprimers

Melting temperature of megaprimers was calculated for the *italic* part of the sequence only according to the Finnzymes T_M calculator (Breslauer et al., 1986).

2.2. Methods

2.2.1. Molecular biological Methods

2.2.1.1. Construction of yeast strains

- **One step gene disruption ("megaprimer method")**

A gene of interest was knocked out by disruption with a linear DNA fragment that contains a marker gene including its promotor and terminator sequence. The essential benefit of this method is that it works in one step and can be performed artificially by PCR. Only the marker gene but not the target gene needs to exist on a plasmid, on the contrary to other methods. The desired marker gene is integrated into the genome by replacing the whole gene of interest or large parts of the gene, triggered by homologous recombination (see Fig. 6). Consequently, homologous flanking sequences between the target gene and the marker gene are mandatory. Therefore, the PCR-amplified marker gene sequence has to contain homologous parts to the genome in order to be integrated at the correct locus. For this condition, megaprimers are used. They are designed to have two parts. One part contains short complementary sequences of approximately 20 bp to the template plasmid DNA sequence in order to be amplified by PCR. Moreover, the primer has an approximately 60 nt long tail with the sequence being complementary to the genomic DNA at the site of replacement (Fig. 5). The longer the homologous sequences the higher chances are for the foreign sequence to be integrated at the exact region in the genome. As a general rule, 30 nt are sufficient for homologous recombination to take place.

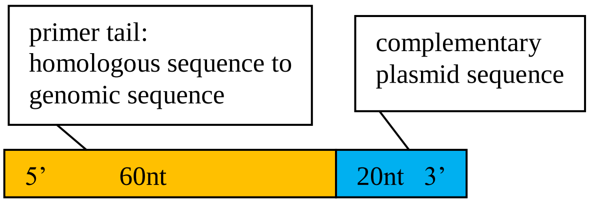

Fig. 5. General design of megaprimer

To avoid unspecific recombination, sequences of the marker gene should not be present in the genome, for example remaining sequences of other disrupted genes. One popular marker gene is *URA3*. It is common to use the *URA3* gene sequence from *Kluyveromyces lactis* for disruptions in order to avoid unspecific recombination.

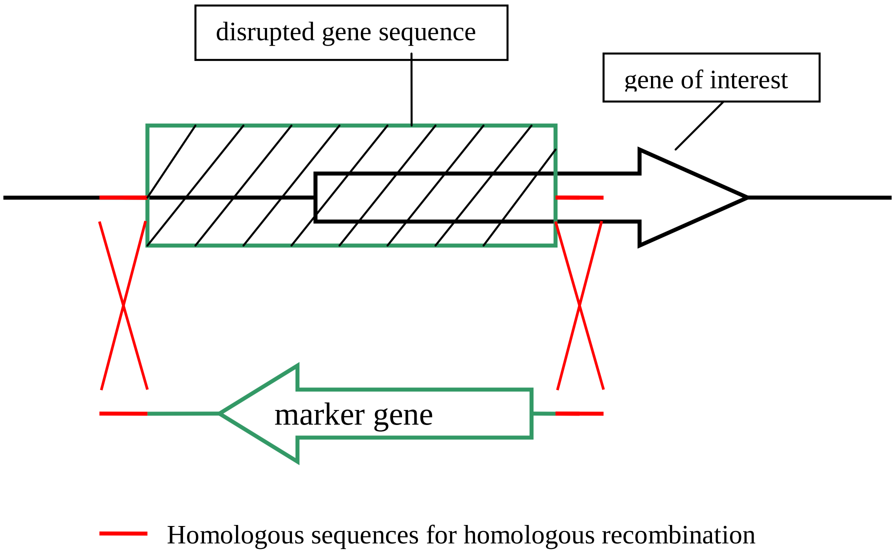
disrupted gene sequence
gene of interest
marker gene
Homologous sequences for homologous recombination

Fig. 6. Disruption of a target gene with a marker gene

- **Two step Gene Replacement (“Loop-in/loop-out”)**

The first step (loop-in) involves a plasmid integration into the genome as illustrated in Fig. 7. The plasmid should have the characteristics of a Yeast Integrating Plasmid (YIp). Furthermore it has to consist of the selectable *URA3* marker and the mutation that should be integrated into the genome, for instance a deletion or an insertion, respectively. The plasmid is linearized within the altered target gene by a restriction enzyme, which defines the integration locus in the genome. The linearized plasmid is transformed into the strain and integration is mediated by homologous recombination.

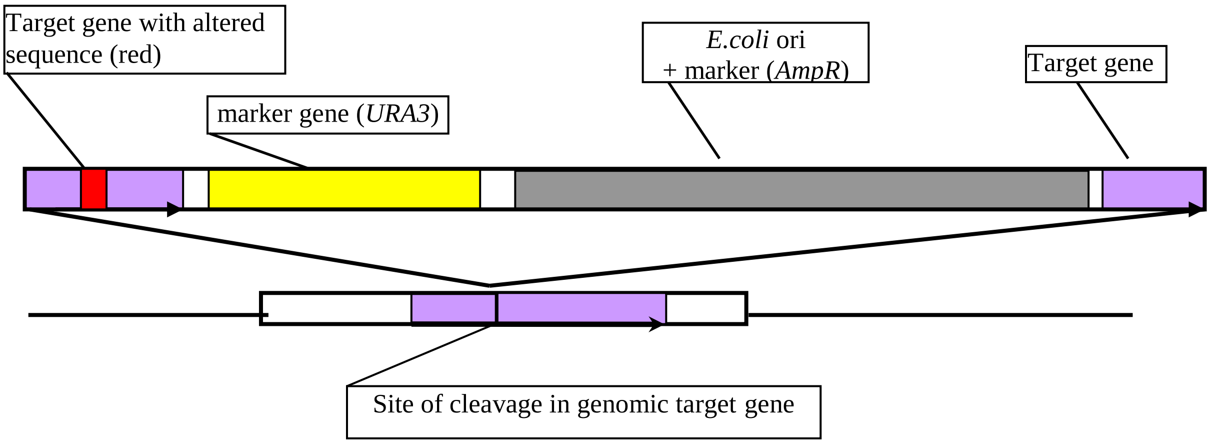
Target gene with altered sequence (red)
E.coli ori
+ marker (*AmpR*)
Target gene
marker gene (*URA3*)
Site of cleavage in genomic target gene

Fig. 7. Integration locus of linearized plasmid sequence into genome

Consequently, clones that successfully took up the plasmid DNA can be differentiated by selection on SC-ura plates due to the marker gene *URA3*. Positive clones have two copies of the target gene; one copy of the wt gene and a second copy of the mutated gene (Fig. 8).

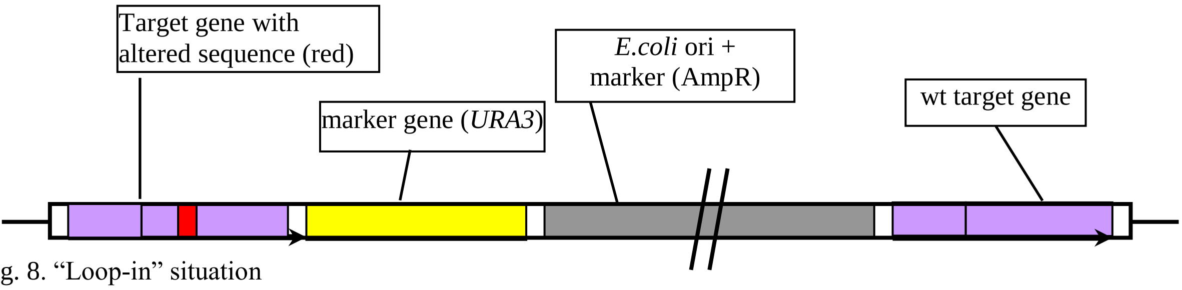
Target gene with altered sequence (red)
E.coli ori + marker (AmpR)
wt target gene
marker gene (*URA3*)

Fig. 8. “Loop-in” situation

Since there are two copies of the target gene another homologous recombination is provoked (Fig. 9), which occurs spontaneously and excludes the plasmid sequence resulting in individuals containing the wt gene and others containing the target gene with the altered sequence. Therefore it is important to be able to distinguish between those two types of clones. The selection of “loop-out” recombinants is based on 5-FOA as a negative selection for URA$^+$ clones. Consequently, all clones where excision of the plasmid occurred can grow on the selective plates. The plasmid will be lost since it has no replicating sequence for yeast. Positive clones still have to be selected for the mutated target gene.

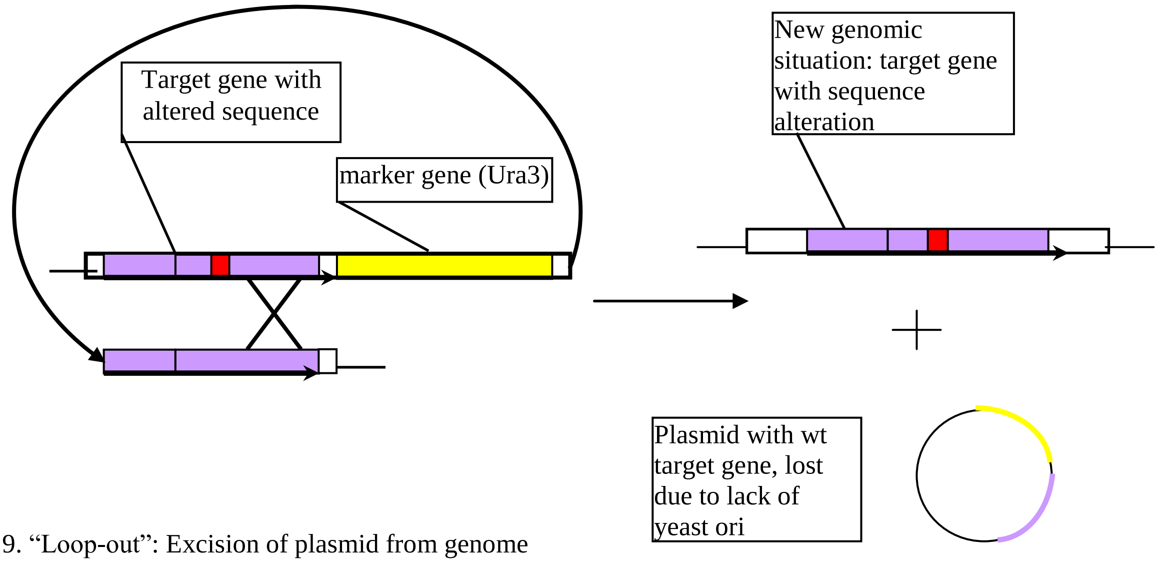
New genomic situation: target gene with sequence alteration
Target gene with altered sequence
marker gene (Ura3)
Plasmid with wt target gene, lost due to lack of yeast ori

Fig. 9. “Loop-out”: Excision of plasmid from genome

2.2.1.2. Yeast Transformation

For yeast transformation two different methods of gene transfer were used. Standard protocol was performed with LiAc transformation. Additionally, in some cases gene transfer was performed with electroporation.

First, LiAc yeast transformation will be described (Gietz RD, 2007):

1) Inoculate a single yeast colony of the host strain into 4 ml YPAD and incubate o/n at 30°C.
2) Determine cell count with microscope and add 2.5 x 10^8 cells to 50 ml pre-warmed YPAD (starting cell density 5 x 10^6 cells/ml).
3) Incubate 4 hours shaking at 30°C .
4) Meanwhile, denature single stranded carrier salmon sperm DNA (Deoxyribonucleic acid Sodiumsalt, Sigma) by incubating 5 min in boiling water and store on ice until needed.
5) Determine cell count of yeast culture with microscope. Cell density should be at least 2 x 10^7 cells/ml.
6) Harvest cells by centrifugation for 5 min at 3500 rpm and remove supernatant.
7) Wash cells with 25 ml ddH_2O twice.
8) Resuspend cell pellet in 1 ml ddH_2O and transfer to eppendorf tube.
9) Centrifuge at full speed for 30 s and discard supernatant.
10) Resuspend pellet in 1 ml ddH_2O and pipet 100 µl (equals 1 x 10^8 cells) per transformation of cells into new tubes.
11) Centrifuge cells at full speed for 30 s and discard supernatant.
12) Prepare the transformation mix:

PEG 50% (w/v)	240 µl
LiAc 1M	36 µl
ss carrier DNA (2 mg/ml)	50 µl
DNA of interest in ddH_2O	34 µl
Total volume	360 µl

13) Add 360 µl of transformation mix to prepared pelleted cells and mix vigorously. Always include a negative control without DNA and a positive control with an

appropriate plasmid (either 2 µm plasmid or CEN and ARS for replication in yeast).

14) Incubate tubes at 42°C for 40 min for heat shock.
15) Centrifuge tubes at full speed for 30 s and discard supernatant.
16) a) Resuspend cells in 1 ml ddH_2O, except for negative control (only 200 µl) by vortexing.
    b) If the transformed DNA corresponds to antibiotic resistance or if a FAO selection follows, add 1 ml YPD and regenerate cells for 2 hours shaking at 30°C. Afterwards wash cells with 1 ml ddH_2O and resuspend in 1 ml ddH_2O (negative control 200 µl).
17) Plate cells on selective media in following concentrations:
    sample: 2 x 200 µl, 100 µl, 50 µl, 20 µl, 10 µl, 2 µl or 5x 200 µl for FOA selection
    positive control: 50 µl and 20 µl
    negative control: 200 µl all on one plate

Alterations of the protocol described by (Gietz RD, 2007):
For the strain YUF and YUFΔlP the protocol was optimized with regard to time of heat shock, amount of ss carrier DNA and sample DNA. The heat shock time was reduced to 20 minutes and the ss carrier DNA amount increased to 70 µl. A minimum of 1 µg DNA was used.

Yeast Transformation with electroporation:

1) Inoculate a single yeast colony in 50 ml YPD and grow o/n shaking at 30°C at 250 rpm.
2) Determine cell count with microscope.
3) Transfer cells in Falcon tubes and stop growth by incubating cells on ice for 15 min.
4) Harvest cells at 3500 rpm for 5 minutes at 4°C and discard supernatant.
5) Resuspend cells in 8 ml ddH_2O and mix by vortexing.
6) Add 1 ml 10x TE and mix by inverting tube.
7) Add 1 ml 1M LiAc and mix by inverting tube.
8) Incubate cell suspension at 30°C shaking at 100 rpm for 45 min (this step makes cells competent).
9) Add 250 µl 1M DTT and incubate for further 15 min at 30°C shaking.

10) Add 40 ml sterile ddH_2O and centrifuge at 3500 rpm for 5 min at 4°C.
11) Remove supernatant and add 5 ml ice-cold sterile ddH_2O → vortex.
12) Add 45 ml sterile ddH_2O and centrifuge with previous settings.
13) Discard supernatant and resuspend pellet in 3 ml ice-cold 1M sorbitol.
14) Centrifuge with same settings and resuspend cell pellet with appropriate volume of 1M sorbitol (cell density should be 2.5×10^{10} cells/ml).
15) Wash 2mm electroporation cuvetts (BioRad or PeqLab) with ddH_2O and EtOH and put on ice to cool them.
16) Prepare DNA in a volume of 5 µl (approximately 100 ng) and cool on ice.
17) Transfer 40 µl competent cells to DNA and mix by pipetting up and down.
18) Incubate on ice for 5 min.
19) Transfer competent cells with DNA to pre-cooled 2mm cuvetts and put into electroporation device (Gene Pulser Xcell, BioRad).

Settings for electroporator:

capacity:	50 µF
voltage:	1,5 kV
resistance:	200 ohm
cuvette:	2 mm
pulse type:	exponential decay

20) Add 1 ml YPD immediately after electric pulse.
21) Transfer electroporated cells to new eppendorf tubes and incubate for 2 hours at 30°C shaking.
22) Centrifuge cells at full speed for 30 s and wash with 1 ml ddH_2O.
23) Plate cells to appropriate selective media in aliquots of 2 x 200 µl, 100 µl, 50 µl, 20 µl, 10 µl, 2 µl.

Positive control is plated on two plates with 50 µl and 20 µl. Whole amount of negative control is plated on 1 plate.

2.2.1.3. *E. coli* transformation

Competent cells:

100 ml LB were inoculated with 1 ml of an o/n-culture with DH5α cells. Incubation was performed at 37°C in an incubator shaker. Once the culture reached an OD of

approximately 0.8 (A_{600}) the cells were harvested by centrifugation at 4°C for 10 minutes (4000 rpm). The pellet was resuspended in 20 ml cold CM1 solution (0,2 volumes) and kept on ice for 20 minutes. After repeating the centrifugation step with the same settings the pellet was resuspended in 2 ml cold CM2 solution.

Then the competent cells were either used right away for transformation or aliquots of 100 µl in tubes were shock-frozen and stored at -80°C.

Transformation step:

50-100 pg DNA or 5-10 µl of a ligation preparation respectively, was added to an aliquot of 100 µl competent *E. coli* cells. Solution was mixed with a pipet tip and kept on ice for 40 minutes. After a heat shock at 42°C for 2 minutes 320 µl LB was added to the cells and the reaction mix was regenerated for 1 hour shaking at 37°C. Further the cells were streaked onto selective plates (LB_{amp} or X-Gal plates).

2.2.1.4. Genomic DNA preparation from yeast

1) Collect cells of 3 ml of an o/n culture

- Spin down 1.5 ml of a YPD o/n culture in a microfuge tube (1 min 13 000 rpm)
- Discard supernatant
- Repeat last two steps in same tube
- Wash pellet with water, spin down

2) Prepare spheroplasts

- Resuspend cells in 500 µl sorbitol buffer (1 M sorbitol, 0.1 M EDTA, pH 7.5).
- Add 12.5 µl DTT stock (2 M), mix
- Add 10 µl Zymolyase (2.5 mg/ml diluted in sorbitol buffer; Seikagaku Corporation) , mix
- Incubate at 37°C for about 1 h. (Conversion of spheroplasts takes 15-120 min. Check for spheroplast formation by mixing 4 µl cells and 4 µl 10 % SDS on a microscope slide. Formation is complete when 80-90% of the cells are "ghost" cells. Compare to a slide without SDS)
- Spin spheroplasts for 30 sec, 13 000 rpm
- Discard the supernatant.
- Resuspend spheroplasts in 500 µl lysis buffer (50 mM Tris-HCl, 20 mM EDTA, pH 7.4) by slowly pipetting up and down.

3) Prepare DNA extracts

- Add 1 µl Proteinase K stock (1mg/ml), mix.
- Add 50 µl SDS (10%), mix and immediately incubate at 65°C for 30 min.
- Add 200 µl 5 M KOAc, mix, and keep on ice for 30 min or longer. (The white precipitate that forms consists mainly of insoluble potassium dodecyl sulfate and denatured proteins.)
- Spin at 13 000 rpm for 5 min.
- Transfer supernatant to a new tube.

4) Precipitate with ethanol

- Add 0.75 ml ice-cold absolute ethanol. (On mixing, the nucleic acids [2% DNA and 98% RNA] and some residual proteins will immediately precipitate.)
- Spin at 13 000 rpm for 1 min
- Remove liquid.
- Air dry pellet for 5-10 min. Do not overdry

5) Dissolve DNA in 200 µl TE (Part of it may be deposited on the wall. Pellet will take a while to dissolve. A 10 min incubation at 50°C in a thermoshaker can help.

6) Digest RNA for 30 min at 37 °C (+1 µl RNaseA stock [10 mg/ml])

7) Precipitate with ethanol

- Add 20 µl 3M NaOAc and 600 µl ice-cold absolute ethanol
- Incubate for 20 min at -20°C
- Spin at 13 000 rpm for 1 min, then remove liquid.
- Wash pellet with 70% EtOH without disturbing it
- Spin at 13 000 rpm for 20 sec, remove liquid
- Air dry pellet for 5-10 min. Do not overdry

8) Resuspend DNA in 50 µl $T_{10}E_{0.1}$, pH 8 (Part of it may be deposited on the wall. Pellet will take a while to dissolve. A 10 min incubation at 50°C in a thermoshaker can help.)

2.2.1.5. Plasmid Preparation of *E. coli*

Plasmid-Miniprep (Sambrook J, 1992)

1) Inoculate one isolated colony in LB_{amp} (or other antibiotics for resistance of strain) and incubate o/n at 37°C.

2) Harvest 1,5 ml of o/n-culture by centrifugation at full speed for 1 min.

3) Remove supernatant by vacuum aspiration.

4) Resuspend cells pellet in 100 µl sterile ddH_2O → vortex

5) Add 100 µl 2x lysis buffer for *E. coli* → vortex and incubate at room temperature for 5 min (cell lysis).

6) Add 50 µl 2M $MgCl_2$, mix by inverting tube and incubate at room temperature for 2 min.

7) Centrifuge at full speed for 5 min.

8) Add 50 µl 3M KAc (pH5; contains 2M glacial acetic acid), mix carefully by inverting tube (pH-neutralisation to precipitate proteins).

9) Incubate for 5 min at room temperature.

10) Centrifuge at full speed for 8 min and transfer supernatant to new tube (this step separates plasmid DNA containing solution from precipitated proteins).

11) Precipitate plasmid DNA with 750 µl 70% EtOH; vortex and incubate on ice for 30 min.

12) Centrifuge at full speed for 15 min.

13) Remove supernatant by vacuum aspiration and dry DNA pellet at room temperature for 10 min.

14) Dissolve pellet in 50 µl ddH_2O + RNaseA (10 ng/µl).

Whenever high plasmid concentrations were required, midiprep was performed with the Jet- star plasmid purification kit according to the manufacturer’s protocol.

2.2.1.6. Ligation

Generally ligation reactions were prepared in 20 µl. The insert was added in a 3 molar overfold, which was calculated for each specific vector and insert.

Reaction:
x µl ddH_2O
2 µl 10x buffer
y µl linearized vector
z µl insert
0,5 µl T4 DNA Ligase (1-3U/µl)
20 µl

The reaction was incubated o/n at a temperature gradient from 0°C to room temperature.

2.2.1.7. Restriction digest of DNA

- Common digest

Enzymes from different companies were used (Roche, Fermentas, Promega, NEB). For analytical digests 10 µl reaction mixes were used, whereas for preparative digests a volume of 50 µl was used. Generally, 1 µg DNA was cleaved by 1 U enzyme. In case of small reaction volumes 0,2 µl enzyme was used. If a double digest was performed two enzymes had to be combined, which were compatible in the same buffer. The digest was performed at 37°C for 1 hour in a thermomixer or o/n in a 37°C incubator.

- FastDigest Fermentas

1 µl restriction enzyme was required for cleaving 1 µg genomic DNA or plasmid DNA respectively within 5 minutes.
General reaction mix:

x µl sterile ddH_2O
1 µl 10x Fast Digest buffer
1 µg DNA
1 µl FastDigest Enzyme
10 µl

The reaction mix was modified if more than one enzyme was used. All FastDigest enzymes could be combined since one buffer was suitable for all enzymes. If the total volume was more than 10 µl the buffer and water volume had to be adjusted. Preparative digests were usually performed in a 50 µl reaction mix.
The reaction mix was incubated at 37°C if not other indicated by the manufacturer for 10-15 minutes to ensure a complete cleavage. Enzymes were heat-inactivated by incubation at 65°C for 15-20 minutes.

2.2.1.8. Polymerase Chain Reaction (PCR)

- Standard PCR

Analytical PCRs were performed with 25 µl per reaction. For quantitative PCRs the volume was doubled.

Reaction mix	**Final concentration**
0.5 µl DNA	< 1µg
2.5 µl10x buffer	1x
0.5 µl dNTPs (10 mM each)	200 µM of each dNTP
1.5 µl primer forward	0.6 µM
1.5 µl primer reverse	0.6 µM
0.5 µl 25 mM $MgCl_2$ (optional)	2 mM
0.15 µl Taq Polymerase	3 U
17.5 µl ddH_2O (or 18 µl if $MgCl_2$ was added)	Total volume 25 µl

Table 8. Reaction mix for standard PCR

Thermocycler settings:

Step	**Time [seconds]**	**Temperature °C**
Initial denaturation	300	94
30 cycles of next 3 steps:		
Denaturation	*30*	*94*
Annealing	*30*	*Tm of primers – 2-5°C*
Extension	*45 s/kb*	*72*
Final extension	300	72

Table 9. Settings for thermocycler

- High fidelity PCR (Phusion Polymerase)

Whenever preparative PCRs were performed in order to amplify a PCR product, which was used for following transformations or cloning, a high fidelity (proofreading) polymerase was used to minimize misincorporations throughout the process of the polymerase chain reaction.

Reaction mix	**Final concentration**
0.5 µl DNA 1:100	< 5 ng for plasmids; <100 ng genomic DNA
4 µl 5x HF buffer	1x
0.4 µl dNTPs (10 mM each)	200 µM of each dNTP
1.25 µl primer forward	0.5 µM
1.25 µl primer reverse	0.5 µM
0.5 µl 25 mM $MgCl_2$ (optional)	2.5 mM
0.2 µl Phusion Polymerase (Finnzymes)	0.02 U/µl
12.5 µl ddH_2O (or 12 µl if $MgCl_2$ was added)	Total volume 20 µl

Table 10. Reaction mix for high fidelity PCR

Thermocycler settings:

Step	**Time [seconds]**	**Temperature °C**
Initial denaturation	30	98
30 cycles of next 3 steps:		
Denaturation	*10*	*98*
Annealing	*30*	*calculated with Finnzymes**
Extension	*15-30 s/kb*	*72*
Final extension	300	72

Table 11. 3-step program for high fidelity PCR

* Annealing temperature was calculated with the Finnzymes T_M calculator (Breslauer et al., 1986)

In some cases the calculated Tm for primers resulted in 72°C or higher. In this case a 2-step program was used for the thermocycler since the extra annealing step was not necessary.

Step	**Time [seconds]**	**Temperature °C**
Initial denaturation	30	98
30 cycles of next 2 steps:		
Denaturation	*10*	*98*
Annealing + Extension	*15-30 s/kb*	*72*
Final extension	300	72

Table 12. 2-step program for high fidelity PCR

- Control PCRs to verify newly constructed strains

As a general rule, clones derived by transformation were always tested with three PCRs to verify integration of the new gene.

a) PCR with two external primers (external for + external rev) in regard to the new gene:

   With this PCR the length difference of positive clones can be compared to the wt. Even if the transformation was not successful and the DNA-fragment did not integrate into the genome, the combination of two external primers should always yield a PCR product. According to the length of the PCR product it can be confirmed if the transformation was successful or if the clone still resembles the host strain.

b) PCR with combination of one external and one internal primer (external for + internal rev according to Fig. 10) to verify beginning of gene:

   The internal primer is located on the newly introduced gene and is combined with one external primer, which can be the same one as in a). For this PCR the successful integration of the gene is required, otherwise no PCR product can be obtained.

c) PCR with the combination of the external and internal primer (external rev + internal for) to amplify the downstream region (according to example in Fig. 10) of the gene.

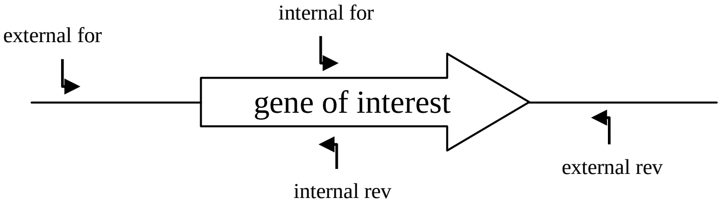

Fig. 10. Positions of external and internal primers

2.2.1.9. Site directed mutagenesis

To insert mutations into a gene of interest (GOI), a site directed mutagenesis was performed in two steps with PCR.

In the first step, a PCR was performed with one mutagenic primer, meaning that the primer contained for instance an insertion or a deletion. The change of one or few nucleotides on the primer does not hinder the annealing of the primer to the template in the PCR. The second primer can be chosen individually to obtain a PCR product which contains part of the target gene including the mutation as shown in Fig. 11.

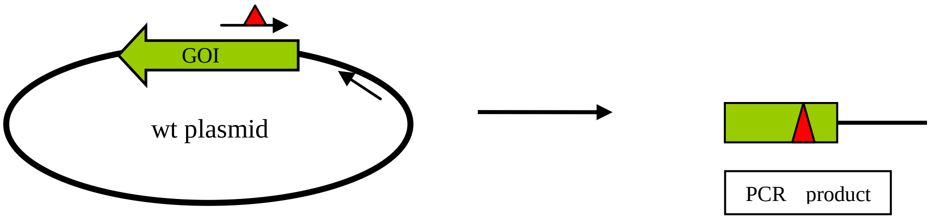
GOI
wt plasmid
PCR product

Fig. 11. First step in PCR mutagenesis with one primer carrying the desired mutation.

The PCR product from the first PCR was purified and served as primer for the second PCR. The second primer was picked external of the ORF of the target gene. The resulting PCR product contains the amplified sequence of the target gene with the mutation which was inserted with the specific primer (Fig. 12).

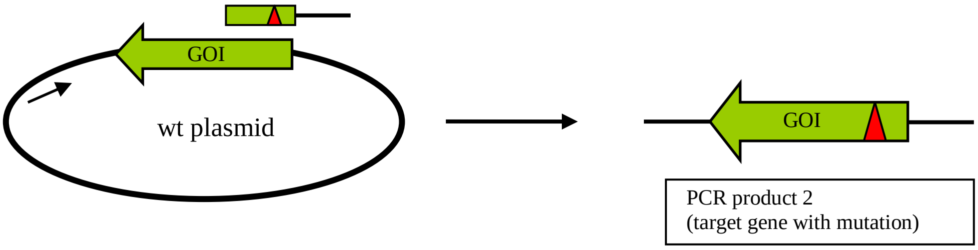
GOI
wt plasmid
GOI
PCR product 2
(target gene with mutation)

Fig. 12. Second step in PCR mutagenesis to generate target gene with mutation

Subsequently, the PCR product was purified and could be used for following subcloning as shown in Fig.13 to avoid potential PCR-derived errors within the sequence.

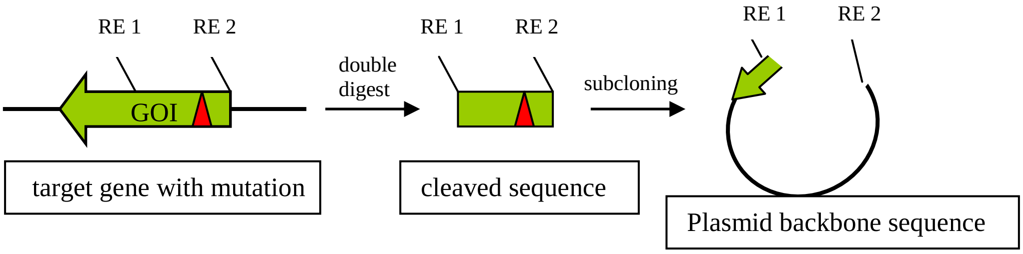
RE 1
RE 2
GOI
target gene with mutation
double digest
RE 1
RE 2
cleaved sequence
subcloning
RE 1
RE 2
Plasmid backbone sequence

Fig. 13. Subcloning with restriction enzymes (RE) of PCR product 2 with mutation into vector backbone

2.2.1.10. Gel electrophoresis

According to the expected bands 0.8%-2% agarose was melted by boiling in 1x TAE buffer (50 ml for a small chamber and 100 ml for a big chamber). After cooling down 1µl ethidiumbromide stock (10 mg/ml) was added and the agarose was poured into the device. For small gels either 8 slot or 12 slot combs were used. In case of the bigger gel 16 slot-combs were used.

After solidifying, the agarose gel was put into the electrophoresis chamber, which has been filled with TAE running buffer. The comb was removed and the gel could be loaded with the samples mixed with 10x loading dye. Furthermore, a DNA marker was loaded on each gel. According to the expected fragments following markers were used: O'Gene Ruler DNA Ladder mix, Mass Ruler High Range or O'Gene Ruler Low Range Marker (Fermentas).

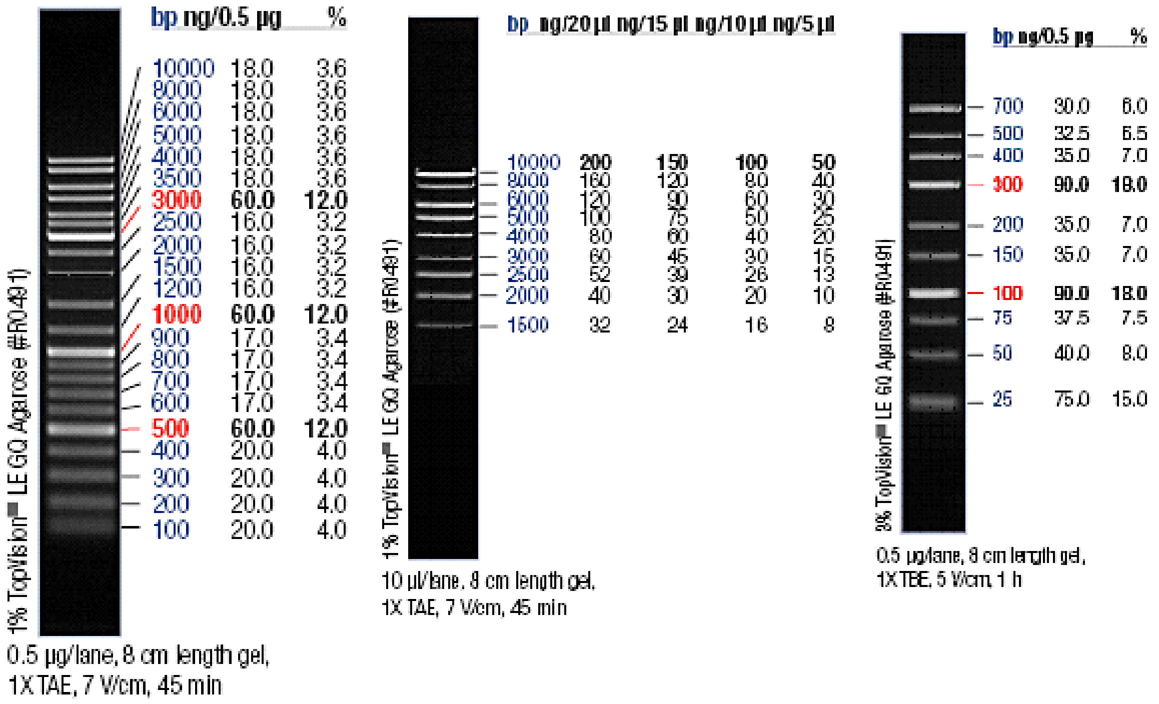
O'Gene Ruler DNA Ladder Mix

Mass Ruler High Range DNA Ladder

O'Gene Ruler Low Range DNA Ladder Mix

bp ng/0.5 µg %
10000 18.0 3.6
8000 18.0 3.6
6000 18.0 3.6
5000 18.0 3.6
4000 18.0 3.6
3500 18.0 3.6
3000 60.0 12.0
2500 16.0 3.2
2000 16.0 3.2
1500 16.0 3.2
1200 16.0 3.2
1000 60.0 12.0
900 17.0 3.4
800 17.0 3.4
700 17.0 3.4
600 17.0 3.4
500 60.0 12.0
400 20.0 4.0
300 20.0 4.0
200 20.0 4.0
100 20.0 4.0
1% TopVision™ LE GQ Agarose (#R0491)
0.5 µg/lane, 8 cm length gel, 1X TAE, 7 V/cm, 45 min
bp ng/20 µl ng/15 µl ng/10 µl ng/5 µl
10000 200 150 100 50
8000 160 120 80 40
6000 120 90 60 30
5000 100 75 50 25
4000 80 60 40 20
3000 60 45 30 15
2500 52 39 26 13
2000 40 30 20 10
1500 32 24 16 8
1% TopVision™ LE GQ Agarose (#R0491)
10 µl/lane, 8 cm length gel, 1X TAE, 7 V/cm, 45 min
bp ng/0.5 µg %
700 30.0 6.0
500 32.5 6.5
400 35.0 7.0
300 90.0 18.0
200 35.0 7.0
150 35.0 7.0
100 90.0 18.0
75 37.5 7.5
50 40.0 8.0
25 75.0 15.0
3% TopVision™ LE GQ Agarose (#R0491)
0.5 µg/lane, 8 cm length gel, 1X TBE, 5 V/cm, 1 h

Fig. 14. DNA markers

Settings for electrophoresis:

	50 ml gel	100 ml gel
Voltage	80 V	100 V
time	> 45 min	> 60 min

2.2.1.11. DNA precipitation

According to the volume of the solution a tenth part 3M NaOAc was added and mixed. After the addition of 0,8 volumes of isopropanol for precipitation of the DNA the solution was incubated at room temperature for 5 minutes. Solutions were centrifuged for 15 minutes at 0°C full speed and supernatant removed by vacuum aspiration. DNA pellets were washed with 70% EtOH and centrifuged again for 5 minutes. The supernatant was removed and the pellets were dried at room temperature for approximately 15 minutes. Then the pellets were resuspended in sterile ddH$_2$O or TE buffer respectively.

2.2.1.12. DNA purification

Two different kits were used to purify DNA of PCR mixtures or from gel bands. If the samples were prepared for following sequencing, DNA was purified with the Cleanmix kit (Talent TA 050 CLN). In all other cases illustra^{TM} GFX PCR DNA and Gel Band Purification kit (GE Healthcare) was used. Both kits use the system of binding the DNA to a column.

DNA was purified according to the manufacturer's protocol.

2.2.1.13. Sequence analysis

Relevant regions of newly constructed strains or plasmids and a selection of revertants were sequenced for verification. In all cases a purified PCR product was sent to VBC Genomics to perform sequencing.

2.2.2. Microbiological Methods

2.2.2.1. Cultivation of yeast strains

Inoculation occurred from a fresh single colony in 4 ml YPD in a plastic 15 ml round-bottom tube. An o/n-culture was shaken for approximately 16 hours at 30°C and 250 rpm. Alternatively, in some cases cultivation occurred in Erlenmeyer glass flasks (100-500 ml flask) in a water bath shaker.

2.2.2.2. Cultivation of *E. coli*

Cultivation of bacteria occurred at 37°C in LB medium. If the strain possesses an antibiotic resistance, for instance against ampicillin, then the required concentration was added to the medium (see media). For o/n-cultures one single colony was usually inoculated in 4 ml LB in a plastic tube or in 100 ml in a glass flask and shaken at 180 rpm.

2.2.2.3. Marker test

In order to verify the characteristics of each yeast strain, the strain of interest was tested for its specific marker genes by replica plating to various selective plates, for instance, YPG, SC-lys, SC-trp, SC-ade, SC-ura, SC-his, FOA, SC-Lactate. In order to determine the mating type the cells were replica plated to 2% plates pre-oculated with a or α mating type tester strains.

2.2.2.4. Adaptive mutation assay

The day before the start of the adaptive mutation assay, prepare 60 SC-Lactate plates (equally heavy +/- 5% to offer same amount of nutrients on each plate). Per subculture 4 plates are needed.

1) Inoculate 16 isolated colonies of same size in 4 ml YPD each (cultures 1-16) with the exception of colonies of the strain YPFA (inoculation in 1 ml YPD)
2) Incubate o/n shaking at 30°C
3) Determine cell count of o/n-cultures 1-4 with microscope (arithmetical mean corresponds to cell density of all 16 cultures)
4) Transfer cultures from inoculation tubes to centrifugation tubes
5) Harvest cells by centrifugation at 3500 rpm for 5 min
6) Discard supernatant
7) Wash each cell pellet with 4 ml sterile ddH_2O --> vortex
8) Centrifuge with same settings and discard supernatant
9) Resuspend cell pellet of first culture with 600 µl sterile ddH_2O by drawing pellet up and down in a 1 ml glass pipet
10) Draw suspension into same pipet (exactly 600 µl) and transfer 4 x 150 µl to four SC-Lactate plates (about 1 x 10^8 cells/plate or in case of strain YPFA 2.5 x 10^7 cells /plate)
11) Use one drigalski spatula to streak cells on all four plates (plate 2, 3 and 4 are supposed to have the smallest variation in cell count)
12) Repeat steps 8-10 for subcultures 2-15
13) Discard subculture 16 (backup) if not needed
14) Incubate plates at 30°C and check for colony formation starting with day 3 (day of plating = day 0) until day 24
15) Determine mutation rate and mutation frequencies

Determination of survival and residual proliferation:
Use plates from subpopulation 14 and 15
Day 0:
1) Rinse plates 14/2 and 15/2 with a total of 4 ml sterile ddH_2O
    - Pipet 2 ml sterile ddH_2O on plate and mobilize cells with a drigalski spatula

- Remove cells and transfer into tube
- Add 1 ml sterile ddH_2O to plate, disperse and collect in tube
- Repeat last step to remove all cells from plate

2) Measure the volume of the collected rinsed cells in a 5 ml glass pipet (important for the determination of residual proliferation)
3) Prepare 1:10 dilutions and determine cell count and CFU with microscope
4) Plate 3 YPD survival plates with 100 CFU
5) Calculate the total cells/plate by multiplying determined cell/ml (microscope) with the measured volume of rinsed cells (will be needed for the determination of residual proliferation, mutation rate and mutation frequency)

Day 1:
1) Repeat procedure of day 0 with plates 14/3 and 15/3
2) Compare calculated cells/plate from day 0 and day 1 for residual proliferation

Day 2-10 and 13-17 and 20-24:
Plates can not be rinsed anymore for the determination of residual proliferation because colonies might start to form on plates. Therefore from day 2 on, only the survival rate will be determined.
1) Punch out two plugs in agar of plates 14/1 and 15/1 (alternatively, 14/4 and 15/4 can be used)
2) Remove all four plugs and pool in a 2 ml eppendorf tube in 1 ml sterile ddH_2O
3) Rinse cells from plugs by vortexing vigorously
4) Prepare 1:10 dilutions and determine CFU/ml with microscope
5) Plate 3 YPD survival plates with appropriate CFU number (the survival will decrease throughout the experiment → increase plated CFU in order to obtain app. 100 colonies/plate)

2.2.2.5. Reconstruction Assay

The reconstruction assay is an experiment to test revertants derived from adaptive mutation assays. Generally, in the setup the conditions of the adaptive mutation assay are simulated to confirm that late-arising revertant colonies are the consequence of spontaneous reversion events occurring in the population of arrested cells, subsequently to plating.
Every revertant should grow into a colony until day 4 if plated on fresh plates, no matter on what day it appeared on the plates of the adaptive mutation assay. If this is the case, then it

can be excluded that late-arising colonies are simply a result of very slowly growing pre-plating revertants carried over from preculture.

To simulate the setup of the mutation assay, cells that cannot grow or revert on SC-Lactate but, nevertheless, compete for nutrients are required. Consequently, the fbp1-k.o. strain YΔF1 was used and plated as a non-reverting background to SC-Lactate plates in the same concentration as in the mutation assay (1 x 10^8 cells or 2.5 x 10^7 when YPFA revertants were characterized). The fbp1-negative cells are seeded with 40 cells per plate of fbp1-positive revertants. YΔF1 cells will arrest in the cell cycle and constitute competition in nutrients for the 40 fbp1-positive cells, that will be able to form colonies.

Reconstruction assays were also performed in a slightly different setup, where it was not the aim to characterize revertants. In one case the newly constructed fbp1-k.o. strain was tested for its effects on fbp1 wt cells. In another setup, a newly constructed strain with a fusion of *hTP53* to *FBP1* was tested for the fbp1 enzyme function in a background of fbp1-negative cells.

3. Results

3.1. *PCK1* deletion

The aim was to develop a glucose-limited system to study mutation frequencies in stationary yeast cells. A so far well established system to study adaptive mutations is based on lysin starvation (Heidenreich and Wintersberger, 1998, 2001). However, starvation for a single amino acid does not reflect natural circumstances. Moreover, the lysine starvation setup still offers glucose in the selection media. This is thought to be one major disadvantage to the system, since glucose represents a growth signal for cells (Granot and Snyder, 1991), which should be avoided when studying adaptive mutations in stationary yeast cells. Therefore, a glucose-limited system should be established, where glucose is merely offered in the inoculation phase but is not present at times of selection.

The idea was to block the gluconeogenesis pathway and consequently obtain a more relevant cell cycle arrest. The hypothesis that a blocked gluconeogenesis results in a cell cycle arrest had to be analyzed first. Therefore, the phosphoenolpyruvate carboxy kinase gene (*PCK1*), which is involved in gluconeogenesis, was disrupted and its effects observed.

3.1.1. Construction of deletion strain YΔPCK1

The gene *PCK1* is responsible for the expression of the enzyme phosphoenolpyruvate carboxy kinase, which converts oxalacetate to phosphoenol pyruvate. This step is involved in gluconeogenesis and is one of the irreversible steps. Therefore the *PCK1* gene was selected as target gene to block gluconeogenesis.

The deletion strain was constructed by replacing the majority of the *PCK1* sequence with the marker gene *URA3* from *Kluyveromyces lactis*. The ORF of *URA3* with its promoter and terminator was PCR-amplified from pUG72. The megaprimer sequence consists of the complementary sequence of the plasmid (Universal primers) and tails for homologous recombination complementary to the genome sequence of *PCK1* as shown in Fig. 16.

The amplification with the primers MPpck1for and MPpck1rev resulted in a fragment of 1709 bp. The PCR product was loaded on a 1% preparative agarose gel (Fig. 15).

step	Time [seconds]	Temperature °C
Initial denaturation	120	95
3 cycles of next 3 steps:		
Denaturation	*20*	*95*
Annealing	*60*	*53*
Extension	*60*	*72*
30 cycles of next 2 steps		
Denaturation	*20*	*95*
Extension	*80*	*72*
Final extension	480	72

50 µl reaction:
1 µl pUG72 1:10
5 µl 10x buffer
2 µl dNTPs
3 µl MPpck1for
3 µl MPpck1rev
1 µl $MgCl_2$
35 µl ddH_2O
0.25 µl Taq Polymerase (Qiagen)

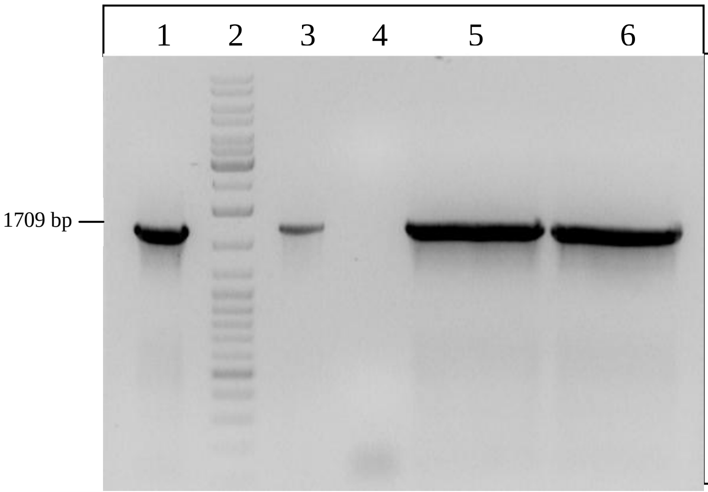

1 → 5 µl PCR product
2 → O'Gene Ruler DNA Ladder Mix (5 µl)
3 → 1 µl PCR product
4 → negative control (5 µl)
5 → 10 µl PCR product
6 → 10 µl PCR product

Fig. 15. Preparative agarose gel with PCR products of *URA3* amplification

The two gel bands from slot 5 and 6 were cut with a scalpel and transferred into two tubes. DNA was purified from the gel slices with the GFX column purification kit from illustra^{TM}. DNA was eluted in a total of 40 µl ddH_2O. 30 µl of the purified DNA were used for a transformation of the yeast strain YLBM. One transformation was performed with ddH_2O instead of DNA and served as negative control. Transformed cells were plated on SC-ura plates with a gradient from 10 µl to 200 µl. Homologous recombination occurred due to the homologous sequences in the genomic DNA of the host strain YLBM and the offered transformed DNA.

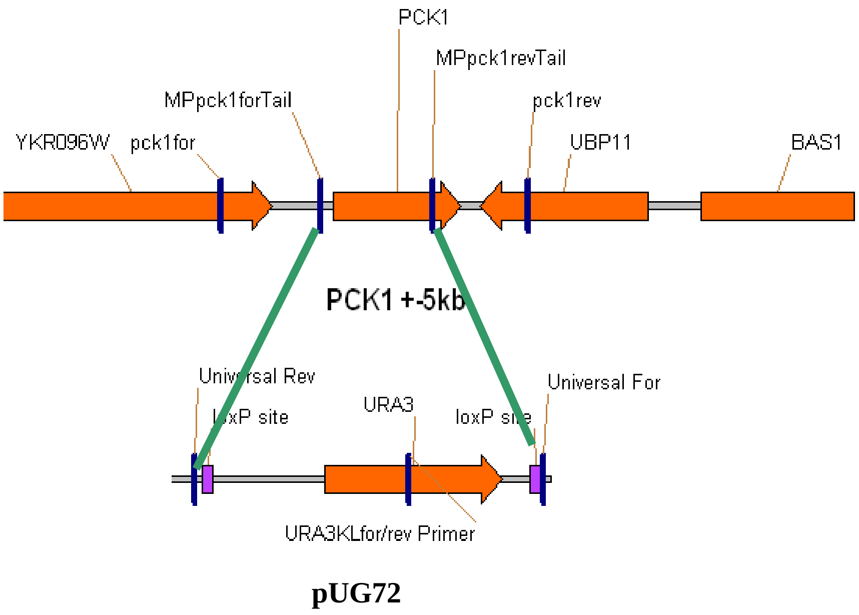
PCK1
MPpck1revTail
MPpck1forTail
pck1rev
YKR096W
pck1for
UBP11
BAS1
PCK1 +-5kb
Universal Rev
loxP site
URA3
loxP site
Universal For
URA3KLfor/rev Primer
pUG72

Fig. 16. Scheme of construction of *PCK1* disruption. Green bold lines indicate area of homologous recombination.

Due to the excision of *PCK1* and the insertion of part of the plasmid sequence with the *URA3* marker a new genomic situation developed as illustrated in Fig. 17. Colonies from the transformation were picked, isolated on fresh SC-ura plates and verified with PCR and marker tests.

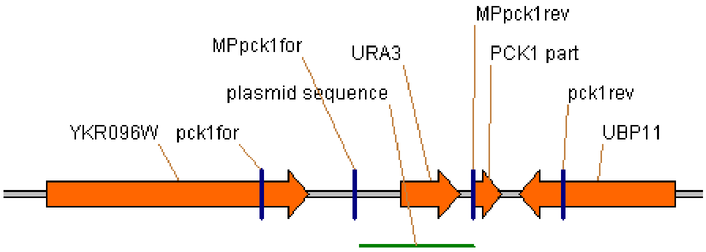
MPpck1rev
MPpck1for
URA3
PCK1 part
plasmid sequence
pck1rev
YKR096W
pck1for
UBP11

Fig. 17. Genomic situation of disruption strain YΔPCK1

In the control PCR two primers (pck1for and pck1rev), which are situated outside the *PCK1* gene were used to verify the difference in fragment length compared to the wild type YLBM. Four transformation clones were chosen to preparate their DNA to be able to verify the sequence with PCR. As a control the same PCR was performed with the host strain YLBM as well as S288C, which should obtain the same length as YLBM.

step	Time [seconds]	Temperature °C
Initial denaturation	300	95
30 cycles of next 3 steps:		
Denaturation	*30*	*95*
Annealing	*30*	*58*
Extension	*180*	*72*
Final extension	300	72

25 µl reaction:
1 µl DNA
2.5 µl 10x buffer
0.5 µl dNTPs
1.5 µl pck1for
1.5 µl pck1rev
18 µl ddH_2O
0.15 µl Taq Polymerase (Qiagen)

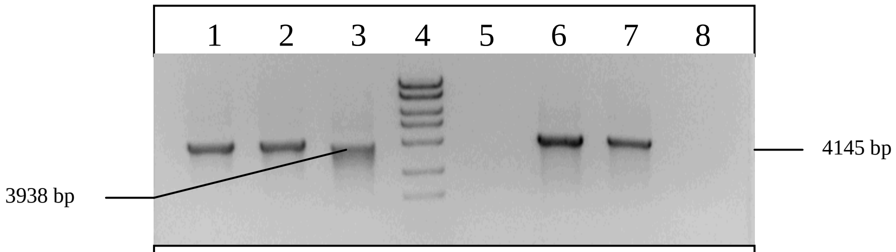

1 → clone 1 (5 µl PCR product)
2 → clone 2 (5 µl PCR product)
3 → YLBM (5 µl PCR product)
4 → O'Gene Ruler High Range (5 µl)
5 → S288c (5 µl PCR product)
6 → clone 3 (5 µl PCR product)
7 → clone 4 (5 µl PCR product)
8 → negative control (5 µl)

Fig. 18. Control PCR with external primers in regard to *URA3*

Positive clones should result in a fragment length of 4145 bp and the controls YLBM and S288C in 3938 bp. For the wt S288C the PCR did not work, consequently no PCR product occurred. However, YLBM showed a PCR product and therefore could be compared to positive clones in their difference in length (Fig. 18). The fragments of all 4 clones are slightly longer compared to the wt, indicating that the gene disruption was successful.

Furthermore, two additional PCRs were performed with the combination of a primer with its complementary sequence internal of the inserted *URA3* sequence and one primer downstream or upstream of *PCK1*. If *URA3* was integrated, the combination of the primers pck1for and ura3Klrev resulted in a fragment of 2318 bp and the combination of pck1rev and ura3KLfor in 1851 bp. The reaction mix was the same as for the first control PCR with external primers. The only alteration was the primer pair combination. PCR settings can be compared with the first PCR as well, with the exception of the extension time, which was reduced from 180 seconds to 82 seconds.

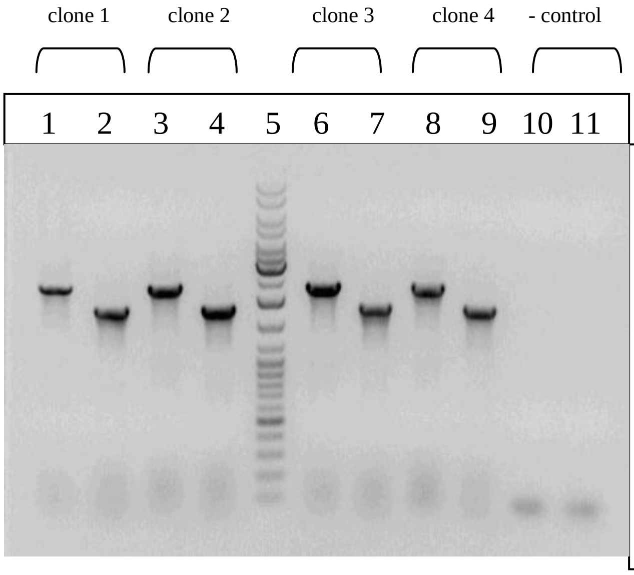

Primer combination pck1for + ura3Klrev:
Lane 1, 3, 6, 8, 10 (5 µl)
→ 2318 bp

Primer combination pck1rev+ura3Klfor:
Lane 2, 4, 7, 9, 11 (5 µl)
→ 1851 bp

5 → O'Gene Ruler DNA Ladder mix (5 µl)

Fig. 19. Two control PCRs with a combination of an internal and external primer of *URA3*.

As evident from Fig. 19 all four clones have been transformed correctly. Clone 2 has been chosen as the future strain YΔPCK1.

Furthermore, the various markers were verified with replica plating, confirming the following genotype:

YΔPCK1: MATa *trp1-Δ his3-Δ200 ura3-52 lys2ΔBgl ade2-1o gal mal CUP*^{r} *pck1::URA3(K.l.)*

The *PCK1* deletion strain was constructed successfully and could be used for further experiments.

3.1.2. Cell cycle arrest and survival on different carbon sources

To determine cell cycle arrest, a glucose-limited starvation assay was developed.

The assay was performed for the strains YΔPCK1 as well as YLBM as a control strain. One fresh single colony of the strain was inoculated in 200 ml YPD (1 l glass flask) and incubated o/n at 30°C shaking. The next morning, cells were counted and harvested at 3500 rpm for 5 minutes. The cell pellet was washed with a total of 180 ml sterile ddH_2O (split in 6 Falcon tubes). Afterwards, the cells were resuspended in 10 ml sterile ddH_2O and the cell count was determined again. Volume was adjusted in order to obtain a concentration of $1x10^8$ cells/150 µl. The experiment was performed on different carbon sources:

SC-Lactate (3%)
SC-Pyruvate (2%)
SC-Lactate/Pyruvate (3%/2%)

18 equally heavy plates of each carbon source were plated with one drigalsky spatula. 150 µl per plate, representing $1x10^8$ cells were streaked per plate for the deletion strain. For the control strain YLBM the number of plates was reduced to 9 SC-lys plates as a reference. On days 0, 1, 2, 3, 4, 6, 8 and 10, two plates per carbon source were rinsed. Cells were resuspended in a total of 4 ml sterile ddH_2O and transferred from each plate to a new tube. From the control strain YLBM only one plate was rinsed for each point of time. The volumes were measured in a 1 ml glass pipet. Cell count and CFU were determined with a microscope. By multiplying the cell count with the volume of rinsed cells from the plate, cells per plate were calculated. Since each plate should hold the same amount of cells, residual proliferation was determined over a time course of 10 days.

For information about the viability of the cells 3 YPD plates per cell suspension were plated at the indicated point of times, starting with 100 CFU. CFU amount was increased gradually at later days.

Obtained results for residual proliferation are presented in Fig. 20. The control cells on SC-lys doubled from day 0 to day 1 in their cell count, meaning that residual proliferation is present in lysine starvation. On the contrary, *pck1*-deficient cells exposed to glucose-limited starvation, showed no residual proliferation. The number of cells per plate stayed constant within a range of +/- 10%, which resulted from plating efficiency. The different carbon sources showed comparable results in residual proliferation. YΔPCK1-cells entered the cell cycle arrest strictly when starved on SC-Lactate, SC-Pyruvate or a combination of both non-sugars, respectively. Therefore, no preference for one of the nutrients was given as all three showed the desired effect. The result suggests that a block in gluconeogenesis leads cells to a relevant cell cycle arrest.

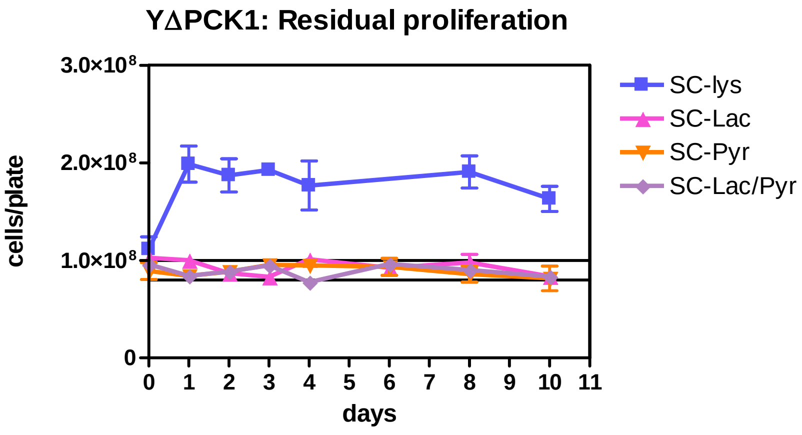

Fig. 20. Residual proliferation of YΔPCK1. Blue line shows the reference strain YLBM on SC-lysine. Other lines represent YΔPCK1-cells on different carbon sources.

The determined survival curves for arrested cells are shown in Fig. 21. The lysine-starved control cells of YLBM showed a higher viability throughout the experiment. *Pck1*-deficient cells derived from SC-Lactate, SC-Pyruvate and a mixture of both carbon sources showed poor survival compared to the control. Their viability was decreased to approximately 20% within three days of starvation.

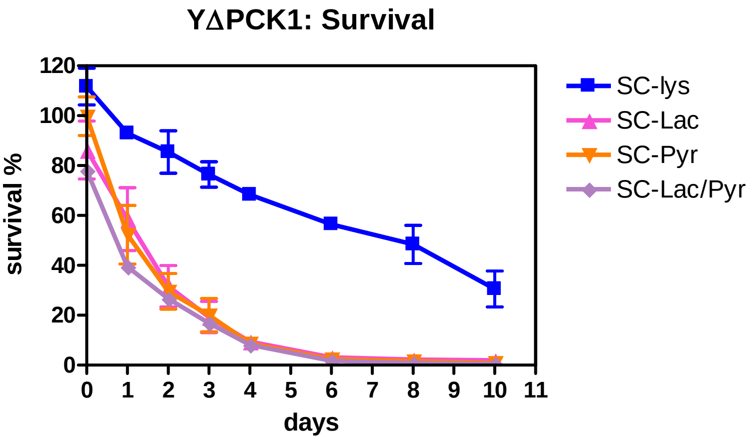

Fig. 21. Survival curves of glucose-limited starved YΔPCK1- cells. The blue line indicates the control YLBM as a control on SC-lysine.

Whereas results of residual proliferation with the *PCK1* disrupted strain showed the desired effect, the viability of arrested cells was not satisfactory enough to continue further experiments with this strain.

3.2. *FBP1* deletion

Since the first target gene *PCK1* did not show comparable survival curves to cells starved with lysine, the second target gene *FBP1* in gluconeogenesis was deleted. *FBP1* regulates the step in gluconeogenesis where fructose-1,6-bisphosphate is dephosphorylated to fructose 6- phosphate. This step poses an irreversible one in gluconeogenesis and therefore does not occur in glycolysis. Consequently, *FBP1* is a suitable target gene to introduce a block in gluconeogenesis.

3.2.1. Construction of the deletion strain YΔF1

The gene *FBP1* was disrupted with the *kanMX* marker gene in the wt strain YLBM. The ORF of *kanMX* as well as its promoter and terminator are situated on the plasmid pUG6. Two megaprimers (MPfbp1for and MPfbp1rev) were constructed, which contain the sequence of the "Universal Primer" forward or reverse. This part of the primer enabled the amplification of the gene *kanMX* in a PCR (Gueldener et al., 2002). The primer was arranged with tails of the complementary sequence of the genomic *FBP1* region, indicating where the foreign DNA should be integrated via homologous recombination. The combination of the Universal primers and the tail sequence was chosen in order to insert the *kanMX* in the opposite orientation of the *FBP1* gene.

The *kanMX* sequence was amplified with PCR with the following settings. Positions of primers are indicated in Fig. 22. Correct amplification results in PCR products of 1733 bp as shown in Fig. 24.

step	**Time [seconds]**	**Temperature °C**
Initial denaturation	120	95
3 cycles of next 3 steps:		
Denaturation	*20*	*95*
Annealing	*60*	*53*
Extension	*60*	*72*
30 cycles of next 2 steps		
Denaturation	*20*	*95*
Extension	*80*	*72*
Final extension	480	72

50 µl reaction:
1 µl pUG6 1:10
5 µl 10x buffer
2 µl dNTPs
3 µl MPfbp1for
3 µl MPfbp1rev
1 µl $MgCl_2$
35 µl ddH_2O
0.25 µl Taq Polymerase (Qiagen)

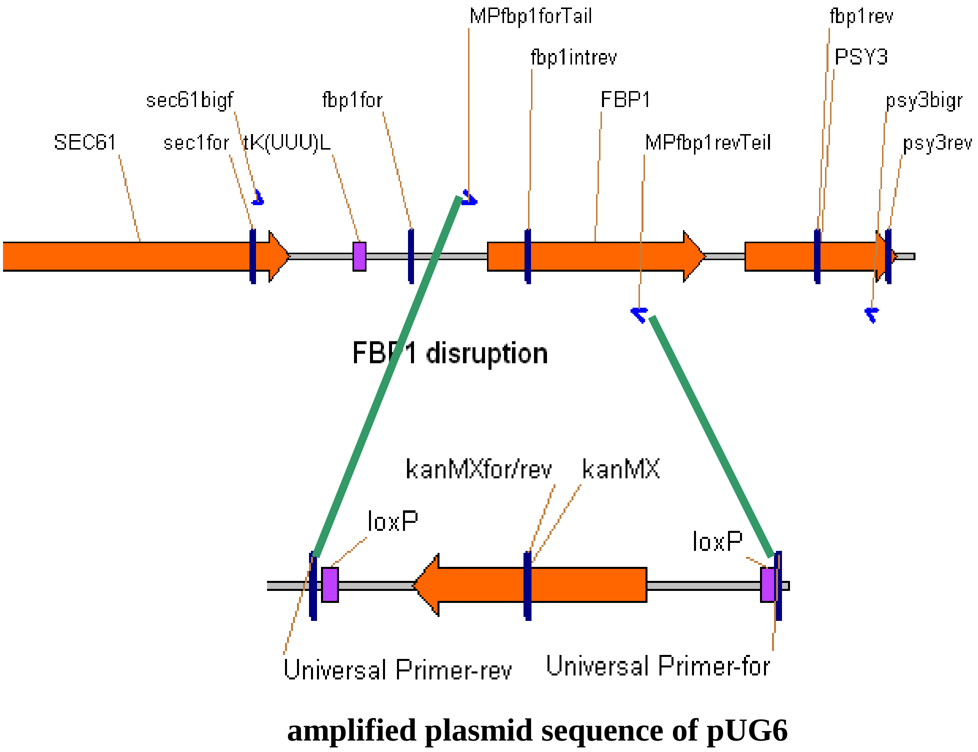
MPfbp1forTail
fbp1rev
fbp1intrev
PSY3
sec61bigf
fbp1for
FBP1
psy3bigr
SEC61
sec1for
tK(UUU)L
MPfbp1revTeil
psy3rev
FBP1 disruption
kanMXfor/rev
kanMX
loxP
loxP
Universal Primer-rev
Universal Primer-for
amplified plasmid sequence of pUG6

Fig. 22. Disruption scheme of *FBP1* with the marker gene *kanMX*. Green bold lines indicate homologous recombination.

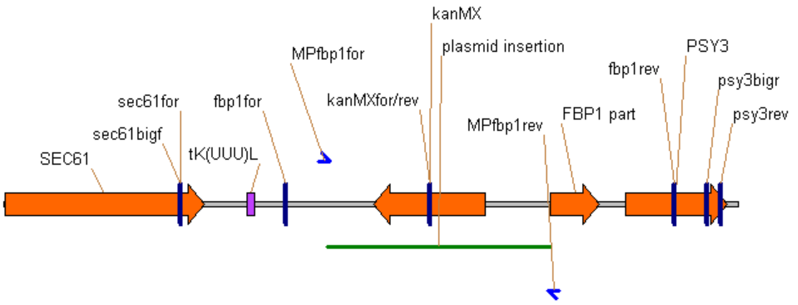
kanMX
plasmid insertion
PSY3
MPfbp1for
fbp1rev
psy3bigr
sec61for
fbp1for
kanMXfor/rev
FBP1 part
psy3rev
MPfbp1rev
sec61bigf
tK(UUU)L
SEC61

Fig. 23. New genomic situation in disruption strain YΔF1.

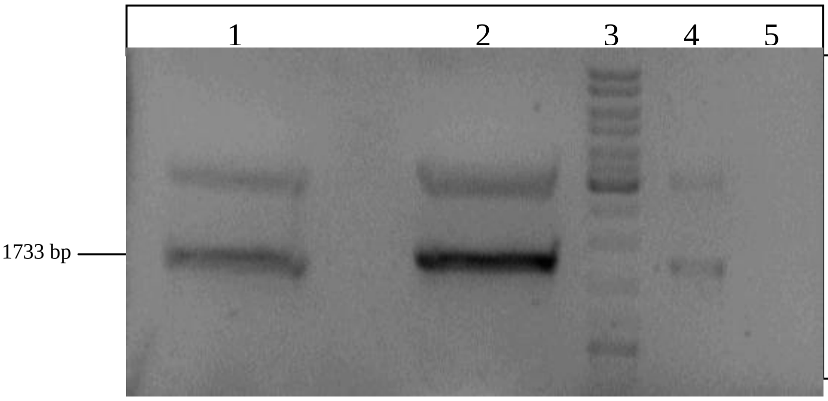
1
2
3
4
5
1733 bp

1 → 24 µl PCR product

2 → 24 µl PCR product

3 → O'Gene Ruler DNA Ladder Mix (5 µl)

4 → 2 µl PCR product

5 → negative control (5 µl)

Fig. 24. Preparative gel with PCR product of *kanMX* amplification from pUG6.

The product was purified with the illustra^{TM} GFX column kit and approximately 700 ng DNA were transformed into the strain YLBM. Due to the marker gene kanMX, selection occurred on G-418 agar plates. Transformation clones were tested with a control PCR to verify the different length due to the altered genomic situation (Fig. 23). The first PCR was performed with the two primers psy3rev and sec61for situated upstream and downstream of *FBP1*, respectively. Positive clones were slightly longer than the amplified product of the positive control, which corresponds to the same length as the host strain YLBM. Since the amplification of the *FBP1* sequence and its surroundings made difficulties, the PCR had to be optimized in order to obtain PCR products. Different polymerases were tried until a PCR product could be yielded with the proof-reading Phusion polymerase (Finnzymes). In this case, annealing temperatures were calculated with the Finnzyme's TM calculator, resulting in temperatures over 72°C. Therefore, the annealing step could be eliminated and a 2-step program was used. For correct clones, where a gene replacement of *FBP1* to *kanMX* took place, a fragment of 3921 bp was expected as shown in Fig. 25, whereas the wt yielded a fragment of 3064 bp.

step	**Time [seconds]**	**Temperature °C**
Initial denaturation	30	98
30 cycles of next 2 steps:		
Denaturation	*10*	*98*
Annealing + Extension	*104*	*72*
Final extension	300	72

20 µl reaction:
1 µl DNA
4 µl 5x buffer
0.4 µl dNTPs
1 µl sec61for
1 µl psy3rev
12.6 µl ddH$_2$O
0.2 µl Phusion Polymerase

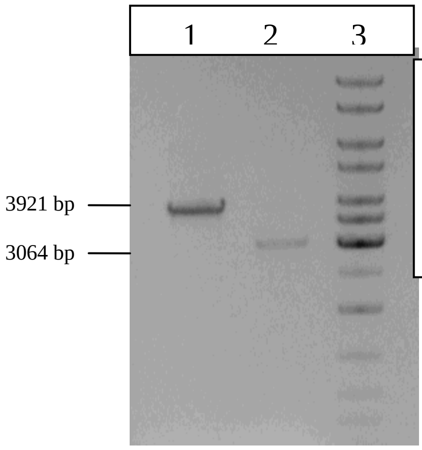

1 → clone 3 (5 µl)
2 → control S288c (5 µl)
3 → O'Gene Ruler DNA Ladder Mix (5 µl)

Fig. 25. Gel of control PCR of *FBP1* disrupted candidate with two external primers sec61for and psy3rev.

Moreover, two PCRs were performed with an internal primer of the gene *kanMX* combined with an external one, which has already been used in the first control PCR. Primer pair combinations were kanMXfor and sec61for as well as kanMXrev and fbp1rev. Furthermore, a third combination with kanMXfor and fbp1for was tested since the PCR did not seem to be equally efficient for all primer pairs. Since clone 3 was the only clone where the PCR worked to some extent, control PCRs were performed only with this clone. Some optimizations in the program of the PCR and the reaction mix were applied to result in successful control PCRs.

step	Time [seconds]	Temperature °C
Initial denaturation	180	95
30 cycles of next 3 steps:		
Denaturation	*30*	*95*
Annealing	*30*	*59*
Extension	*61*	*72*
Final extension	300	72

25 µl reaction:
1 µl DNA
2.5 µl 10x buffer
0.5 µl dNTPs
1.5 µl fbp1rev *
1.5 µl kanMXrev *
18 µl ddH_2O
0.15 µl Taq Polymerase (Qiagen)

* Same conditions were used for the two other primer pairs fbp1for + kanMXfor and sec61for + kanMXfor.

Results of PCR are shown in Fig. 26. For correct clones following fragments were produced.

fbp1rev + kanMXrev	1789 bp
sec61for + kanMXfor	1818 bp
fbp1for + kanMXfor	1060 bp

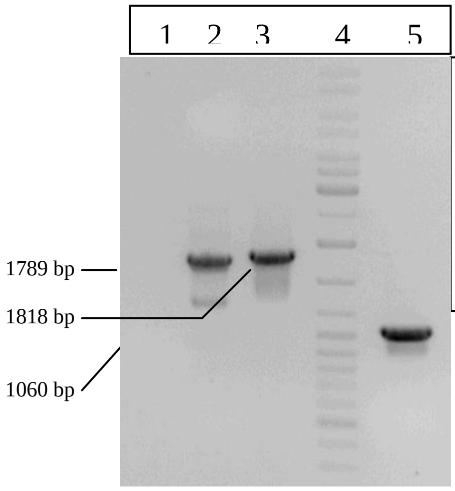

1 → negative control (5 µl)
2 → primer fbp1rev + kanMXrev (5 µl)
3 → primer sec61for + kanMXfor (5 µl)
4 → O'Gene Ruler DNA Ladder Mix (5 µl)
5 → primer fbp1for + kanMXfor (5 µl)

Fig. 26. Gel of control PCR products with combination of internal primers with external ones.

Clone 3 was successfully verified with four control PCRs for the replacement of *FBP1* with *kanMX*. Additionally, the new strain was tested for its markers by replica plating as described in Materials and Methods (2.2.2.3.) and following genotype was confirmed:

YΔF1: MATa *trp1-Δ his3-Δ200 ura3-52 lys2ΔBgl ade2-1o gal mal CUP*^{r} *fbp1::kanMX*

3.2.2. Cell cycle arrest and survival on different carbon sources

To study the stringency of cell cycle arrest in the fbp1-deficient strain YΔF1 the effect of the block in gluconeogenesis was analyzed in a glucose-limited starvation assay. The details of the starvation assay were described previously in chapter 3.1.2. The experiment was performed with the strain YLBM as a control for lysine starvation. Additionally to the carbon sources SC-Lactate (3%) and SC-Pyruvate (2%), SC-Glycerol (2%) was used as well. This nutrient source was not used for YΔPCK1 since a *pck1*-deficient strain cannot utilize glycerol.

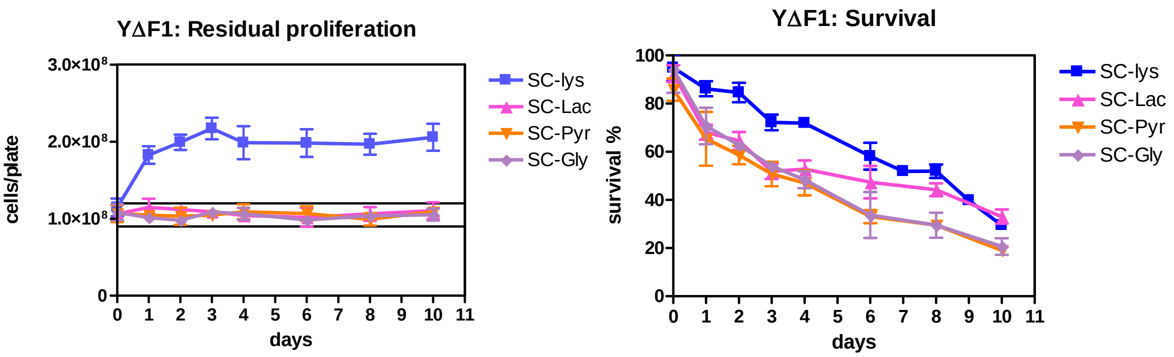

Fig. 27. Residual proliferation and survival curves of *fbp1*-deficient cells. Blue line represents the control YLBM starved on SC-lysine.

The control cells of YLBM with lysine starvation showed residual proliferation evident by a doubling of the cell number from day 0 to day 1. Fbp1-deficient cells that entered the cell cycle arrest due to the block in gluconeogenesis did not show any residual proliferation as evident from Fig. 27 (left). Consequently, cells entered a strict cell cycle arrest from the beginning of glucose-limited starvation. The three types of non-fermentable carbon sources SC-Lactate, SC-Pyruvate and SC-Glycerol showed no significant differences in the effect of arrest. Cells stayed reasonably viable as shown in Fig. 27 (right). The survival of cells on SC-Pyruvate and SC-Glycerol revealed very similar curves. The viability on SC-Lactate was equal to SC-Pyruvate and SC-Glycerol within the first three days. However, after day 4 the survival rate stays slightly higher compared to the two other nutrient sources. Thus, SC-Lactate was considered more favorable as a constant alternative carbon source. Compared to the viability of arrested cells of the *PCK1* knock-out strain where a viability loss of 80% took place, *fbp1* disrupted cells only lost approximately 50% viability during three days of glucose limitation.

3.2.3. YΔF1 in a Reconstruction Assay

A reconstruction assay with the *fbp1*-deficient strain was performed for various reasons. First, it should provide information about the point of time when colonies appear under competitive conditions. The background layer of non-replicating cells can affect the growth of replicating cells due to the competition for nutrients.

Second, the reconstruction assay was performed on SC-Lactate, SC-Pyruvate and SC-Glycerol to be able to determine the carbon source with optimal growth.

Third, the day when to draw a line between replication-dependent revertants and adaptive revertants can be estimated. This information will be important when adaptive mutation assays are performed with frameshift strains.

The experiment was performed with YΔF1 as background strain seeded with YLBM, which is able to grow colonies on the tested carbon sources due to its intact *FBP1*. In Fig. 28 results of the reconstruction assays for the three non-sugars are presented.

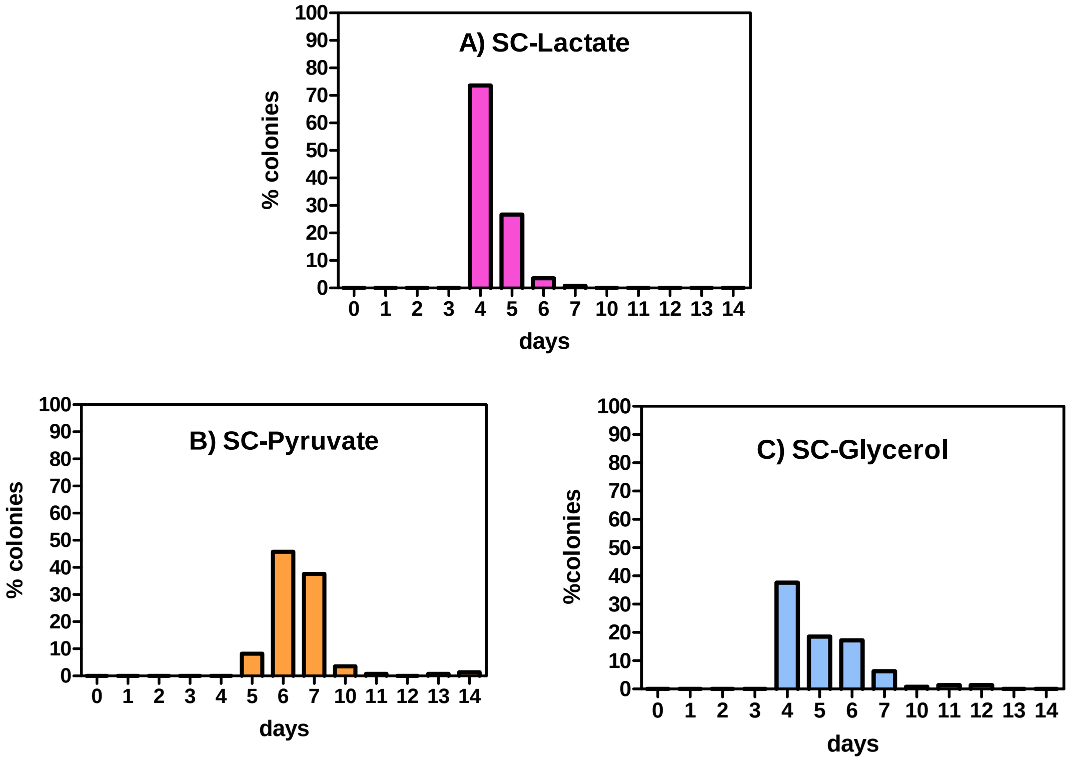

Fig. 28. Reconstruction assay of YΔF1 on different carbon sources

Colonies appeared on day four when plated to SC-Lactate or SC-Glycerol (Fig. 28 A and C). On the contrary, on SC-Pyruvate colony formation was delayed one day and starts on day 5 (Fig. 28 B). A peak was reached on day four in cases of lactate and glycerol. For SC-Pyruvate the delay of one day was observed again. Moreover, colony formation on SC-Pyruvate showed a peak distributed to day 6 and 7. The sharpest peak was achieved with SC-Lactate as a carbon source. Furthermore, SC-Lactate also had the most homogenous colony appearance since almost 80% appeared on day 4. These reasons made SC-Lactate the most favorable carbon source for further experiments.

If SC-Lactate is considered the media of choice a prediction can be made for adaptive mutation assays which day should be chosen to draw the line between replication-dependent reversions and adaptive reversions. According to the results, day 6 would be set to 0 assuming that after this point of time only adaptive revertants will appear.

3.3. *FBP1* +1 Frameshift

After confirming that a non-functional *FBP1* gene results in a blocked gluconeogenesis and cells enter a strict cell cycle arrest, a strain with a revertible mutation was constructed to be able to study mutation frequencies.

In summary, I tried three approaches for the construction of the strain. All three strategies (one-step gene replacement, modified one-step gene replacement and two-step gene replacement) are described below. The approach with a two step gene replacement was the one to be successful first. Before the frameshift strain could be constructed, a precursor strain had to be constructed first and the frameshift strategy designed.

3.3.1. Construction of URA$^+$ precursor strain YUF

The precursor strain was constructed in order to use it as new host strain for various following frameshift strain constructions. The essential part was to insert the marker gene *URA3* with its promoter and terminator between the start codon of *FBP1* and its promoter to create a URA$^+$ strain. Afterwards, the *URA3* gene can be replaced in further constructions, which are based on a negative selection for *URA3*.

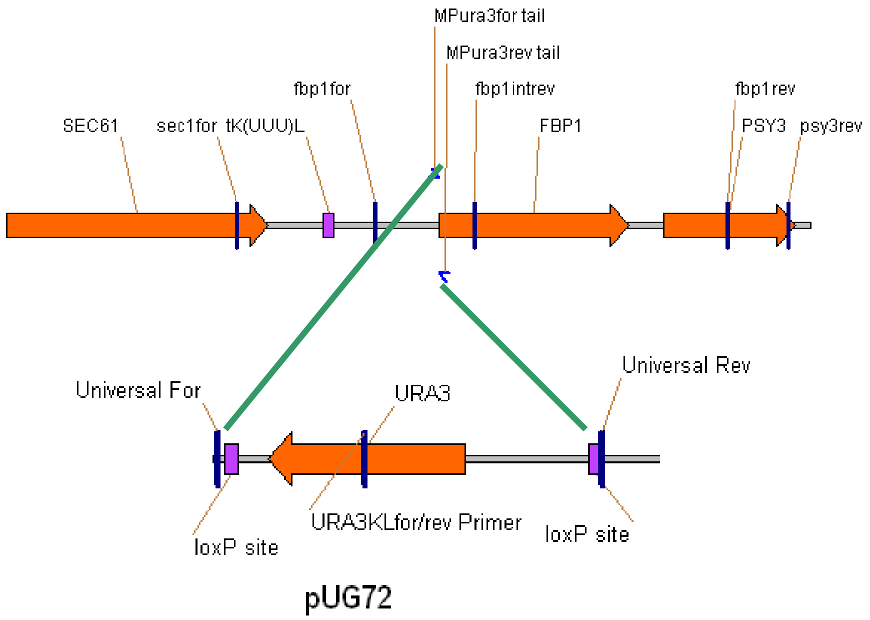
MPura3for tail
MPura3rev tail
fbp1for
fbp1intrev
fbp1rev
SEC61
sec1for
tK(UUU)L
FBP1
PSY3
psy3rev
Universal For
URA3
Universal Rev
URA3KLfor/rev Primer
loxP site
loxP site
pUG72

Fig. 29. Construction of YUF

The marker gene *URA3* was amplified from pUG72 (Fig. 29) with the same conditions as for the construction of YΔPCK1 (see chapter 3.1.1.). DNA was transformed into the host strain YLBM, transformants selected on SC-ura plates and verified by PCR with the primers fbp1intrev, fbp1for, ura3KLfor and ura3KLrev respectively. Locations of primers are indicated in Fig. 30.

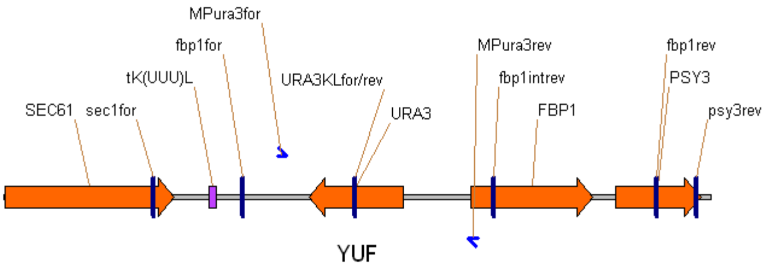
MPura3for
fbp1for
tK(UUU)L
SEC61
sec1for
URA3KLfor/rev
URA3
MPura3rev
fbp1intrev
FBP1
fbp1rev
PSY3
psy3rev
YUF

Fig. 30. New genomic situation in strain YUF

The first PCR to verify the difference in length due to the insertion of *URA3* was performed with the two external primers fbp1for and fbp1intrev. Correct clones obtained PCR products of 2170 bp, whereas the control stain, missing the *URA3* insertion produced a fragment of only 578 bp as shown in Fig. 31.

step	**Time [seconds]**	**Temperature °C**
Initial denaturation	300	95
30 cycles of next 3 steps:		
Denaturation	*30*	*95*
Annealing	*30*	*56*
Extension	*65*	*72*
Final extension	300	72

25 µl reaction:
1 µl DNA
42.5 µl 10x buffer
1 µl dNTPs
1.5 µl fbp1for
1.5 µl fbp1intrev
0.5 µl $MgCl_2$
17 µl ddH_2O
0.15 µl Taq Polymerase

The two control PCRs with the combination of an internal primer and an external primer required following alterations of the settings. Expected fragment lengths, when *URA3* was inserted, are indicated in the table as well. Furthermore the reaction mix was prepared with and without increased $MgCl_2$ concentration. PCR products were yielded only with higher concentrations of $MgCl_2$.

Primer pair	Annealing temperature	Extension	PCR product
fbp1for + URA3Klfor	58°C	45 s	986 bp
fbp1intrev + URA3Klrev	56°C	54 s	1208 bp

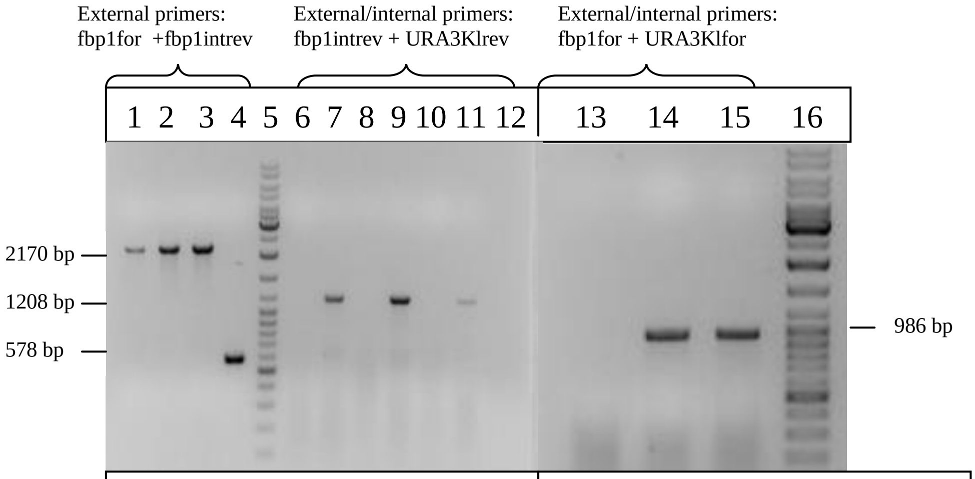
External primers:
fbp1for +fbp1intrev
External/internal primers:
fbp1intrev + URA3Klrev
External/internal primers:
fbp1for + URA3Klfor
1 2 3 4 5 6 7 8 9 10 11 12
13 14 15 16
2170 bp
1208 bp
578 bp
986 bp

1 → clone 2 (1 µl)
2 → clone 3 (1 µl)
3 → clone 3 (1µl)
4 → positive control YLBM (5 µl)
5/16 → O'Gene Ruler DNA Ladder Mix (5 µl)
6 → clone 2 (5 µl)
7 → clone 2 + extra $MgCl_2$ (5 µl)
8 → clone 3 (5 µl)

9 → clone 3 + extra $MgCl_2$ (5 µl)
10 → clone 4 (5 µl)
11 → clone 4 + extra $MgCl_2$ (5 µl)
12 → negative control (5 µl)

13 → negative control (5 µl)
14 → clone 3 (5 µl)
15 → clone 4 (5 µl)

Fig. 31. Control PCRs with external primers and combination of external and internal primers

All 3 clones showed the correct length, indicating that the *URA3* sequence was inserted into the genome. Clone 3 was selected to be the new strain YUF. Its markers were tested by replica plating, confirming following genotype:

YUF: MATa *trp1-Δ his3-Δ200 ura3-52 lys2ΔBgl ade2-1o gal mal CUP*^{r} *fbp1::URA3*

The URA$^+$ strain was used for various constructions when *URA3* should be replaced by another gene sequence. Selection is based on negative selection for *URA3* on 5-FOA plates, which is toxic for URA$^+$ strains.

3.3.2. Frameshift insertion strategy in *FBP1*

The aim was to introduce a +1 frameshift into the *FBP1* gene to allow a study of adaptive mutations in a glucose-limited system. The frameshift mutation will result in a non-functional *FBP1* since the reading frame will change to +1 and the triplets coding for amino acids are changed.

Since only the original reading frame codes for the correct protein sequence, the other two reading frames contain stop codons that truncate the protein sequence. Consequently, the insertion of a nucleotide to shift the reading frame will also shift the codons from this point on and will lead to an altered amino acid sequence. Sooner or later the frame will provide a stop codon, where the gene product will be truncated and as a consequence protein functionality will be lost.

As a result of the frameshift mutation, a reversion window, which is defined by two out-of-frame stop codons, is created. This window defines the region, where mutations possibly are able to reverse the frameshift mutation. A deletion of one nucleotide within this window compensates the frameshift insertion and leads back to the original coding frame. Consequently, the complete gene can be read and the translation into a functional protein sequence is possible. Generally, there are more situations which lead to the original reading frame. The +1 insertion can as well be compensated by a -1, -4, -7, (…) deletion or a +2, +5, +8, (…) insertion.

Following aspects had to be considered, when planning a +1 frameshift mutation for the *FBP1* gene:

a) Length of reversion window:

The two out of frame stop codons that define the reversion window should provide a sequence of at least 150 nt. The bigger the reversion window, the higher chances are for adaptive mutations to occur. Mononucleotide repeats within this window are hot spots for mutations to take place.

b) The position should not affect any active centers in the protein sequence: Due to the insertion of one nucleotide, the amino acid sequence will be changed within the reversion window. Since the functionality of the translated protein is essential, it should be avoided to place the reversion window in conserved sequences within the *FBP1* gene, so that active centers are not disturbed.

c) No other stop codons should be present within the window.

An additional manipulation (destruction of a stopcodon) might increase the length of the reversion window

The choice of the inserted nucleotide has to be considered well. According to the introduced nucleotide more variants for a new amino acid in the coding frame are possible. Of course no new stop codon may be created, due to the insertion. Another aspect is the creation of a new recognition site as a result of the insertion of the frameshift, which can be a benefit during strain construction.

Fig. 32 shows the concept of the frameshift insertion in the *FBP1* gene under all aspects described above. The underlined sequence represents the primer fbp1ins1, which introduces the frameshift mutation and additionally carries one mismatch.

The insertion of the frameshift mutation was chosen to occur after position 127 nt. A guanine was inserted between two thymines and the new codon results in the amino acid cystein.

At position 82 nt a mismatch is introduced with the primer to manipulate a stop codon. This allows a bigger reversion window. If the stop codon would not be manipulated, the reversion window would have a size of 109 nt. Due to the manipulation, the window can be elongated to 176 nt. Therefore, the codon TAA was changed to TAC. The cytosin was chosen based on the resulting amino acid leucine in the original frame, which is conserved in other organisms at this position. Furthermore, with the change from adenine to cytosine, a new enzyme recognition site for XhoI is created. This proposed an advantage for the strain construction, since clones could be tested for the new recognition site.

The *FBP1* gene shows conserved sequences starting 210 bp after the start codon of the ORF. The designed reversion window in *FBP1* ranges from 14 to 188 bp. Therefore, interference with conserved regions of the gene was avoided as good as possible.

A)

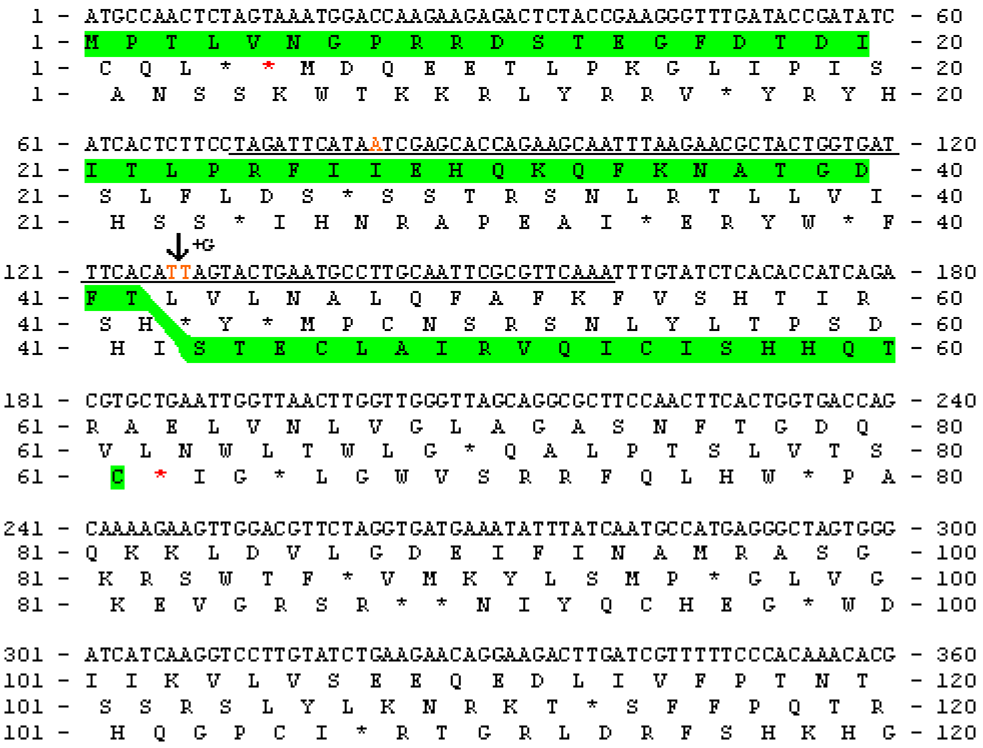

```
  1 - ATGCCAACTCTAGTAAATGGACCAAGAAGAGACTCTACCGAAGGGTTTGATACCGATATC - 60
  1 - M  P  T  L  V  N  G  P  R  R  D  S  T  E  G  F  D  T  D  I   - 20
  1 -  C  Q  L  *  *  M  D  Q  E  E  T  L  P  K  G  L  I  P  I  S  - 20
  1 -   A  N  S  S  K  W  T  K  K  R  L  Y  R  R  V  *  Y  R  Y  H - 20

 61 - ATCACTCTTCCTAGATTCATAATCGAGCACCAGAAGCAATTTAAGAACGCTACTGGTGAT - 120
 21 - I  T  L  P  R  F  I  I  E  H  Q  K  Q  F  K  N  A  T  G  D   - 40
 21 -  S  L  F  L  D  S  *  S  S  T  R  S  N  L  R  T  L  L  V  I  - 40
 21 -   H  S  S  *  I  H  N  R  A  P  E  A  I  *  E  R  Y  W  *  F - 40
                 +G
121 - TTCACATTAGTACTGAATGCCTTGCAATTCGCGTTCAAATTTGTATCTCACACCATCAGA - 180
 41 - F  T  L  V  L  N  A  L  Q  F  A  F  K  F  V  S  H  T  I  R   - 60
 41 -  S  H  *  Y  *  M  P  C  N  S  R  S  N  L  Y  L  T  P  S  D  - 60
 41 -   H  I  S  T  E  C  L  A  I  R  V  Q  I  C  I  S  H  H  Q  T - 60

181 - CGTGCTGAATTGGTTAACTTGGTTGGGTTAGCAGGCGCTTCCAACTTCACTGGTGACCAG - 240
 61 - R  A  E  L  V  N  L  V  G  L  A  G  A  S  N  F  T  G  D  Q   - 80
 61 -  V  L  N  W  L  T  W  L  G  *  Q  A  L  P  T  S  L  V  T  S  - 80
 61 -   C  *  I  G  *  L  G  W  V  S  R  R  F  Q  L  H  W  *  P  A - 80

241 - CAAAAGAAGTTGGACGTTCTAGGTGATGAAATATTTATCAATGCCATGAGGGCTAGTGGG - 300
 81 - Q  K  K  L  D  V  L  G  D  E  I  F  I  N  A  M  R  A  S  G   - 100
 81 -  K  R  S  W  T  F  *  V  M  K  Y  L  S  M  P  *  G  L  V  G  - 100
 81 -   K  E  V  G  R  S  R  *  *  N  I  Y  Q  C  H  E  G  *  W  D - 100

301 - ATCATCAAGGTCCTTGTATCTGAAGAACAGGAAGACTTGATCGTTTTTCCCACAAACACG - 360
101 - I  I  K  V  L  V  S  E  E  Q  E  D  L  I  V  F  P  T  N  T   - 120
101 -  S  S  R  S  L  Y  L  K  N  R  K  T  *  S  F  F  P  Q  T  R  - 120
101 -   H  Q  G  P  C  I  *  R  T  G  R  L  D  R  F  S  H  K  H  G - 120
```

B)

nt	82
wt	TAA TCG AG
mismatch	TA***C TCG AG***

C)

nt	127	128	129	130
wt	T	T	A	
FS	T	**G**	T	A

Fig. 32. A) First 360 nt of the wt *FBP1* ORF. Stars indicate stopcodons in the reading frames. Red stars define the reversion window starting with nucleotide 14 and ending at the position of 186 nt. Underlined sequence corresponds to primer fbp1ins1 that introduces the mismatch and frameshift mutation. Red A at position 82 represents planned mismatch on primer to manipulate stopcodon. Red TT at position 127 and 128 is the position where one G is inserted for the +1 frameshift. Green bold line indicates the prospective reading frame of the +1 frameshift allele, which shifts at the site of frameshift insertion and stops at the end of the reversion window.

B) Detail of manipulation of stopcodon on position 82. The change from A to C creates a recognition site for the enzyme XhoI. Bold italic letters indicate the recognition site.

C) Detail of frameshift insertion at position 127. Between nt 127 and 128 one Guanine is inserted to create a +1 frameshift mutation.

3.3.2.1. One step gene replacement

A fragment of the *FBP1* gene was amplified from pBY011-FBP1 with one long primer (fbp1ins1) containing the frameshift mutation and the mismatch to manipulate the stop codon to be able to introduce the mutation into the genome. The second primer was a megaprimer fbp1for2 with sequence complementary to the first 20 nt of the *FBP1* ORF. The tail of the megaprimer was complementary to the promoter sequence of *FBP1*. A basic overview is given in Fig. 33. The amplification of the sequence resulted in a short PCR product of 220 bp. The transformation was performed in the host strain YUF, which has the marker *URA3* placed between the promoter sequence of *FBP1* and its start codon. Due to homologous recombination the marker gene should be replaced. This was expected not to be a trivial step due to an abnormal length difference of approximately 1600 bp.

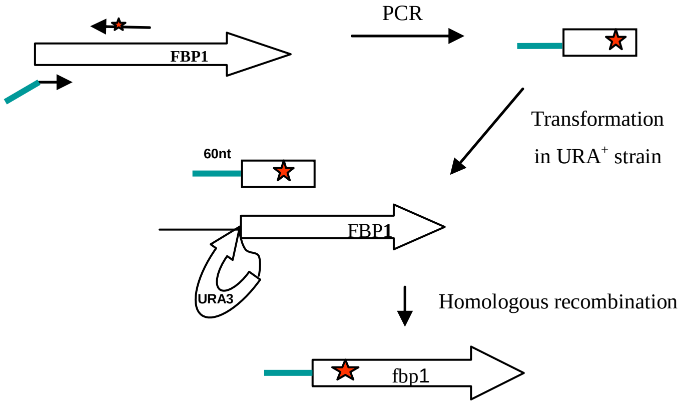

Fig. 33. principle of strategy

Genomic DNA of 42 FOA resistant clones was isolated and a control PCR was performed with two external primers (fbp1for and fbp1intrev) to detect the length difference. Only 7 clones were tested positive with the control PCR. Furthermore, the manipulated stopcodon was analyzed. Due to the introduced mutation to get rid of the stop codon, a recognition site for the enzyme XhoI was created. DNA of positive clones was tested for the recognition site in a DNA restriction digest with XhoI. If the site was active and the PCR product cleaved, it would indicate that additional to the mutation of the manipulated stopcodon also the frameshift mutation was integrated into the genome. Unfortunately, none of the four clones was tested positive for the XhoI recognition site, suggesting that the clones also did not carry the frameshift mutation. Therefore, the remaining PCR product that was used for transformation was tested for the XhoI cleavage site and could be confirmed positive. Consequently, it could be excluded that the transformed linear DNA fragment lacked the mutations. It was assumed that the error occurred in vivo during homologous recombination. A possible reason could be that the homologous sequence was not long enough. Homologous flanks at the 5’ end proposed 60 nt in the promoter region of *FBP1* and 81 nt to the mismatch and at the 3’ end 79 nt up to the mutation and 33 nt to the frameshift mutation, respectively, as seen in Fig. 34.

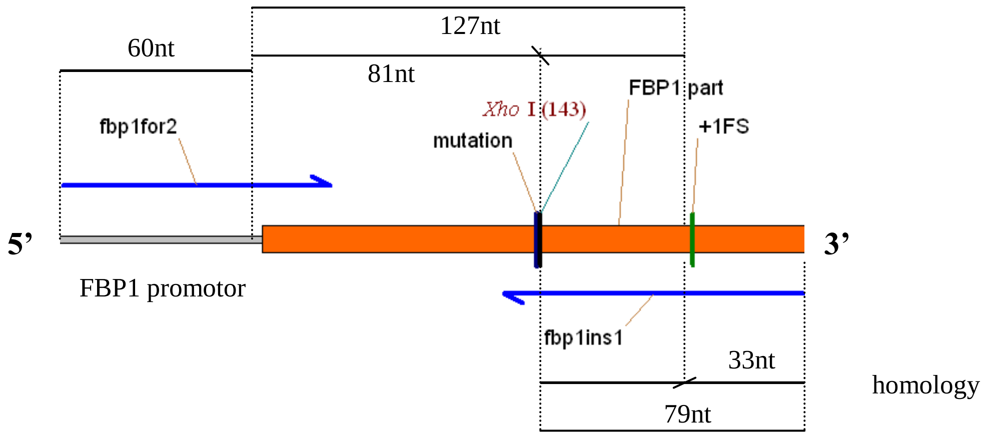

Fig. 34. Homologous flanks of PCR product regarding to the 5' and 3' end.

The desired frameshift strain could not be constructed with this method. Thus, another strategy was applied.

3.3.2.2. Modified one-step gene replacement

In the first approach the problem arose that the frameshift mutation was not integrated into the genome. It was assumed that the homologous sequence was not long enough (79 nt), the mismatch recognized therefore, and the strand degraded so that the wt-sequence stayed intact.

Therefore, a new approach was to elongate the downstream sequence as shown in Fig. 36. A plasmid which contains the mutagenic *FBP1* with the frameshift mutation and the manipulated stop codon was newly constructed for the method of the two-gene replacement, which was started parallel. Therefore, the plasmid YIpFBP1FS+1 could be used as template in this approach. Details of the construction of the plasmid are described in the next subchapter 3.3.2.3.

The primers fbp1for2 and verif2fbp1 (Fig. 35) were used to amplify part of the *FBP1* gene with the frameshift mutation and the manipulated stopcodon. Since the gene on the plasmid is lacking its promoter, the upstream sequence could not be elongated to achieve a longer homologous flank at this end. Fig. 36 shows the new situation of homologous sequences of the PCR product to the genomic DNA.

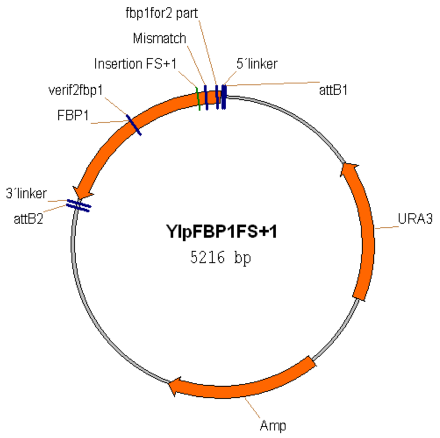
fbp1for2 part
Mismatch
Insertion FS+1
5´linker
verif2fbp1
attB1
FBP1
3´linker
attB2
YIpFBP1FS+1
5216 bp
URA3
Amp

Fig. 35. Plasmid map of YIpFBP1FS+1 with primers to amplify part of the *FBP1* sequence with the frameshift mutation and the mismatch.

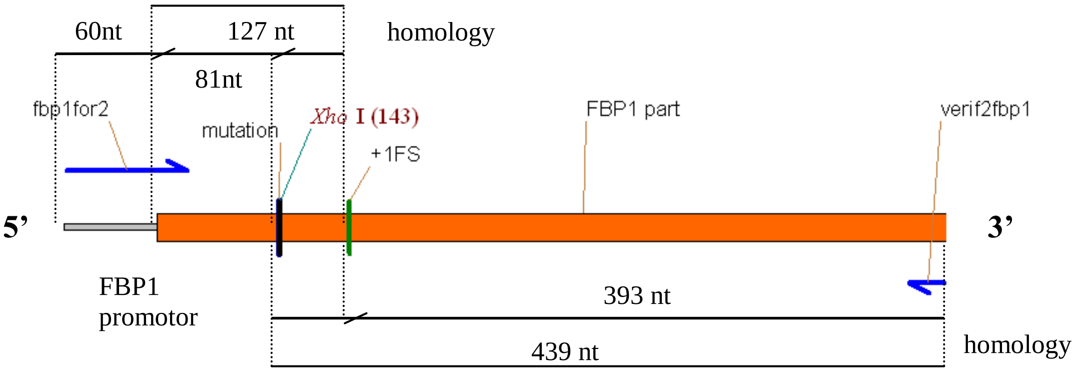
60nt
127 nt
homology
81nt
fbp1for2
mutation
Xho I (143)
+1FS
FBP1 part
verif2fbp1
5'
3'
FBP1
promotor
393 nt
439 nt
homology

Fig. 36. Elongated downstream region of *FBP1* gene. Length of homologous flanks are indicated. Compared to the PCR product yielded in the previous strategy, the 5' end is identical and the 3' end longer (compare with Fig. 34)

The PCR product was transformed into the URA$^+$ strain YUF as in the previous method. Subsequently, genomic DNA of clones was isolated and analyzed with PCR. Clones tested positive with PCR were further characterized for their XhoI cleavage site. However, the same problems as in the previous construction were observed. None of the clones had the mutation integrated into the genome.

Therefore, the second approach did not lead to the desired strain. A third approach had been started parallel.

3.3.2.3. Two step gene replacement („loop-in/loop-out")

The principle of the method was described in Materials and Methods (2.2.1.1.). Two general steps had to be performed in order to start the two step gene replacement. First, a plasmid with the *FBP1* ORF had to be modified to make it suitable for loop-in/loop-out.

Second, the frameshift mutation and the manipulated stop codon had to be introduced on the plasmid sequence of *FBP1*.

The required plasmid with the ORF of *FBP1* was commercially acquired. The plasmid pBY011-FBP1 holds the gene *FBP1* under a Gal1-10 promotor. For the technique of a two step gene replacement, the plasmid was further modified by removing the sequences of CEN and parts of ARS. The CEN on the plasmid would propose a problem once the linearized plasmid sequence is integrated into the genome. It would introduce a second centromer on the chromosome, which has to be avoided. Therefore, the CEN was removed from the plasmid.

The plasmid was cleaved with two compatible single-cutter restriction enzymes XbaI and NheI (Promega; Multicore buffer). After an o/n-incubation at 37°C the digested plasmid was loaded on an agarose gel and the 5215 bp band cut from the gel.

The DNA was purified from the cut gel band and its compatible ends religated with T4 DNA Ligase as shown in Fig. 37.

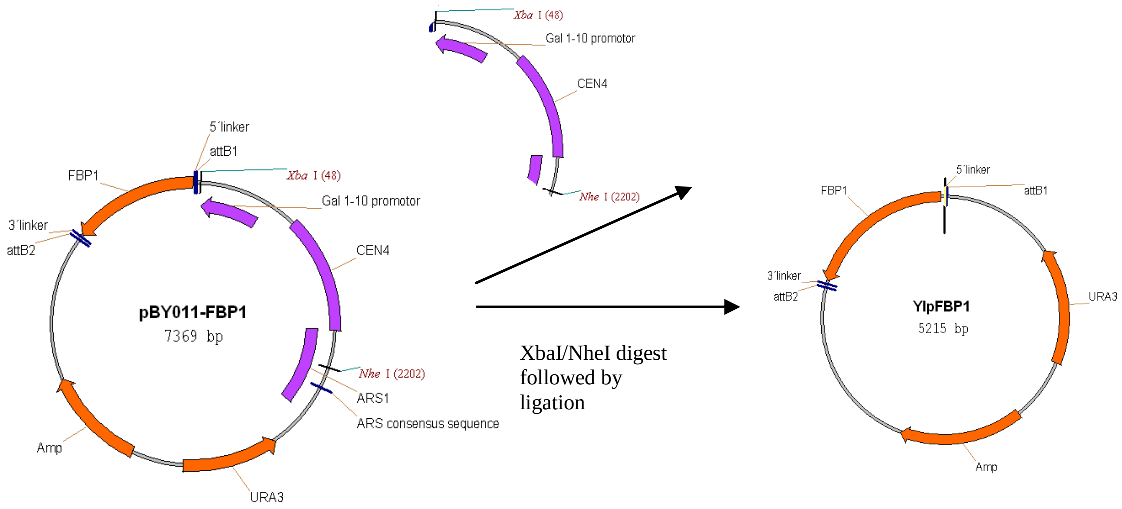
Xba I (48)
Gal 1-10 promotor
CEN4
Nhe I (2202)
5´linker
attB1
FBP1
3´linker
attB2
pBY011-FBP1
7369 bp
ARS1
ARS consensus sequence
Amp
URA3
XbaI/NheI digest followed by ligation
YIpFBP1
5215 bp

Fig. 37. Construction of YIpFBP1

Half of the ligation reaction was transformed in competent DH5α *E. coli* cells and selection for positive clones occurred on LB$_{amp}$ plates. 14 transformants were picked for plasmidprep and a control restriction digest with the enzyme SspI (Promega, buffer E) performed. Following fragments were expected.

pBY011-FBP1 (control)	YIpFBP1
2988 bp	2910 bp
2910 bp	2309 bp
1471 bp	-

The restriction enzyme cuts the control plasmid into three fragments but only two fragments were expected in correct clones.

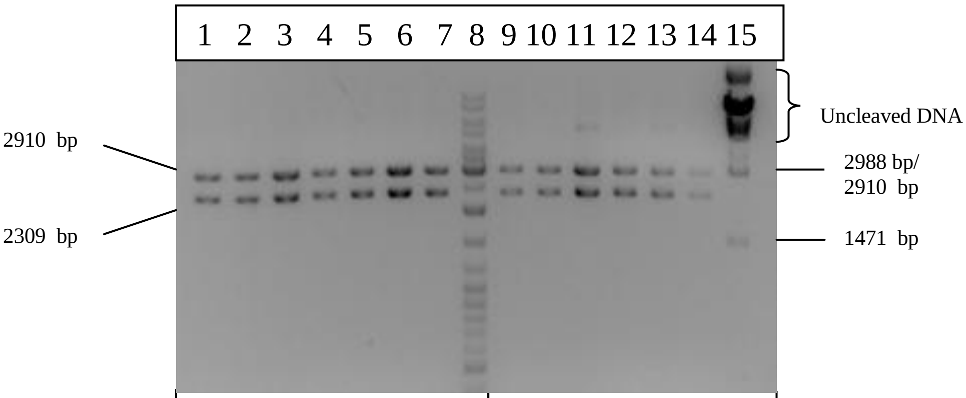

1 → clone 1	9 → clone 9
2 → clone 2	10 → clone 10
3 → clone 3	11 → clone 11
4 → clone 4	12 → clone 12
5 → clone 5	13 → clone 13
6 → clone 6	14 → clone 14
7 → clone 7	15 → control pBY011-FBP1
8 → O’Gene Ruler DNA Ladder Mix (5 µl)	

Fig. 38. Gel of control digest of candidates for YIpFBP1.

All 13 clones showed the expected two fragments of 2910 bp and 2309 bp as shown in Fig. 38. Transformant number 11 additionally shows a higher molecular band, which indicated that the DNA digest was not complete. Clone 5 was chosen to be the new plasmid YIpFBP1.

In further steps a +1 frameshift and the mismatch were introduced to *FBP1* on the plasmid with a mutagenesis PCR, which was described in Materials and Methods (2.2.1.9.). For both steps of the mutagenesis the PCRs had to be optimized to obtain a PCR product with high specificity. Due to an unspecific band, optimizations of concentrations in plasmid, primer and $MgCl_2$ were required. Highest specificity could be yielded in a reaction with a decreased primer final concentration of 0.2 µM instead of the standard conditions of 0.5 µM. Only successful PCRs are listed here. The primer fbp1ins1 carries the +1 FS as well as the manipulated stop codon.

First step of mutagenesis PCR:

step	Time [seconds]	Temperature °C
Initial denaturation	300	98
30 cycles of next 3 steps:		
Denaturation	*10*	*98*
Annealing	*30*	*70*
Extension	*16*	*72*
Final extension	300	72

50 µl reaction
1 µl YIpFBP1 (1:100)
10 µl 5x HF buffer
1 µl dNTPs
1 µl fbp1ins1
1 µl uraSCintf
35.5 µl ddH$_2$O
0.5 µl Phusion Polymerase

Part of the PCR product was loaded on a gel to verify a band at 1055 bp (Fig. 39) and the remaining volume of the PCR product was purified with the DNA purification kit from illustra^{TM}.

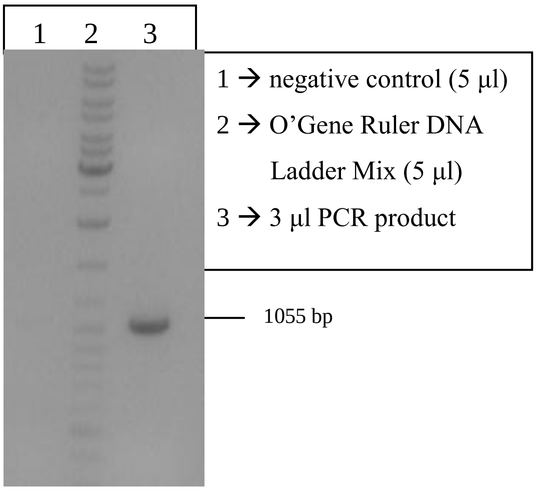
1 2 3
1 → negative control (5 µl)
2 → O'Gene Ruler DNA Ladder Mix (5 µl)
3 → 3 µl PCR product
1055 bp

Fig. 39. PCR product 1 of mutagenesis

Second step of mutagenesis PCR:

The PCR product of the first PCR was used as "primer" in the second PCR. The PCR required many optimizations to yield a specific product. Due to the use of the first PCR product as a primer the consequence was that there would always be an "unspecific" product at 1055 bp resulting alone from this one "primer". However, this effect cannot be avoided. Therefore the main focus was to optimize the ratio between the unspecific primer band and the PCR product that was desired. The primer concentration seemed to be a crucial factor. Consequently, the PCR product 1 was titrated to obtain the best results possible, which required a high amount of PCR product 1. The final PCR conditions were the following:

50 µl reactions:
1 µl YIpFBP1 (1:1000)
10 µl 5x HF buffer
1 µl dNTPs
2 µl PCR product 1 (0.22 pmol)
2.8 µl fbp1rev2 (1:100/1.38 pmol))
2 µl $MgCl_2$
29.5 µl ddH_2O
0.4 µl Phusion Polymerase

Step	**Time [seconds]**	**Temperature °C**
Initial denaturation	30	98
30 cycles of next 2 steps:		
Denaturation	*10*	*98*
Annealing + Extension	*27*	*72*
Final extension	300	72

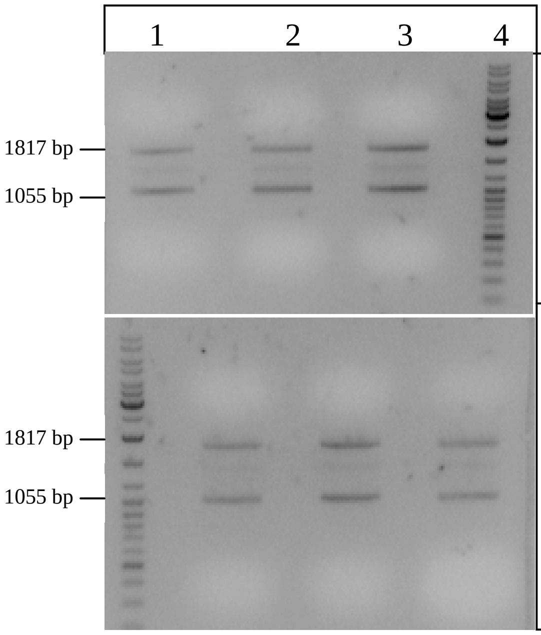

1 → PCR product 2 (25 µl)
2 → PCR product 2 (25 µl)
3 → PCR product 2 (25 µl)
4→ O'Gene Ruler DNA Ladder Mix (5 µl)

1 → O'Gene Ruler DNA Ladder Mix (5 µl)
2 → PCR product 2 (25 µl)
3 → PCR product 2 (25 µl)
4→ PCR product 2 (25 µl)

Fig. 40. Preparative gel of second PCR step in mutagenesis. Unspecific band at 1500 bp is present, but hardly visible.

In all cases a further unspecific band at 1500 bp occurred to complicate the matter. Consequently, the specific bands in Fig. 40 had to be cut from the gel and purified. Since the yield was not sufficient to use for a following subcloning reaction, all six bands at 1817 bp were cut from the gel and purified before the DNA was used for a re-PCR to yield more DNA, which can be used for further experiments. Since the DNA content was too low to be measured by Nanodrop it could not be estimated how much of it would be needed in the PCR reaction. Therefore, one reaction with 1 µl template (one fifteenth of purified DNA) and a second one with 2 µl were performed. As positive controls the plasmid YIpFBP1 was used. Program and PCR reaction (for 1 µl template) are indicated below.

step	Time [seconds]	Temperature °C
Initial denaturation	30	98
30 cycles of next 3 steps:		
Denaturation	*10*	*98*
Annealing	*15*	*70*
Extension	*27*	*72*
Final extension	300	72

20 µl reaction
1 µl template (PCR product 2)
4 µl 5x HF buffer
0.4 µl dNTPs
1 µl fbp1rev2
1 µl uraSCintf
12.4 µl ddH$_2$O
0.2 µl Phusion Polymerase

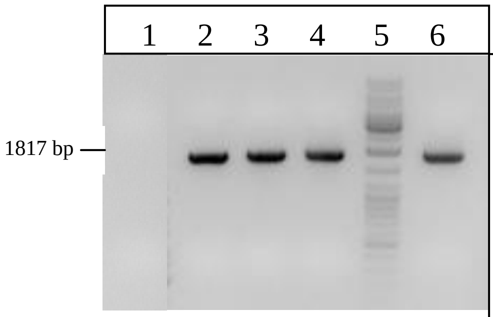

1 → negative control (5 µl)
2 → 1 µl template
3 → 2 µl template
4→ YIpFBP1 + 1 µl template
5 → O'Gene Ruler DNA Ladder Mix (5 µl)
6 → YIpFBP1 (positive control) 5 µl

Fig. 41. Re-PCR of PCR product 2

The re-PCR was successful and specific for the amplification of interest as the bands at 1817 bp show in Fig. 41. Therefore, the DNA could be purified directly from the remaining PCR solutions of both reactions with 1 and 2 µl, respectively. To create a plasmid that carries the mutated *FBP1*, subcloning was performed with YIpFBP1 as vector and the re-PCR product. Both templates were cleaved with the single cutters SgrAI and SalI, resulting in a 461 bp fragment carrying both mutations in *FBP1*. This sequence was removed from YIpFBP1, as it served as backbone vector, where the altered *FBP1* was inserted as shown in Fig. 42. The two enzymes did not create compatible ends, therefore religation of the vector was avoided.

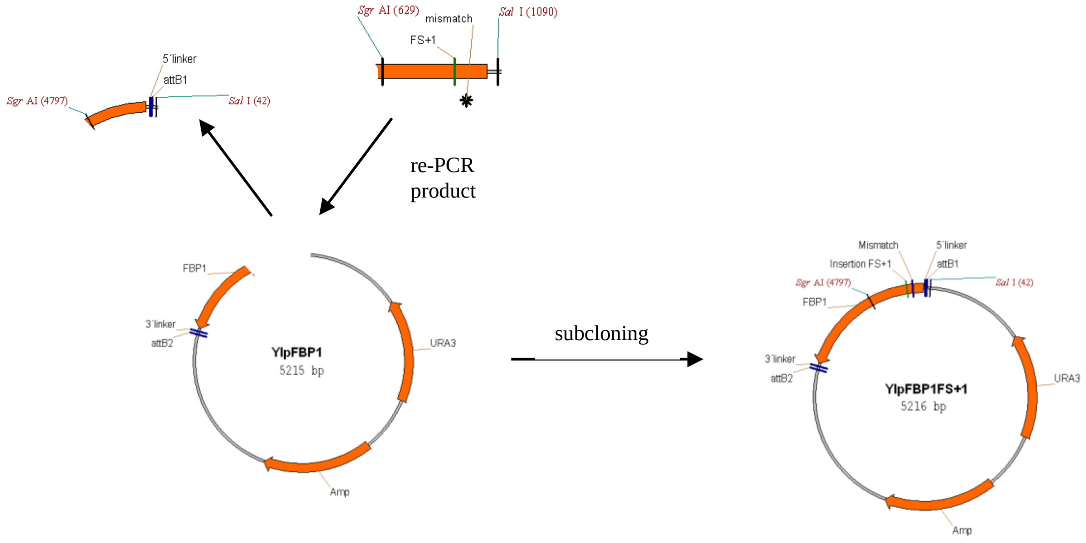
Sgr AI (629)
mismatch
Sal I (1090)
FS+1
5´linker
attB1
Sgr AI (4797)
Sal I (42)
re-PCR
product
FBP1
3´linker
attB2
YIpFBP1
5215 bp
URA3
Amp
subcloning
Mismatch
Insertion FS+1
5´linker
attB1
Sgr AI (4797)
Sal I (42)
FBP1
3´linker
attB2
YIpFBP1FS+1
5216 bp
URA3
Amp

Fig. 42. Subcloning of YIpFBP1 with Re-PCR product to construct YIpFBP1FS+1

The ligated plasmid was transformed in DH5α competent cells and clones were selected on LB$_{amp}$ plates. After isolating plasmid DNA, clones were verified by control restriction digests and one clone was sequenced and declared the new YIpFBP1FS+1.

To perform “loop-in”, the plasmid YIpFBP1FS+1 was linearized with the restriction enzyme HpaI, purified and the DNA used in transformation with electroporation in YLBM. Selection occurred on SC-ura plates, genomic DNA was isolated from 14 clones. Control PCRs were performed to verify the plasmid integration. Unfortunately, optimal PCR conditions could not be found to be able to detect PCR products from clones. Therefore, it was assumed, that clones that showed no wt band, might have the plasmid integrated into the genome.

The second step of the gene replacement (loop-out) was performed with a variety of clones, which were tested negative for a wt band with PCR. The “loop-out” was triggered by plating on FOA plates, a negative selection for *URA3*. However, most of the clones showed 100% growth, even though the step of the excision of the plasmid is a rarely occurring event. Therefore, only a fraction of the cells should lose *URA3* and thus be able to form colonies on FOA plates. Clones that showed reduced growth were picked for further characterizations with PCR and replica plating. First, replica plating to SC-Lactate should distinguish clones carrying the *FBP1* wt copy from clones with the mutated *FBP1* copy. Clones with the wt gene can grow normally on lactate, whereas clones with a frameshift mutation should not grow. 92 clones were screened by replica plating to SC-Lactate, yielding only 7 clones with absent growth. These clones were tested by PCR. After the excision of the plasmid, correct clones should have the same length as the wt strain YLBM. Unfortunately, clones showed no PCR product, on the contrary to the positive control with the wt. Thus, this approach did not lead to a successful construction of a frameshift insertion in *FBP1*.

One consideration why the above described approach failed, was that the truncated ARS in the plasmid, which still consists of the replication origin, might have an effect on the loop-in technique. Consequently, the remaining parts of ARS should be removed from the plasmid as well. The easiest way would have been to cut it from the YIpFBP1 but the lack of two enzymes which produced compatible ends, made this impossible. Hence, the only way was to go back to the initial plasmid pBY011-FBP1. Furthermore, the only enzymes producing compatible ends were ClaI and NarI. Since ClaI is sensitive to methylation sites it would not be possible to cleave plasmid DNA derived from *E. coli* strain DH5α. Thus, the first step was a transformation of the plasmid into a dam-deficient *E. coli* strain JM110. Once the plasmid was present in the dam-deficient strain, plasmid DNA was isolated. The preparative double digest with ClaI and NarI resulted in 2 fragments of 5360 bp and 2009 bp (Fig. 43 left). The 5360 bp fragment was cut from the gel, purified and religated (Fig. 44).

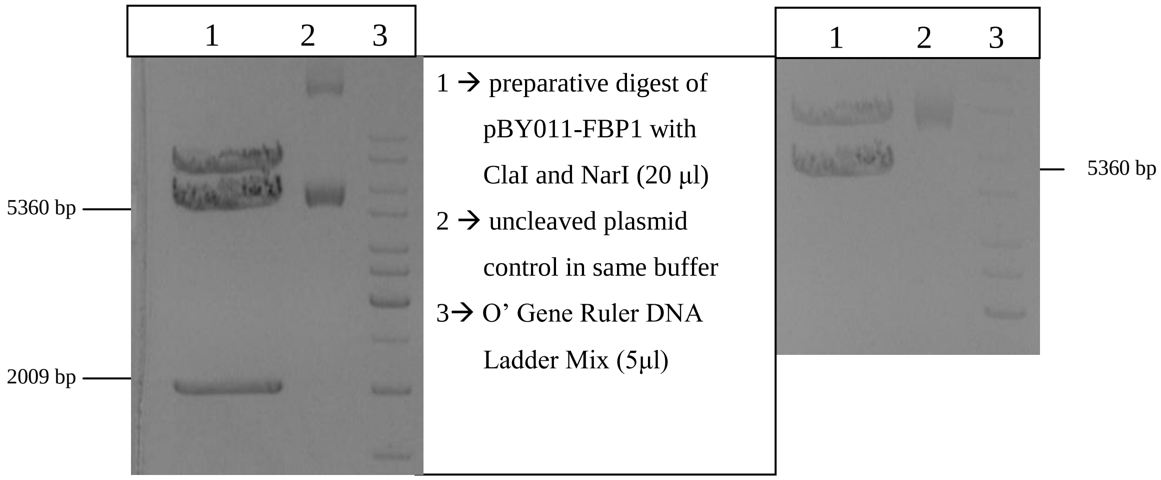
1
2
3
5360 bp
2009 bp
1 → preparative digest of pBY011-FBP1 with ClaI and NarI (20 µl)
2 → uncleaved plasmid control in same buffer
3→ O' Gene Ruler DNA Ladder Mix (5µl)
1
2
3
5360 bp

Fig. 43. Restriction digest of pBY011-FBP1 in JM110 with ClaI and NarI to eliminate the complete ARS sequence. On the right hand side, the same gel is shown after a longer running time with better separation of high molecular bands.

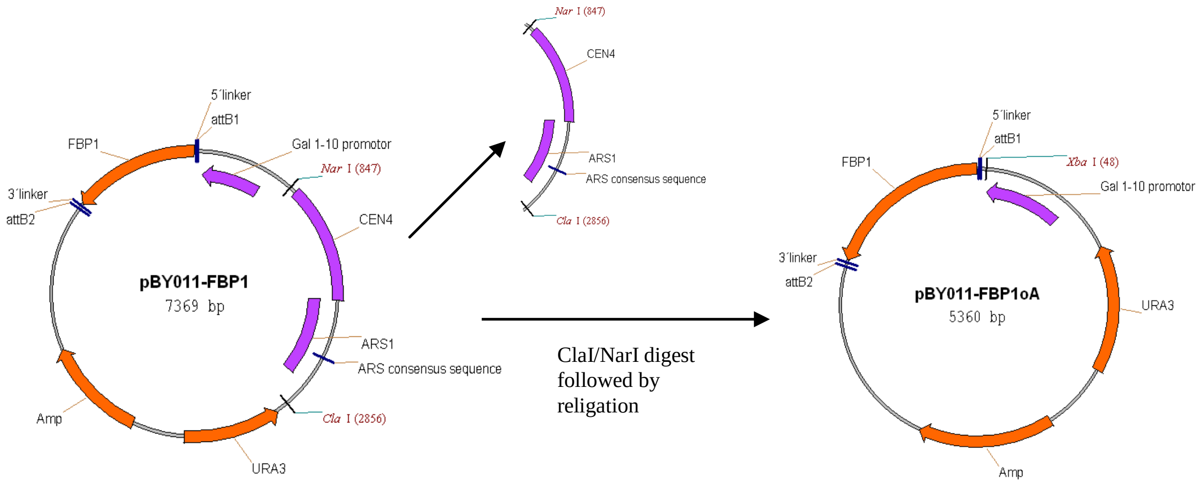
5´linker
attB1
FBP1
Gal 1-10 promotor
Nar I (847)
3´linker
attB2
CEN4
pBY011-FBP1
7369 bp
ARS1
ARS consensus sequence
Amp
Cla I (2856)
URA3
Nar I (847)
CEN4
ARS1
ARS consensus sequence
Cla I (2856)
ClaI/NarI digest
followed by
religation
5´linker
attB1
FBP1
Xba I (48)
Gal 1-10 promotor
3´linker
attB2
pBY011-FBP1oA
5360 bp
URA3
Amp

Fig. 44. Religation of the vector with removal of complete ARS sequence and CEN sequence.

After religation the DNA was transformed in competent JM110 *E. coli* cells. Positive clones were selected on LB_{amp} plates. Furthermore, they were tested in a control DNA restriction digest with the enzymes NcoI and XbaI. As seen in Fig. 45 on the left, correct clones are cleaved into three fragments with the size of 3031 bp, 1499 bp and 830 bp. On the contrary, the control pBY011-FBP1 only shares the fragments 3031 bp and 830 bp, whereas the third fragment provides 3508 bp.

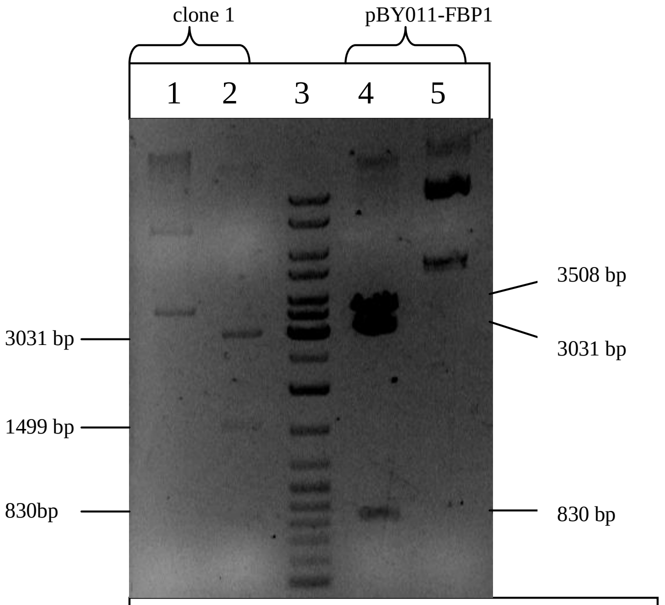
clone 1
pBY011-FBP1
1
2
3
4
5
3508 bp
3031 bp
3031 bp
1499 bp
830bp
830 bp

1 → uncleaved DNA (5 µl)
2 → NcoI/XbaI digest (5 µl)
3→ O’ Gene Ruler DNA Ladder Mix (5µl)
4 → NcoI/XbaI digest (5 µl)
5 → uncleaved DNA (5 µl)

Fig. 45. Control double digest with NcoI/XbaI of candidate for pBY011-FBP1oA. The 830 bp fragment on lane 2 is hardly visible.

Fig. 45 shows that clone 1 is correct and was therefore defined as pBY011-FBP1oA. This new plasmid does not contain any parts of ARS or CEN and was used for further constructions in the loop-in/loop-out method.

Next, the frameshift mutation as well as the manipulated stop codon had to be placed in the plasmid.

Since the plasmid with the frameshift mutation and the mismatch already existed (YIpFBP1FS+1), it was used as template for subcloning. The altered *FBP1* gene was cleaved with the restriction enzymes HindIII and SalI from YIpFBP1FS+1 and replaced in pBY011-FBP1oA to create the new plasmid YIpFBP1FS+1oA, which lacks the sequences of ARS and CEN but consists of the target gene *FBP1* with its mutations (see Fig. 46). The chosen enzymes did not produce compatible ends of the vector, therefore religation of the backbone of the plasmid was avoided.

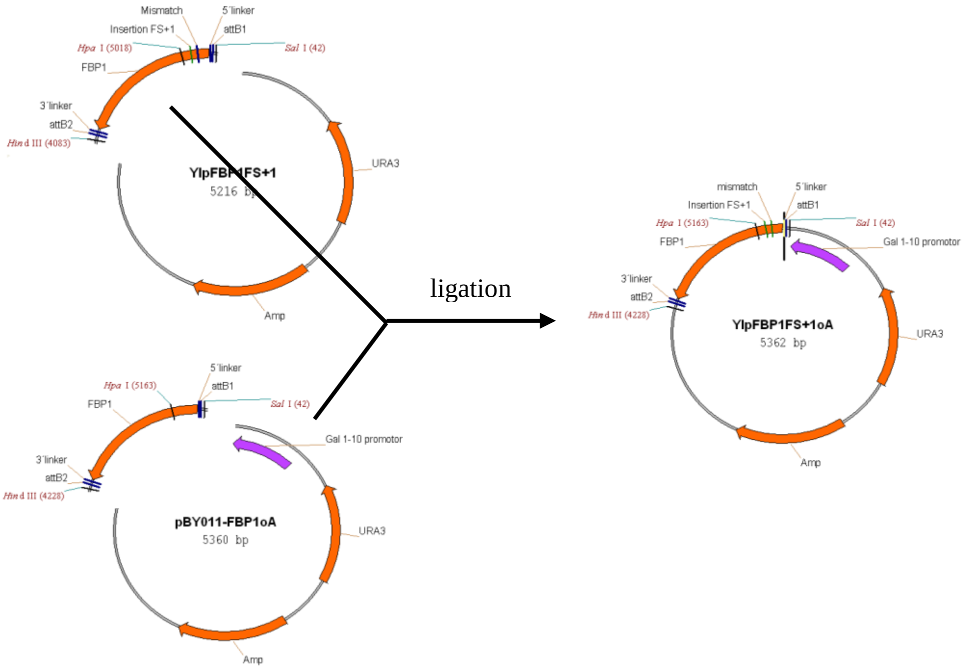
Mismatch
5´linker
Insertion FS+1
attB1
Hpa I (5018)
Sal I (42)
FBP1
3´linker
attB2
Hind III (4083)
YIpFBP1FS+1
5216 bp
URA3
Amp
ligation
mismatch
5´linker
Insertion FS+1
attB1
Hpa I (5163)
Sal I (42)
FBP1
Gal 1-10 promotor
3´linker
attB2
Hind III (4228)
YIpFBP1FS+1oA
5362 bp
URA3
Amp
5´linker
Hpa I (5163)
attB1
FBP1
Sal I (42)
Gal 1-10 promotor
3´linker
attB2
Hind III (4228)
pBY011-FBP1oA
5360 bp
URA3
Amp

Fig. 46. Construction of YIpFBP1FS+1oA by double digest with HindIII and SalI with following subcloning

The plasmid pBY011-FBP1oA was cleaved with SalI and HindIII in a double digest (FastDigest) resulting in two fragments of the sizes 1175 bp and 4186 bp (Fig. 47), latter being cut from the gel and its DNA purified.

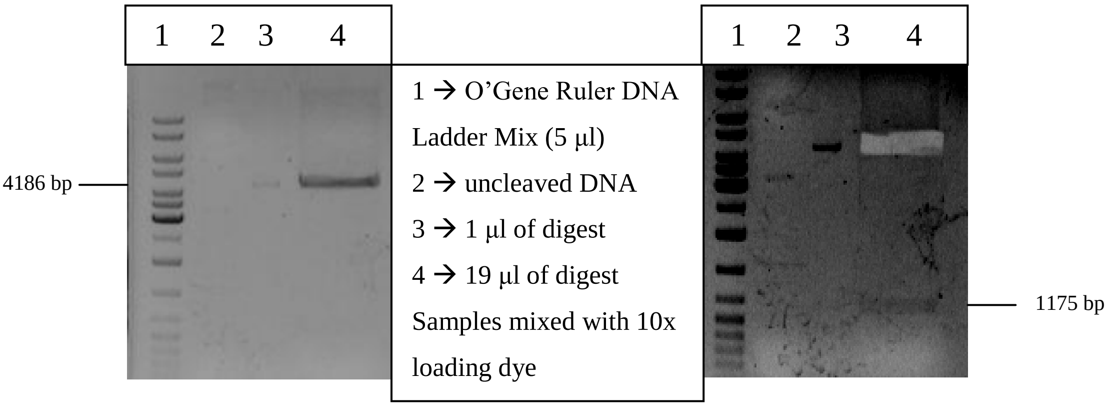

1 → O'Gene Ruler DNA Ladder Mix (5 µl)
2 → uncleaved DNA
3 → 1 µl of digest
4 → 19 µl of digest
Samples mixed with 10x loading dye

Fig. 47. SalI and HindIII double digest of pBY011-FBP1oA

On the left the 1175 bp fragment cannot be seen. The fragment of interest (4186 bp) was first cut from the gel and removed. On the right hand side, the gel was photographed with longer exposure time to UV to be able to detect the 1175 bp fragment.

For YIpFBP1FS+1 the double digest resulted in complications. Therefore, the enzymes SalI and HindIII were used from Promega in an o/n digest at 37°C. Since the enzymes were not active in the same buffer, the plasmid was first linearized with HindIII (buffer E). Afterwards SalI (buffer D) was added and digested for 3.5 hours at 37°C.

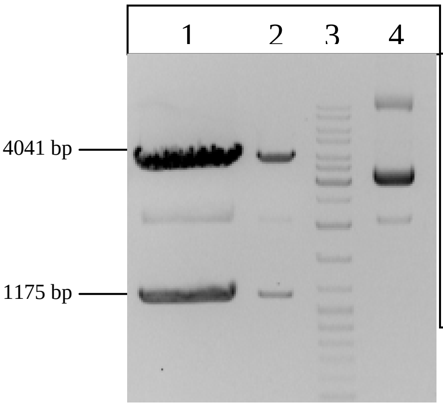

1 → 19 µl of digest
2 → 1 µl of digest
3 → O'Gene Ruler DNA Ladder Mix (5 µl)
4 → uncleaved DNA (5 µl)

Fig. 48. preparative digest of YIpFBP1FS+1 with SalI and HindIII

The obtained 1175 bp band as seen in Fig. 48 was cut from the agarose gel and purified with the Talent DNA purification kit. The vector and its insert were calculated in a molecular ratio of 1:3 for the ligation. The ligation mix was transformed in competent DH5α-cells and selected on LB_{amp} plates. Some clones were chosen for plasmid isolation and control digests to verify correct clones. Two double digests were performed with XhoI, which only cleaves if the mismatch is present in the *FBP1* sequence, and NdeI. Furthermore, NcoI and HpaI were used as for a double digest. Following fragments were obtained:

	correct clone	control pBY011-FBP1oA
XhoI/NdeI	3431 bp; 1930 bp	5360 bp
NcoI/HpaI	3031 bp; 1745 bp; 585 bp	3031 bp; 1744 bp; 585 bp
DrdI/ApaI	2385bp; 1799 bp; 1178 bp	2385bp; 1799 bp; 1178 bp

According to the control digests shown in Fig. 49 all tested clones are positive. Transformant 3 was further tested with a second double digest and was declared the new YIpFBP1FS+1oA.

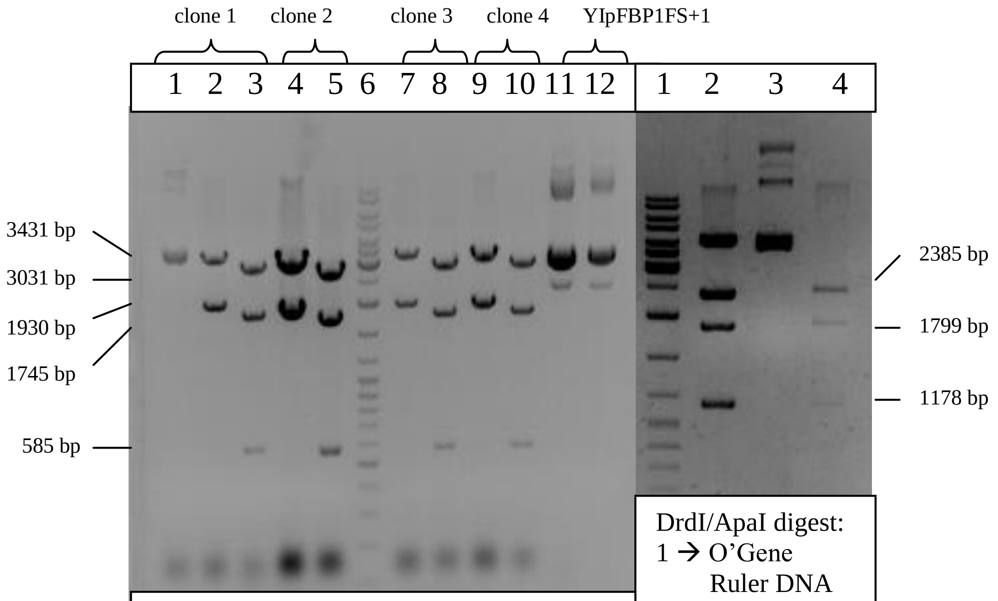

1 → uncleaved DNA

XhoI/NdeI digest: lanes → 2, 4, 7, 9, 11

NcoI/HpaI digest: lanes → 3, 5, 8, 10, 12

6 → O’Gene Ruler DNA Ladder mix (5µl)

6 µl were loaded on gel.

DrdI/ApaI digest:
1 → O’Gene Ruler DNA Ladder mix (5µl)
2 → clone 3
3 → clone 3 uncleaved
4 → pBY011-FBP1oA

7 µl of each sample was loaded on gel.

Fig. 49. Control digests of YIpFBP1FS+1oA candidates

For the loop-in the plasmid was linearized with the restriction enzyme HpaI, purified over an agarose gel and the DNA used in transformation with electroporation in YLBM. Selection occurred on SC-ura plates, genomic DNA was isolated from 2 clones and their loop-in was tried to be verified by PCR.

The verification should normally be done with an external primer and an internal one in regard of the integrated plasmid sequence. As an external primer seqfbp1r in the terminator sequence of the target gene was chosen. The internal primer should be upstream of the newly introduced mutation within the target gene. Since the mutation lies in the beginning of the *FBP1* gene, it was not possible to use a primer there. Alternatively, the primer uraSCintf was chosen, which is situated on the plasmid derived sequence. Consequently, with those two primers, clones which did not integrate the plasmid sequence do not yield a PCR product, since the internal primer uraSCintf can only anneal in positive clones. Unfortunately, I had no positive control for this PCR. Since experience with PCRs amplifying regions around *FBP1* showed that it bears difficulties, a positive control is mandatory to exclude the possibility that the PCR did not work. Therefore, a third primer was used for the PCR to be able to amplify the wt sequence for a control. For this purpose the primer sec61for upstream of the integration locus was selected. In the case of the positive control the primers sec61for and seqfbp1r produce a PCR product of 2305 bp. The primer uraSCintf does not anneal in the positive control or in clones that have no plasmid insert. In the case of correct clones, the primers uraSCintf and seqfbp1r should be responsible for the amplification with a fragment of 2083 bp. Even though the third primer sec61for has complementary sequence, amplification of sec61for and seqfbp1r would yield a fragment of over 7500 bp, which is too long for PCR amplifications. All primers are indicated in Fig. 50.

The wt YLBM could be detected. However, the “loop-in” clones did not result in a PCR product. Consequently, clones definitely did not have the same sequence as the wt. It was speculated that the loop in took place but could not be detected with PCR.

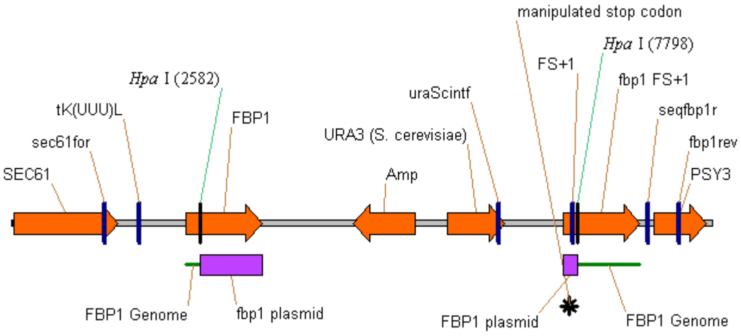

Fig. 50. Loop-in situation of clones with integrated plasmid

Both loop-in clones were cultivated for a loop-out and plated on FOA plates in concentrations of 1 x 10^7 and 5 x 10^7 cells/plate. Only one of the two clones resulted in colonies when selected on FOA. Consequently, the loop-in clone where no loop-out could be derived was not considered for further experiments.

Loop-out clones were further distinguished if they carried the wt gene of *FBP1* or the frameshift gene. This was achieved on SC-Lactate plates. 80 loop-out clones were isolated and replica plated on SC-Lactate to determine their growth conditions. 25 clones had the desired absent growth on SC-Lactate, meaning that they should carry the mutated *FBP1* mutation, which impairs clones to grow on lactate. From these clones, genomic DNA was isolated and control PCR performed. In this case, positive clones should produce the same size as the wt YLBM, since only one additional nucleotide for the frameshift is present.

step	**Time [seconds]**	**Temperature °C**
Initial denaturation	30	98
30 cycles of next 3 steps:		
Denaturation	*10*	*98*
Annealing	*30*	*65*
Extension	*33*	*72*
Final extension	300	72

20 µl reaction:
1 µl DNA
4 µl 5x HF buffer
0.4 µl dNTPs
1.25 µl sec61for
1.25 µl seqfbp1r
0.5 µl $MgCl_2$
12 µl ddH_2O
0.2 µl Phusion Polymerase

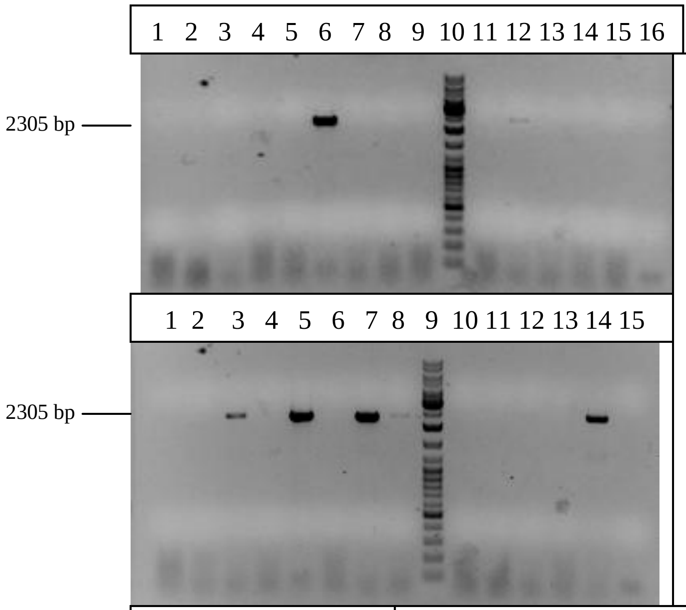

Top gel:
1 → clone 5
2 → clone 8
3 → clone 12
4→ clone 14
5 → clone 17
6 → control YLBM
7 → clone 24
8 → clone 28
9 → clone 38
10 → O’Gene Ruler DNA Ladder Mix (5 µl)
11 → clone 39
12 → clone 44
13 → clone 47
14 → clone 57
15 → clone 59
16 → negative control

Bottom gel:
1 → clone 60
2 → clone 61
3 → clone 63
4→ clone 64
5 → control YLBM
6 → clone 65
7 → clone 66
8 → clone 67
9 → O’Gene Ruler DNA Ladder Mix (5 µl)
10 → clone 72
11 → clone 73
12 → clone 75
13 → clone 77
14 → clone 78
15 → negative control

6 µl of samples were loaded on gel.

Fig. 51. Control PCR of loop-out clones

Five loop-out clones showed a PCR product with the same size of 2305 bp as the control YLBM. The rest of the clones did not yield a PCR product (Fig. 51). Consequently, the 5 clones (44, 63, 66, 67 and 78) with the desired fragment were further characterized to clarify them as positive clones.

First, the clones were tested if the manipulated stop codon was present in the sequence. The mutated *FBP1* should consist of the frameshift mutation as well as of this additional alteration, which created a recognition site for the enzyme XhoI. Thus, only clones where the enzyme cuts, are positive ones.

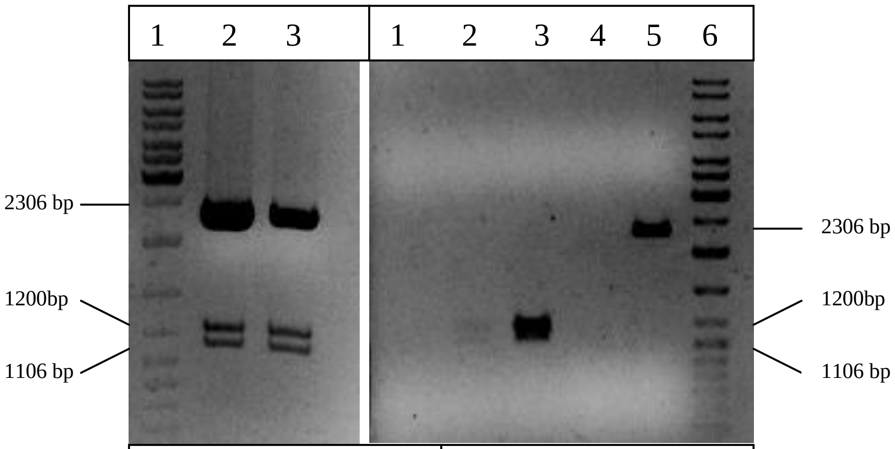

Left hand side	Right hand side:
1 → O'Gene Ruler DNA Ladder Mix (5 µl) 2 → clone 44 (7 µl) 3 → clone 67 (7 µl)	1 → clone 44 (7 µl) 2 → clone 63 (7 µl) 3 → clone 66 (7 µl) 4 → clone 67 (7 µl) 5 → clone 78 (7 µl) 6 → O'Gene Ruler DNA Ladder Mix (5 µl)

Fig. 52. XhoI digest of candidates for the *FBP1* frameshift strain. Clones 44 and 67 were repeated because there was not enough DNA present when digested first (picture on the right). Gel bands at 2306 bp on the left represent undigested DNA. Lower molecular bands derived from cleavage of XhoI.

As seen in Fig. 52, clone 78 did not carry a recognition site for XhoI, therefore, this loop-out clone is not of interest. The other clones carry the recognition site of XhoI as two fragments of 1200 bp and 1106 bp were present, although the bands from clone 63 were not very well visible on the gel.

In a further analysis the four loop-out clones were successfully tested if they revert when plated on SC-Lactate. Consequently, one clone (63) was chosen, sent for sequencing analysis and verified as YFAM.

Subsequently, the new strain was tested for its markers by replica plating and the genotype was confirmed as follows:

YFAM: MATa *trp1-Δ his3-Δ200 ura3-52 lys2ΔBgl ade2-1o gal mal CUP*^{r} *fbp1FS-128*

3.3.3. Adaptive mutation assay with YFAM

Adaptive mutation assays were performed with the *FBP1* frameshift strain. The non-functional gene leads to a block in gluconeogenesis. Due to the lack of the ability to synthesize glucose, cells enter cell cycle arrest in a glucose-limited system where lactate instead of glucose is offered as an alternative carbon source.

Only cells that produce a reversion within the reversion window are able to overcome the arrest and enter cell cycle again. This results in colony formation, which is detected in the adaptive mutation assay. Details of the setup of the assay are described in Materials and Methods (2.2.2.4.).

The mutation rate as well as the mutation frequencies were determined. The mutation rate describes the number of mutations per cell division. Thus, the mutation rate is calculated for early arising colonies that are supposed to be replication-dependent revertants. On the contrary, mutation frequencies are related to the number of mutations independent of cell division and represent the adaptive mutations in the assay.

For this purpose, a line has to be drawn between colonies formed as a result of replication-dependent and replication-independent mutation events, respectively. According to the results of the reconstruction assay (chapter 3.2.3.), day 6 was predicted as the last day of early arising colonies.

Another indicator for the line between replication-dependent colonies and replication-independent adaptive mutations are jackpots, which become manifest in high numbers of colonies in the early days and then abruptly decrease their number of newly arising colonies.

Since no clear line could be drawn, two variants for the adaptive mutation frequency were proposed. In one case day 5 was considered to include all replication-dependent derived colonies. In the second case, day 6 was the line to be drawn. Consequently, mutation rates were once determined for day 5 and in the second variant for day 6, both according to the p_0 method (Luria and Delbruck, 1943; Rosche and Foster, 2000).

d5	6.21×10^{-10}
d6	8.58×10^{-10}

For the determination of the mutation frequency, the number of early colonies was subtracted.

Likewise, mutation frequencies were calculated starting with day 6 or day 7 as shown in Fig. 53. Depending on the starting day, mutation frequencies reached approximately 15 revertants per 10^{10} cells.

Compared to mutation frequencies derived in mutation assays with lysine starvation, the frequencies obtained with the new system of glucose limitation are decreased by a factor three.

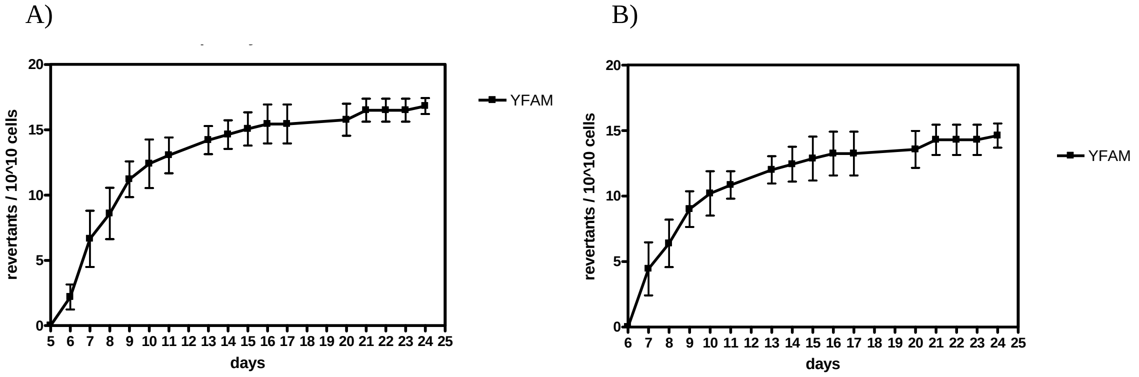

Fig. 53. A) Time course of the accumulation of adaptive revertants starting day 6 determined from 4 individual experiments. B) Time course of the accumulation of adaptive revertants starting day 7 determined from 4 individual experiments.

Throughout the experiment the survival rate of arrested cells was determined as well, which is shown in Fig. 54. The determined viability of arrested cells was satisfactory with 30% viable cells at the end of the experiment at day 24.

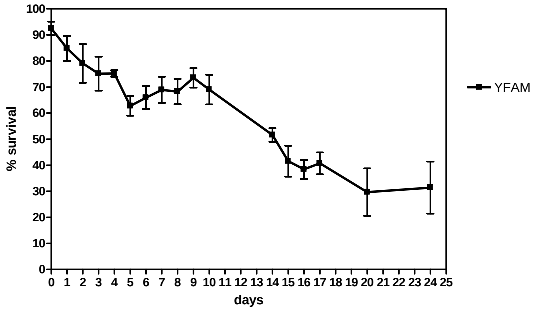

Fig. 54. Survival curve of 4 individual experiments

Four revertants (from day 8, 11 and two from day 9), were sequenced to characterize the reversion events. The genomic DNA was preparated and a PCR performed.

step	Time [seconds]	Temperature °C
Initial denaturation	30	98
30 cycles of next 2 steps:		
Denaturation	*10*	*98*
Annealing + Extension	*92*	*72*
Final extension	300	72

50 µl reaction:
1 µl DNA
10 µl 5x HF buffer
1.5 µl dNTPs
2 µl sec61for
2 µl psy3rev
0.5 µl $MgCl_2$
21.8 µl ddH_2O
0.5 µl Phusion Polymerase

PCR products were purified with the purification kit (Talent) and an aliquot was loaded on a gel to verify correct length of 3064 bp. Samples were sent to VBC Genomics for sequence analysis with the sequencing primer fbp1prof. The primer is situated in the promoter sequence of the *FBP1* gene, so that the sequence analysis will include the sequence of the reversion window.

The sequence confirms that reversion events took place in all four tested revertants, restoring the original reading frame in the bulk of the gene as seen in Fig. 55. In detail, in the sequences of revertants from day 8 and day 11 a TG-duplication was observed at the same spot. The two revertants from day 9 showed a 5-run duplication (TGAAT) in the case of d9I and a deletion (G) in case of d9II.

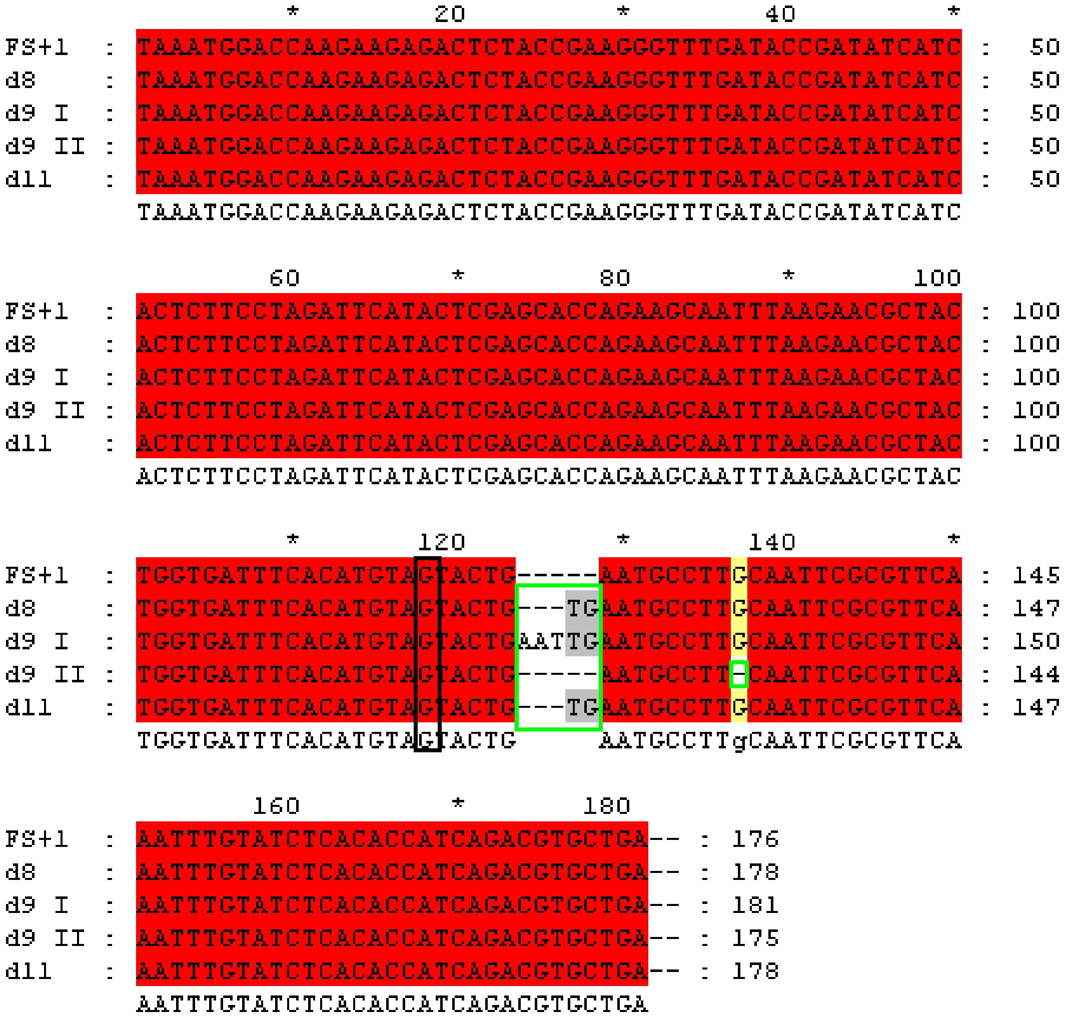

```
                   *        20         *        40         *
FS+1   : TAAATGGACCAAGAAGAGACTCTACCGAAGGGTTTGATACCGATATCATC :  50
d8     : TAAATGGACCAAGAAGAGACTCTACCGAAGGGTTTGATACCGATATCATC :  50
d9 I   : TAAATGGACCAAGAAGAGACTCTACCGAAGGGTTTGATACCGATATCATC :  50
d9 II  : TAAATGGACCAAGAAGAGACTCTACCGAAGGGTTTGATACCGATATCATC :  50
d11    : TAAATGGACCAAGAAGAGACTCTACCGAAGGGTTTGATACCGATATCATC :  50
         TAAATGGACCAAGAAGAGACTCTACCGAAGGGTTTGATACCGATATCATC

                 60         *        80         *       100
FS+1   : ACTCTTCCTAGATTCATACTCGAGCACCAGAAGCAATTTAAGAACGCTAC : 100
d8     : ACTCTTCCTAGATTCATACTCGAGCACCAGAAGCAATTTAAGAACGCTAC : 100
d9 I   : ACTCTTCCTAGATTCATACTCGAGCACCAGAAGCAATTTAAGAACGCTAC : 100
d9 II  : ACTCTTCCTAGATTCATACTCGAGCACCAGAAGCAATTTAAGAACGCTAC : 100
d11    : ACTCTTCCTAGATTCATACTCGAGCACCAGAAGCAATTTAAGAACGCTAC : 100
         ACTCTTCCTAGATTCATACTCGAGCACCAGAAGCAATTTAAGAACGCTAC

                   *       120         *       140         *
FS+1   : TGGTGATTTCACATGTAGTACTG-----AATGCCTTGCAATTCGCGTTCA : 145
d8     : TGGTGATTTCACATGTAGTACTG---TGAATGCCTTGCAATTCGCGTTCA : 147
d9 I   : TGGTGATTTCACATGTAGTACTGAATTGAATGCCTTGCAATTCGCGTTCA : 150
d9 II  : TGGTGATTTCACATGTAGTACTG-----AATGCCTT-CAATTCGCGTTCA : 144
d11    : TGGTGATTTCACATGTAGTACTG---TGAATGCCTTGCAATTCGCGTTCA : 147
         TGGTGATTTCACATGTAGTACTG     AATGCCTTgCAATTCGCGTTCA

                160         *       180
FS+1   : AATTTGTATCTCACACCATCAGACGTGCTGA-- : 176
d8     : AATTTGTATCTCACACCATCAGACGTGCTGA-- : 178
d9 I   : AATTTGTATCTCACACCATCAGACGTGCTGA-- : 181
d9 II  : AATTTGTATCTCACACCATCAGACGTGCTGA-- : 175
d11    : AATTTGTATCTCACACCATCAGACGTGCTGA-- : 178
         AATTTGTATCTCACACCATCAGACGTGCTGA
```

Fig. 55. Sequence analysis. Sequence shown represents the reversion window. Top sequence FS+1 shows the original sequence of the strain YFAM. d8, d9 I, d9 II and d11 are the revertants isolated from the mutation assay. Black box indicates position of introduced +1FS. Green boxes indicate position of reversion events.

The amino acid sequence changed according to the reversion events. Due to the new arrangement of codons, different amino acids are created. All revertants retain a stretch of altered amino acids between the site of the introduced frameshift and the reverting frameshift as shown in Fig. 56.

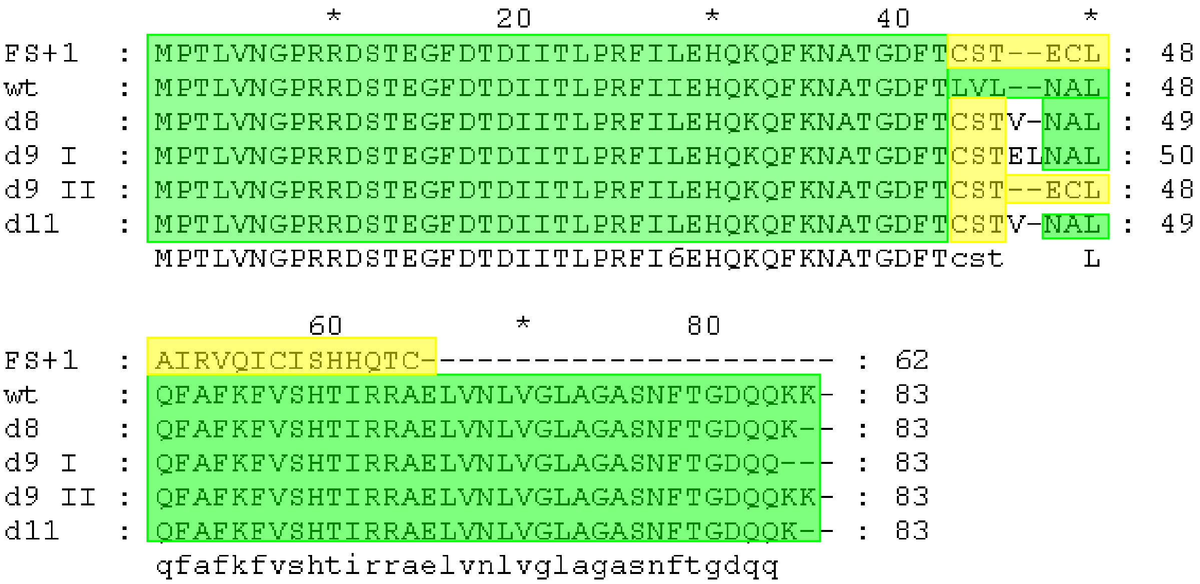

```
                  *         20         *        40         *
FS+1   : MPTLVNGPRRDSTEGFDTDIITLPRFILEHQKQFKNATGDFTCST--ECL : 48
wt     : MPTLVNGPRRDSTEGFDTDIITLPRFIIEHQKQFKNATGDFTLVL--NAL : 48
d8     : MPTLVNGPRRDSTEGFDTDIITLPRFILEHQKQFKNATGDFTCSTV-NAL : 49
d9 I   : MPTLVNGPRRDSTEGFDTDIITLPRFILEHQKQFKNATGDFTCSTELNAL : 50
d9 II  : MPTLVNGPRRDSTEGFDTDIITLPRFILEHQKQFKNATGDFTCST--ECL : 48
d11    : MPTLVNGPRRDSTEGFDTDIITLPRFILEHQKQFKNATGDFTCSTV-NAL : 49
         MPTLVNGPRRDSTEGFDTDIITLPRFI6EHQKQFKNATGDFTcst    L

                60         *        80
FS+1   : AIRVQICISHHQTC--------------------- : 62
wt     : QFAFKFVSHTIRRAELVNLVGLAGASNFTGDQQKK- : 83
d8     : QFAFKFVSHTIRRAELVNLVGLAGASNFTGDQQK-- : 83
d9 I   : QFAFKFVSHTIRRAELVNLVGLAGASNFTGDQQ--- : 83
d9 II  : QFAFKFVSHTIRRAELVNLVGLAGASNFTGDQQKK- : 83
d11    : QFAFKFVSHTIRRAELVNLVGLAGASNFTGDQQK-- : 83
         qfafkfvshtirraelvnlvglagasnftgdqq
```

Fig. 56. Amino acid sequences of frameshift strain YFAM (FS+1), wt strain and revertants. First 83 aa of *FBP1* are shown with the exception of the frameshift strain, where only 62 aa are shown, since the protein is truncated at this spot due to the following stopcodon.

Green indicates the original aa sequence; yellow represents the altered amino acid sequence in the FS strain. White background color indicates newly created amino acids.

The crossover from green to yellow in FS+1 represents the change of aa sequence due to the introduced frameshift.

3.3.4. Reconstruction Assay with YFAM revertants

Some revertants of the adaptive mutation assay were picked for further characterization. A total of two reconstruction assays were performed and the colony formation observed. Eight revertants (colony formation on day 5, 7, 8, 9, 10, 11, 14 and 15 in mutation assay) were chosen for the first reconstruction assay and 9 (colony formation on day 4, 5, 6, 7, 9 and 13 in mutation assay) for the second one. Details of the reconstruction assay were described in Materials and Methods (2.2.2.5.). Colony formation was monitored for 14 days and 17 days, respectively.

In the first reconstruction assay all revertants appeared with a peak on day 3 or 4 with the exception of one revertant from day 14 as evident from Fig. 57. Also after repetition it showed the same pattern. Therefore, the revertant from day 14 is defined as an outlier. Nevertheless, colony formation still took place before day 6, which was defined as the threshold between replication-dependent and replication-independent revertants.

The survival is indicated in Fig. 58. Revertants from day 5 and 8 show 100% viability; all other revertants yield a survival between 60 and 80 % in the reconstruction assay.

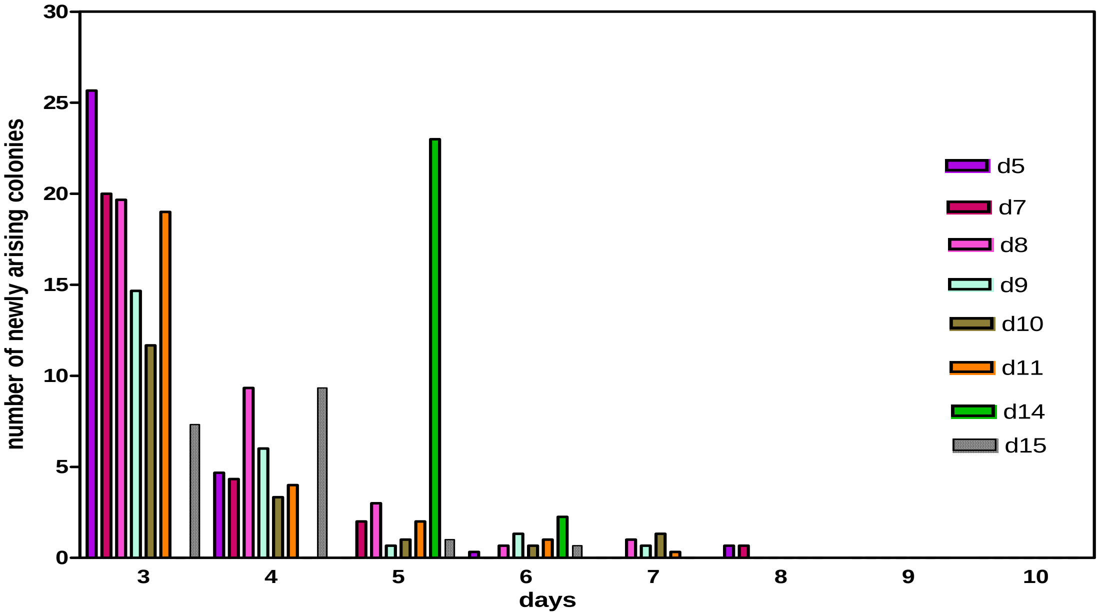

Fig. 57. Reconstruction assay of revertants from first series of adaptive mutation assay. X-axis is truncated at day 10 since no new colonies arose from day 9 on.

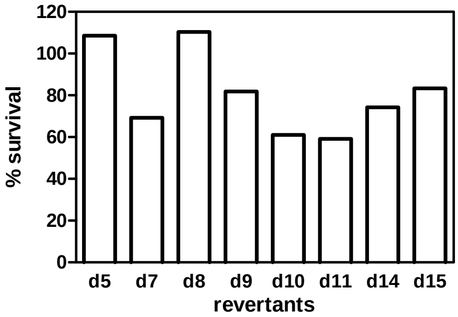

Fig. 58. Normalized survival of revertants tested in the reconstruction assay. 100% is normalized to plating efficiency, which was obtained with YPD plates.

The second reconstruction assay showed similar patterns of colony appearance for the isolated revertants. As Fig. 59 shows, all nine revertants appeared with a peak on day 4, indicating that all of them developed replication-independently in the mutation assay.

The survival rate is indicated in Fig. 60. Over a time course of 17 days only 50% of colonies from revertant 9 appeared in the reconstruction assay. The reason for the low survival is unknown. Rest of plated revertants showed a survival between 60 and 80%.

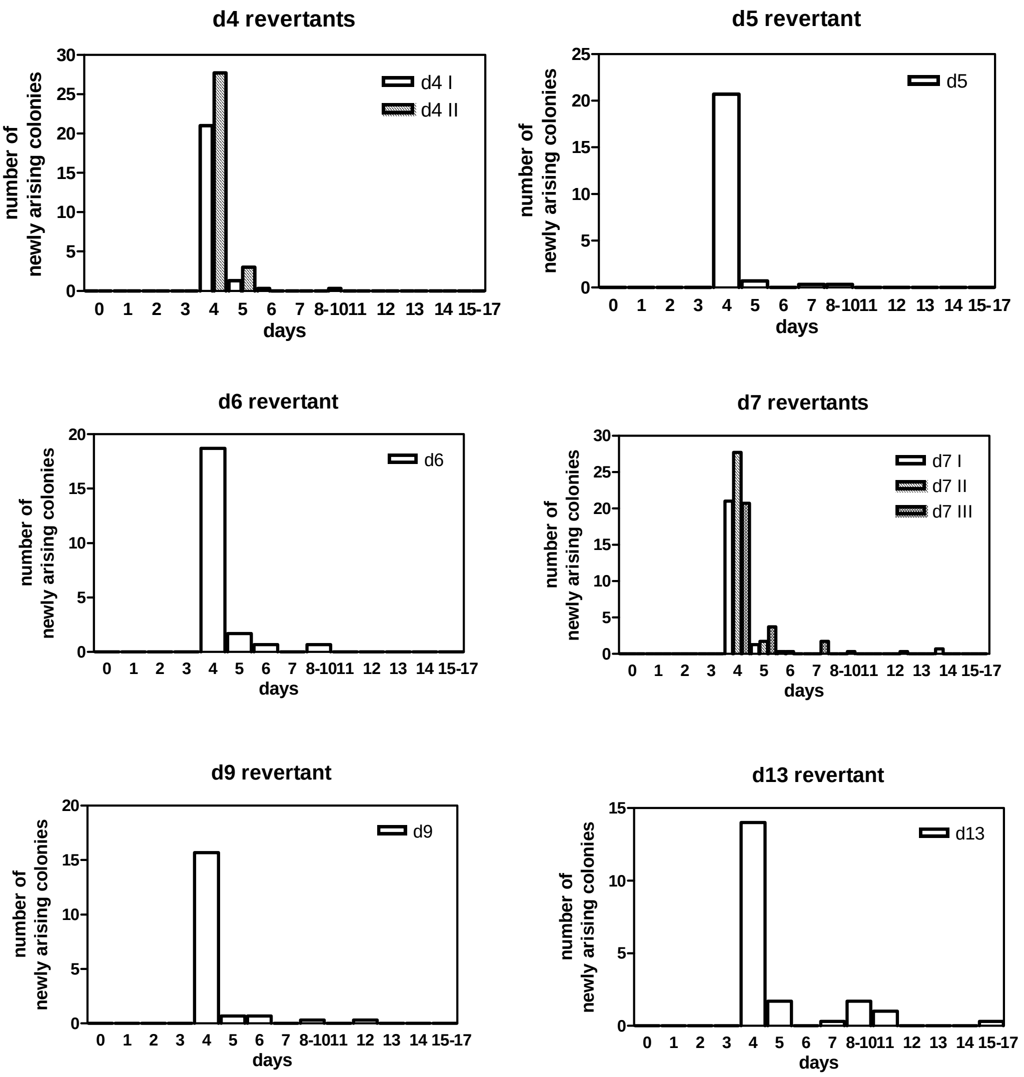

Fig. 59. Results of second reconstruction assay

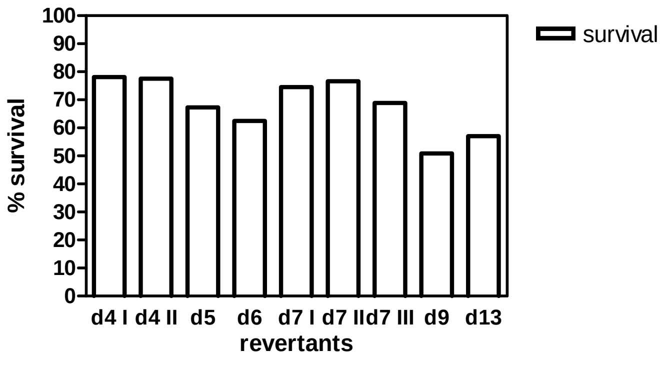

Fig. 60. Normalized survival of revertants tested in the second reconstruction assay. 100% is normalized to plating efficiency, which was obtained with YPD plates.

3.3.5. Implementation of the new assay for DNA repair studies

The DNA repair gene *RAD27* encodes the protein 5'-flap endonuclease which has multiple functions. It is involved in Okazaki processing and in base excision repair (BER). The flap endonuclease is responsible for cleavage of the 5' flap in both pathway. Rad27 is the homolog of human FEN1 (Reagan et al., 1995; Tishkoff et al., 1997).

In previous experiments, a knock-out of the DNA repair gene *RAD27* was analyzed in an adaptive mutation assay for reversions of a *lys2ΔBgl*-mediated lysine auxotrophy. Unfortunately, with this assay, it was not possible to study the frequency of late-arising adaptive reversions, since at late times the plates were already covered by an excess of early arising replicaion-dependent revertant colonies. To overcome this problem, we needed an assay with lower reversion rate. Since this is the case for the newly established *FBP1* assay, we decided to use it for an analysis of adaptive mutation in a *RAD27* knockout strain.

3.3.5.1. Construction of YFA27

The disruption cassette for the Rad27 gene was derived from the plasmid pDR27H (Fig. 61). This plasmid contains upstream and downstream fragments of the Rad27 gene, which has been disrupted by a central *HIS3* marker gene (Heidenreich et al., unpublished).

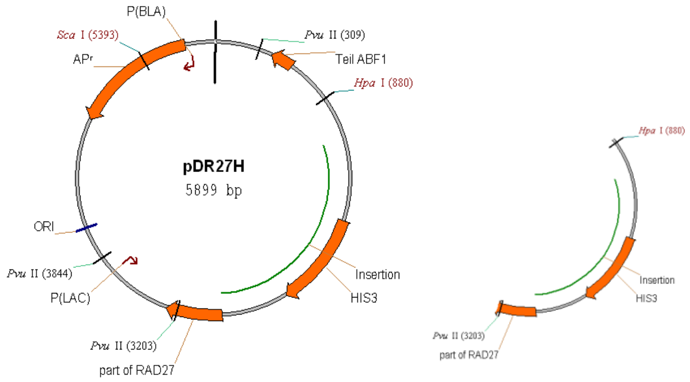

Fig. 61. Plasmid map of pDR27H on the left and the fragment that was used for transformatin

After verifying the plasmid with restriction digests, a preparative restriction digest was performed to obtain a fragment with *Rad27::HIS3*.

The plasmid was digested with the FastDigest restriction enzymes HpaI, PvuII and ScaI to obtain 5 fragments with the sizes indicated in Fig. 62.

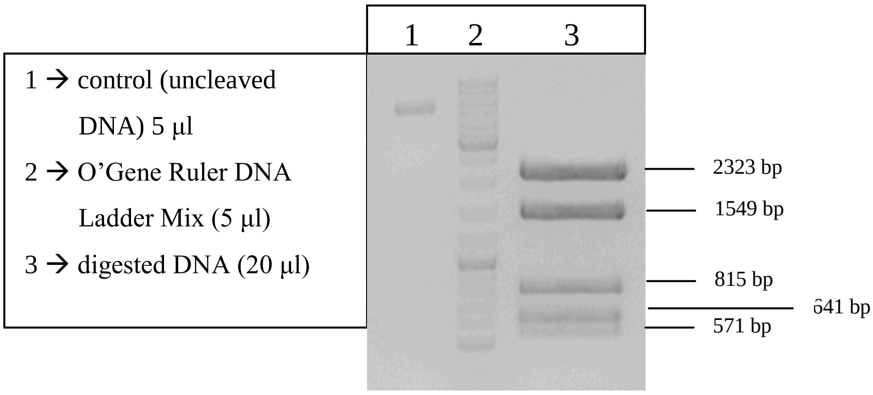
1
2
3
1 → control (uncleaved DNA) 5 µl
2 → O'Gene Ruler DNA Ladder Mix (5 µl)
3 → digested DNA (20 µl)
2323 bp
1549 bp
815 bp
641 bp
571 bp

Fig. 62. Digest of pDR27H to cleave *Rad27::HIS3* sequence from the plasmid.

The fragment with a length of 2323 bp was cut from the agarose gel and the DNA purified with the illustra^{TM} DNA purification kit.

The purified DNA (100 ng) was transformed in the host strain YFAM via electroporation. The remaining part of the *rad27* gene and the homologous region upstream derived from the plasmid acted as substrates for homologous recombination in the genome. The selection for clones with successful gene replacement occurred on SC-his plates. Transformants were selected and isolated on fresh SC-his plates. After a genomic preparation clones were verified via 3 PCRs with internal and external primers.

The first control PCR with external primers was performed with Taq-Polymerase (NEB). Composition of reaction mix as well as conditions for PCR are indicated below.

step	Time [seconds]	Temperature °C
Initial denaturation	300	95
30 cycles of next 3 steps:		
Denaturation	*30*	*95*
Annealing	*30*	*56*
Extension	*210*	*72*
Final extension	300	72

25 µl reaction:
0.5 µl DNA
2.5 µl 10x standard buffer
1 µl dNTPs
1.5 µl r27down
1.5 µl r27up
0.5 µl $MgCl_2$
16.5 µl ddH_2O
0.15µl Taq Polymerase

Positive clones should result in a fragment size of 3539 bp. YFAM provides another control since it was the host strain in the transformation. The PCR yields a band at 2500 bp as shown in Fig. 63.

5 out of 10 tested clones show the correct size of 3539 bp, the rest of the transformants provide the same size as their host strain YFAM.

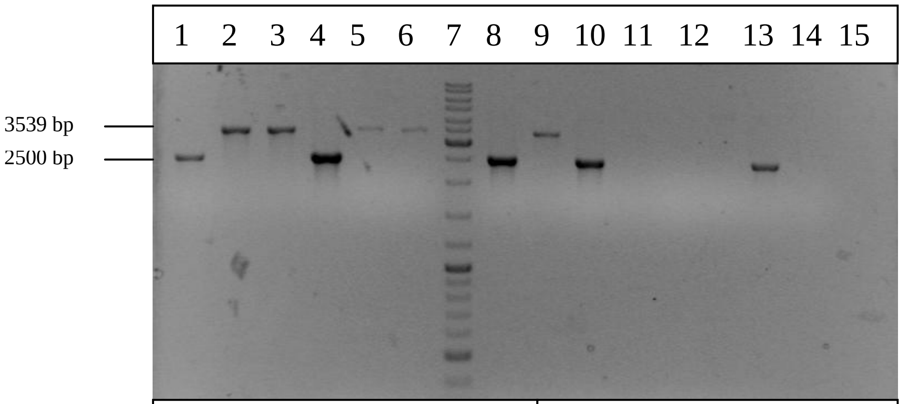

1 → control YFAM
2 → clone 13
3 → clone 14
4→ clone 16
5 → clone 17
6 → clone 18
7 → O’Gene Ruler DNA Ladder Mix (5 µl)

8 → clone 19
9 → clone 20
10 → clone 21
11 → clone 23
12 → clone 24
13 → control YFAM
14 → control YLB327
15 → negative control

Fig. 63. Gel with PCR products with primer pair r27up and r27down

The conditions for the second PCR with an external and internal primer combination (His3for and r27up) were slightly changed according to annealing temperature of the primer pair and the expected length of PCR fragment. Consequently, the annealing temperature was reduced from 56°C to 55°C and the elongation time reduced to 102 seconds, since the product was expected to be 1888 bp long.

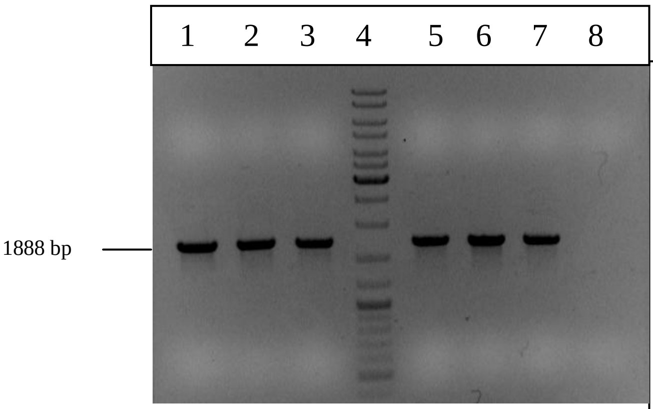

1 → clone 13 (7 µl)
2 → clone 14 (7 µl)
3 → clone 17 (7 µl)
4→ O’Gene Ruler DNA Ladder Mix (5 µl)
5 → clone 18 (7 µl)
6 → clone 20 (7 µl)
7 → control YLB27 (7 µl)
8 → negative control (7 µl)

Fig. 64. Gel with PCR products from primer pair His3for and r27up

All five transformants showed a band with correct length and therefore could be categorized as positive clones (Fig. 64). Clone 13 was chosen to verify with the third PCR to amplify the other part of the disrupted gene (Fig. 65).

The PCR conditions for the third PCR with the combination of the internal primer His3rev and the external primer r27down were adjusted for the size of the amplified product. Therefore, the extension time was reduced to 102 seconds, as the expected product is shorter.

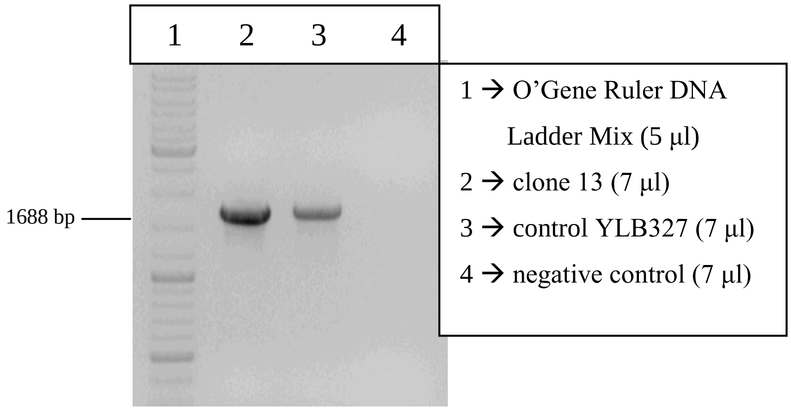
1 2 3 4
1688 bp
1 → O'Gene Ruler DNA Ladder Mix (5 µl)
2 → clone 13 (7 µl)
3 → control YLB327 (7 µl)
4 → negative control (7 µl)

Fig. 65. Gel with PCR products with primer pair His3rev and r27down

For further characterization, clones were tested for their decreased resistance to methyl methanesulfonate (MMS). Rad27-deficient strains typically are very sensitive to MMS.

Positive transformants according to PCR were streaked onto an MMS gradient plate as well as three controls, YLBM and YFAM were used as positive control. Both strains have a functional *RAD27* gene and therefore are capable of growing on MMS. In contrast, the negative control YLB27 has a *rad27* knock out and consequently does not grow on MMS. Thus, the phenotype of the transformants should resemble the control YLB27.

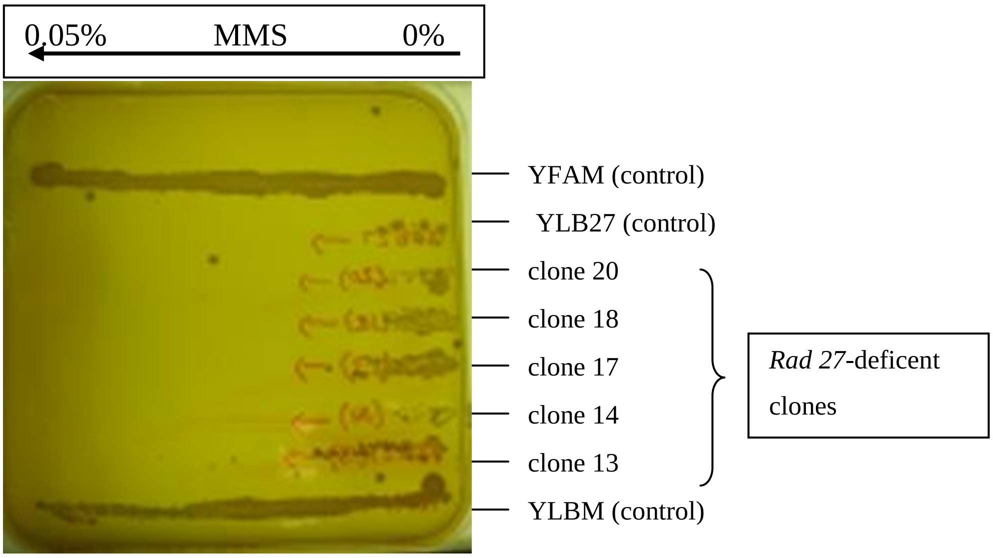
0,05%
MMS
0%
YFAM (control)
YLB27 (control)
clone 20
clone 18
clone 17
clone 14
clone 13
YLBM (control)
Rad 27-deficent clones

Fig. 66. MMS gradient plate from 0% to 0.05%.

All clones show the expected effect that their resistance to MMS is decreased when *rad27* is non functional as evident from Fig. 66. Clone 13 was chosen to be the new strain YFA27. The strain was further tested for its markers by replica plating to confirm following genotype:

YFA27: MATa *trp1-Δ his3-Δ200 ura3-52 lys2ΔBgl ade2-1o gal mal* CUP^r *fbp1FS-128 rad27::HIS3*

3.3.5.2. Adaptive mutation assay with YFA27

After constructing a *rad27* knock out in the *FBP1* frameshift strain, the effects on mutation frequencies were analyzed. The hope was to have a reduced mutation rate compared to analyses with lysine starvation so that replication-independent reversion events can be studied in the *FBP1* assay.

The mutation assay was performed as described in 2.2.2.4. Six individual experiments were performed. As described in the adaptive mutation assay with YFAM, two variants for the day of determination for the mutation rate are presented. In the first case day 5 is considered the day when all replication-dependent reversions are included and in the second variant day 6 still includes early arising colonies. Mutation rates were determined with the method of the median (Lea and Coulson, 1949; Rosche and Foster, 2000). Following mutation rates were determined:

d5	3.77×10^{-9}
d6	4.30×10^{-9}

The mutation rate therefore was about 5.5-fold higher than in the isogenic Rad27 proficient strain (compare section 3.3.3). However, it was successfully decreased in the *FBP1* assay compared to the *lys2ΔBgl* assay, where a mutation rate of 2.2×10^{-7} was determined (Heidenreich et al., unpublished). With the new *FBP1* assay, a reasonably number of replication-dependent revertants appeared, so that SC-Lactate plates still provided enough space for the expected replication-independent adaptive revertants. Therefore, the mutation assay could be proceeded to study adaptive mutations in the *rad27* knock out strain, whereas in the *lys2ΔBgl* system, experiments had to be broken off at this point.

For the determination of the mutation frequency, the number of replication-dependent colonies was subtracted. Mutation frequencies were calculated starting with day 6 or day 7.

According to the starting day, mutation frequency reached approximately 50 revertants per 10^{10} cells for the earlier starting point (Fig. 67 A) and 30 revertants per 10^{10} cells for the later starting point (Fig. 67 B). Unfortunately, even after six individual experiments the error bars were not diminished. Compared to mutation frequencies with YFAM revertants, the *rad27* knock out caused an approximately 3-fold increase in adaptive revertants.

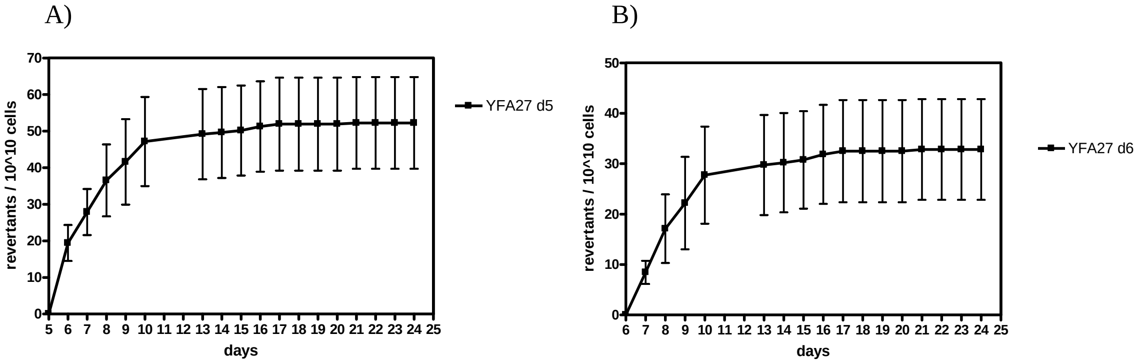
A) B)

Fig. 67. A) Time course of the accumulation of adaptive revertants starting day 6 determined from 6 individual experiments. B) Time course of the accumulation of adaptive revertants starting day 7 determined from 6 individual experiments.

The viability of arrested cells was monitored throughout the experiment. Half way through the experiment, cells still showed a survival of 40%. Around day 20 only 15 % viable cells were observed (Fig. 68).

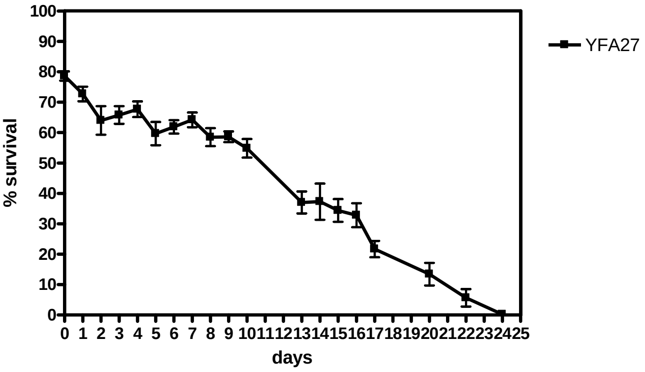

Fig. 68. Survival of arrested cells

3.4. *hTP53-FBP1* Fusiongene

Since the mutation frequency in the *FBP1* frameshift strain was low, the plan was to achieve an increase by preparing a bigger reversion window of a frameshift in a fusion construct, where the frameshift would act on the downstream *FBP1* gene. The human tumor suppressor gene p53 was chosen for this approach. From here on, *hTP53* will describe the coding human gene and p53 will refer to the tumor suppressor protein (Olivier and Taniere, 2011). Before the frameshift is inserted into the p53 and introduced into the yeast genome, it had to be tested if the fusion of p53 to the ORF of *FBP1* would have any effects on the enzyme activity of *FBP1*. Only if the function of the enzyme can be maintained, it makes sense to introduce a frameshift in p53 to continue with this strategy. Therefore, a strain with a fusion of p53 and *FBP1* was constructed in a first step without frameshift to be able to analyze the enzyme functionality first.

3.4.1. Construction of fusion strain *hTP53-FBP1* (YPF63)

The aim was to construct the strain YPF63, which should comprise a fusion of the human tumor suppressor p53 ORF upstream of *FBP1*. The gene p53 will be regulated by the *FBP1* promoter and will be in-frame with *FBP1*.

The host strain for the construction of the fusion strain will be the previously constructed URA^+ strain YUF, described in 3.3.1.

The human p53 ORF originated from the plasmid pC53-SN3. Since the backbone of this plasmid was uncertain, the p53 ORF was first rescued by subcloning into a defined backbone. The vector pC53-SN3 has two recognition sites for BamHI downstream and upstream of p53, so that the ORF with flanks can be cut from the plasmid. The plasmid pUC19 served as new backbone for p53 as shown in Fig. 69.

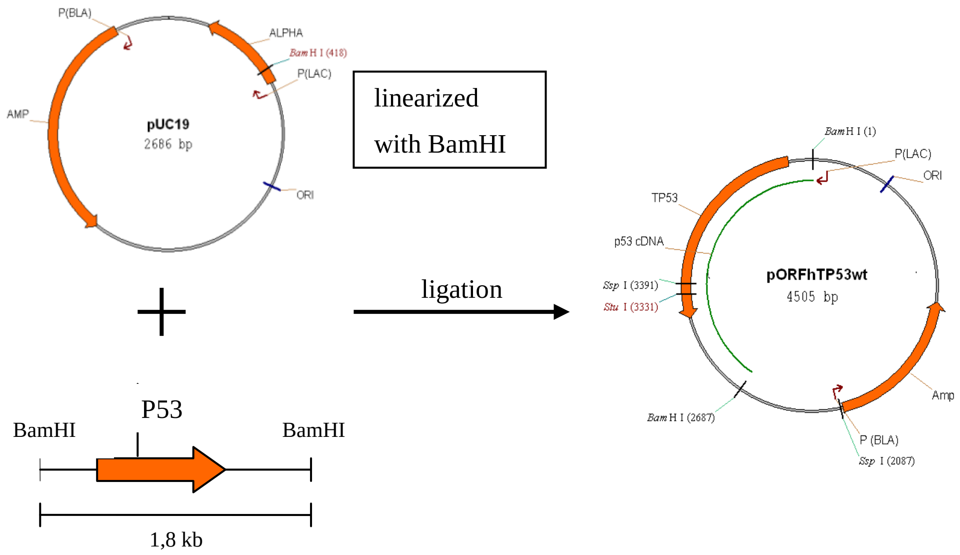
P(BLA)
ALPHA
BamH I (418)
P(LAC)
AMP
pUC19
2686 bp
ORI
linearized
with BamHI
+
ligation
P53
BamHI
BamHI
1,8 kb
BamH I (1)
P(LAC)
ORI
TP53
p53 cDNA
Ssp I (3391)
Stu I (3331)
pORFhTP53wt
4505 bp
Amp
BamH I (2687)
P (BLA)
Ssp I (2087)

Fig. 69. Construction of pORFhTP53wt from pUC19 as backbone and p53 as insert.

The cleaved pC53-SN3 resulted in two fragments of approximately 6000 bp and 1800 bp (Fig. 70). The smaller fragment was used to ligate with the linearized pUC19.

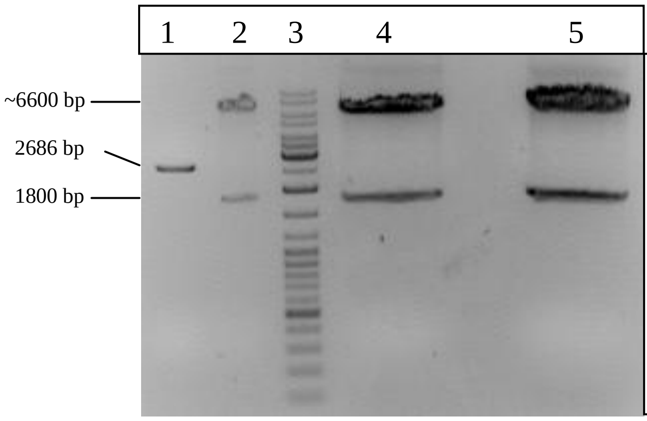

BamHI digest:

1 → pUC19 (1 µl)

2 → pC53-SN3 (4 µl)

3 → O'Gene Ruler DNA Ladder Mix (5µl)

4 → pC53-SN3 (6 µl)

5 → pC53-SN3 (8 µl)

Fig. 70. Preparative digests of pC53-SN3 and pUC19 with BamHI. 1800 bp from pC53-SN3 were cut from gel and the DNA purified.

The ligation was transformed in competent DH5α cells and positive clones selected with a Blue/White-Screening on X-Gal. Due to the linearization with BamHI the LacZ gene on pUC19 was destroyed. LacZ encodes the enzyme β-galactosidase, which metabolizes X-Gal, developing a blue dye. Consequently, clones that carry the religated pUC19 will form blue colonies due to their functional LacZ. On the contrary, clones with successful transformation of the ligated plasmid with *hTP53* are not able to cleave X-Gal due to lack of β-galactosidase and therefore produce white colonies.

Plasmid DNA of white colonies was isolated and restriction site analysis was performed to verify positive clones. Moreover, the possibility of concatemeres was ruled out with the single cutter enzyme StuI and the direction of integration of the insert determined with SspI.

Expected fragments are indicated below and the correct bands shown in Fig. 71:

BamHI	SspI	StuI
2686 bp	2786 bp	4505 bp
1800 bp	1719 bp	---

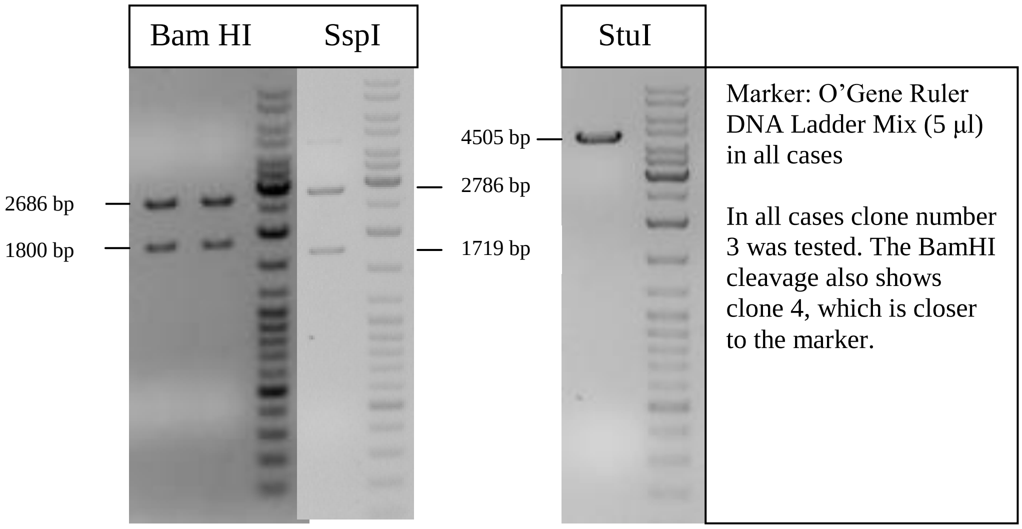

Marker: O’Gene Ruler DNA Ladder Mix (5 µl) in all cases

In all cases clone number 3 was tested. The BamHI cleavage also shows clone 4, which is closer to the marker.

Fig. 71. Control digests to verify pORFhTP53wt

Clone 3 was verified and defined the new plasmid pORFhTP53wt.
It was used as a template to amplify the *hTP53* gene for the fusion strain construction.

The *hTP53* ORF was amplified without its stopcodon in order to produce a direct fusion to the ORF of *FBP1*. By choosing appropriate megaprimer sequences, homologous ends were attached to the p53 ORF to target it to the *FBP1* locus.
PCR conditions and settings for PCR with the meagprimers MPp53for and MPp53rev are indicated below. Expected length of PCR product was 1296 bp as seen in Fig. 72.

step	Time [seconds]	Temperature °C
Initial denaturation	30	98
3 cycles of next 3 steps:		
Denaturation	*10*	*98*
Annealing	*30*	*68*
Extension	*39*	*72*
30 cycles of next 2 steps:		
Denaturation	*20*	*98*
Annealing	*80*	*72*
Final extension	300	72

50 µl reaction:
1 µl DNA
10 µl 5x HF buffer
1 µl dNTPs
2.5 µl MPp53for
2.5 µl MPp53rev
33 µl ddH$_2$O
0.5 µl Phusion Polymerase

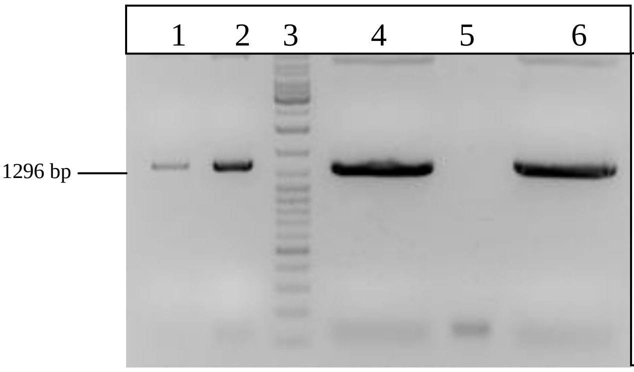
1
2
3
4
5
6
1296 bp

1 → 1 µl PCR product
2 → 5 µl PCR product
3 → O'Gene Ruler DNA Ladder Mix (5 µl)
4 → 20 µl PCR product
5 → negative control (5 µl)
6 → 20 µl PCR product

Fig. 72. Preparative gel of p53 amplification

The 1296 bp fragments were cut from the gel and the DNA purified. Afterwards, it was transformed into the URA$^+$ host strain YUF (Fig. 73). Since positive clones should replace the *URA3* marker with p53 (Fig. 74), negative selection for *URA3* occurred on 5-FOA plates.

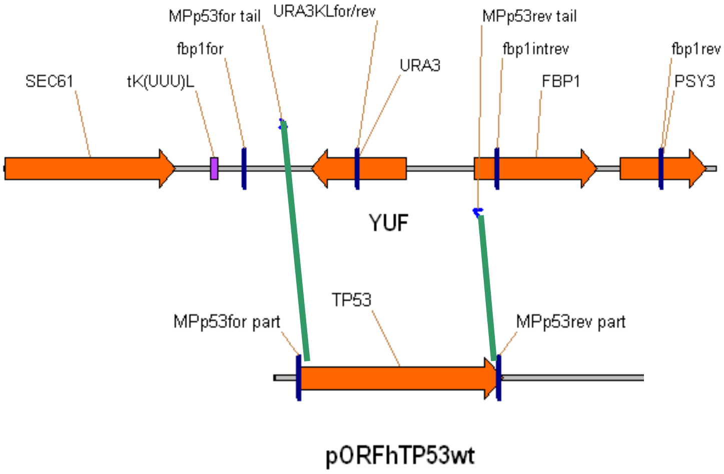
MPp53for tail
URA3KLfor/rev
MPp53rev tail
fbp1for
fbp1intrev
fbp1rev
URA3
SEC61
tK(UUU)L
FBP1
PSY3
YUF
TP53
MPp53for part
MPp53rev part
pORFhTP53wt

Fig. 73. Gene replacement of *URA3* with *hTP53* to fuse the new gene upstream of the *FBP1* gene. Green bold lines indicate sites of homologous recombination

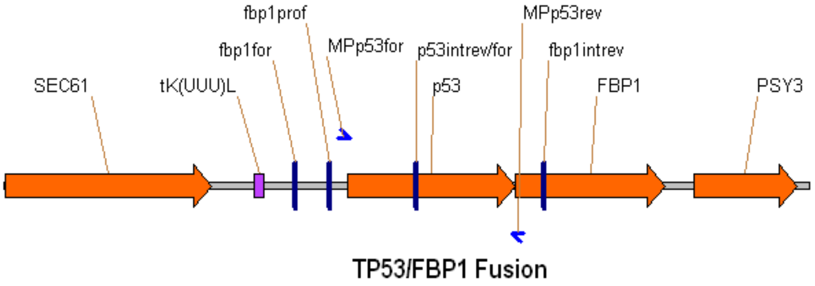
fbp1prof
MPp53rev
fbp1for
MPp53for
p53intrev/for
fbp1intrev
SEC61
tK(UUU)L
p53
FBP1
PSY3
TP53/FBP1 Fusion

Fig. 74. Genomic situation in new strain YPF63

Since during FOA selection difficulties occurred, the conditions for transformation were altered. The selection resulted in false positive clones of two different kinds. First, *URA3* forward mutants developed that were able to grow on FOA. Second, "loxP-artifacts" were present. The strain YUF contains parts of the plasmid pUG72 as described in 3.3.1. The marker gene *URA3* (*K.l.*) is flanked by direct repeats of 32 bp, which represent the loxP sites. Generally, those sites are present at the plasmid to be able to work with a cre/lox system (Gueldener et al., 2002; Guldener et al., 1996).

Due to the amplification of *URA3* with universal primers, it was inevitable to produce an amplicon with these loxP sites, since they are positioned internal of both universal primers. Consequently, the loxP sites were inevitably integrated into the yeast genome, when the strain YUF was constructed.

Some of the unwanted artifacts when using YUF as a host strain obviously are the result of recombination between the two loxP sites. Due to the homologous recombination of these two sites, the *URA3* gene is excluded from the genome and these clones were able to grow on FOA. However, such clones can be identified with PCR, since their PCR product resulted in a much shorter fragment. Nevertheless, to reduce false positive clones, some alterations during the LiAc transformation were tried. No improvement could be observed after an increase of ss salmon sperm DNA. On the contrary, a reduced heat shock time of 20 minutes instead of 40 minutes achieved a reduction of false positive colonies on negative control FOA plates. Consequently, all further transformations in regard to YUF as host strain were performed with a 20-minute heat shock.

Transformants were verified for their p53 integration into the genome with three PCRs. The first PCR was performed with two external primers fbp1for and fbp1intrev. All primers are indicated in Fig. 74. Clones with the correct length, show a band at 1756 bp, in contrast to the control YUF with 2169 bp as shown in Fig. 75 on the left gel.

step	Time [seconds]	Temperature °C
Initial denaturation	300	95
30 cycles of next 3 steps:		
Denaturation	*30*	*95*
Annealing	*30*	*56*
Extension	*80*	*72*
Final extension	300	72

25 µl reaction:
1 µl DNA
2.5 µl 10x buffer
1 µl dNTPs
1.5 µl fbp1for
1.5 µl fbp1intrev
0.5 µl $MgCl_2$
17 µl ddH_2O
0.15 µl Taq Polymerase (Qiagen)

Transformant that have been verified positive with the first PCR, were tested with two further PCRs with combination of an internal p53 primer and an external primer. PCR conditions were slightly altered. The extension time was decreased from 80 s to 39 s for both PCRs. The reaction mix was the same with exception of the primer pairs. In one case, p53intfor and fbp1intrev were combined, in the second case, p53intrev and fbp1for were used as primer pair. Fig. 75 (right) shows the expected fragment lengths, which is 916 bp in the first case and 864 bp in the second case.

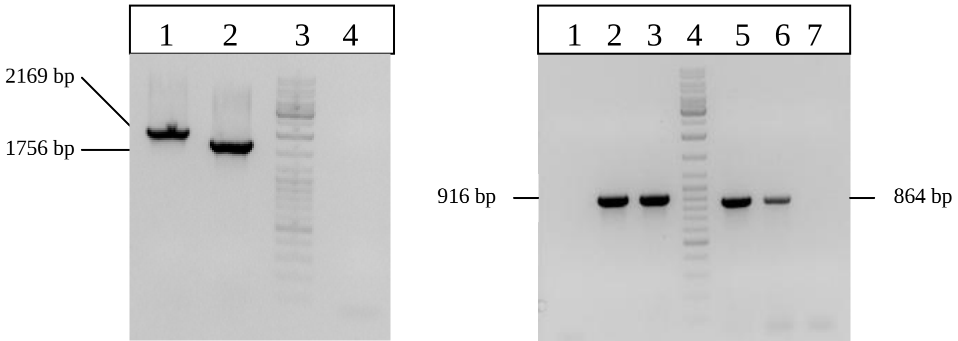

1 → positive control
YUF (5 µl)
2 → clone 63 (5 µl)
3 → O'Gene Ruler
DNA Ladder Mix (5 µl)
4 → negative control (5 µl)

p53intfor+fbp1intrev:
1 → negative control (5 µl)
2 → clone 63 (5 µl)
3 → clone 72 (5 µl)
4 → O'Gene Ruler DNA Ladder Mix (5 µl)
p53intrev+fbp1for:
5 → clone 63 (5 µl)
6 → clone 72 (5 µl)
7 → negative control (5 µl)

Fig. 75. Control PCRs for the verification of positive YPF63 clones

Furthermore, both clones were tested for their markers with replica plating. Additional to the typical marker tests of SC-ade, SC-trp, SC-his, SC-lys, SC-ura, YPG and MATa/α, clones were also replica plated on SC-Lactate. Positive clones should be able to grow on lactate due to a functional *FBP1* gene. Clone 63 was chosen to be the new strain YPF63.

YPF63: MATa *trp1-Δ his3-Δ200 ura3-52 lys2ΔBgl ade2-1o gal mal CUP*^{r} *FBP1::hTP53*

Generally, the construction of the strain turned out to be complicated. 53% of tested clones corresponded to the host strain YUF, 44% of the clones derived from loxP artifacts. Consequently, the remaining 3% were positive clones.

3.4.2. Reconstruction Assay with YPF63

The fusion strain of *hTP53* and *FBP1* was tested for the enzyme activity of Fbp1 in a reconstruction assay. If its activity is maintained, then colony formation on SC-Lactate should not be different compared to a control strain. The experiment was performed with strain YLBM as control and additionally clone 72 from the YPF63 construction. The *fbp1*-deficient strain YΔF1 was used as background strain to provoke nutrient competition.

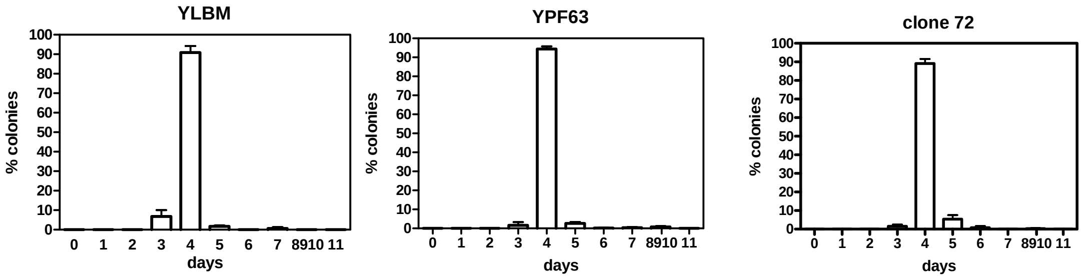

Fig. 76. Reconstruction assay of YLBM (control), YPF63 and clone 72

In all three cases the first colonies appeared on day 3 and a peak was observed on day 4 as shown in Fig. 76. Colony formation appeared homogenous. Consequently, no negative effect of the gene fusion could be observed and it could be concluded that the Fbp1 enzyme function was maintained.

3.5. *hTP53* +1 Frameshift

After verification that the fbp1 enzyme activity stays intact after a fusion between the genes *hTP53* and *FBP1*, a frameshift could be inserted.

3.5.1. Frameshift insertion strategy in *hTP53-FBP1*

The concept of the insertion of the frameshift in *hTP53* meets slightly different criteria than for the frameshift construction directly in the *FBP1* gene. The introduced frameshift in *hTP53* will act directly on the downstream situated in-frame *FBP1* ORF. One major difference is, that in the case of *hTP53* I have more freedom to choose a reversion window since cells are not dependent on the protein function of hTP53. The effect of changes in amino acid sequences is not relevant within hTP53. Furthermore, no special attention has to be paid to active centers or conserved regions in order not to harm them. Without these restrictions, it was possible to choose a reversion window that consisted of 316 nt. On the contrary, the reversion window in the *FBP1* FS+1 strain was only 176 nt. The hope was to achieve higher mutation frequencies in adaptive mutation assays due to a bigger reversion window.

No special notice was necessary to which nucleotide was used to insert the frameshift. The aspect to create a new recognition site by virtue of the frameshift was considered but was not possible at this position. The choice fell on guanine between position 319 and 320 nt, which created the new amino acid valine.

Basics of the principle of a frameshift mutation were described in 3.3.2.

Details of the *hTP53* frameshift insertion are shown in Fig. 77. The underlined sequence indicates the primer p53ins1. It contains the extra nucleotide guanine to introduce a +1 frameshift. The resulting reversion window is defined by the two out-of-frame stop codons, located at positions 128 nt and 444 nt. No other stop codons interfere within this range.

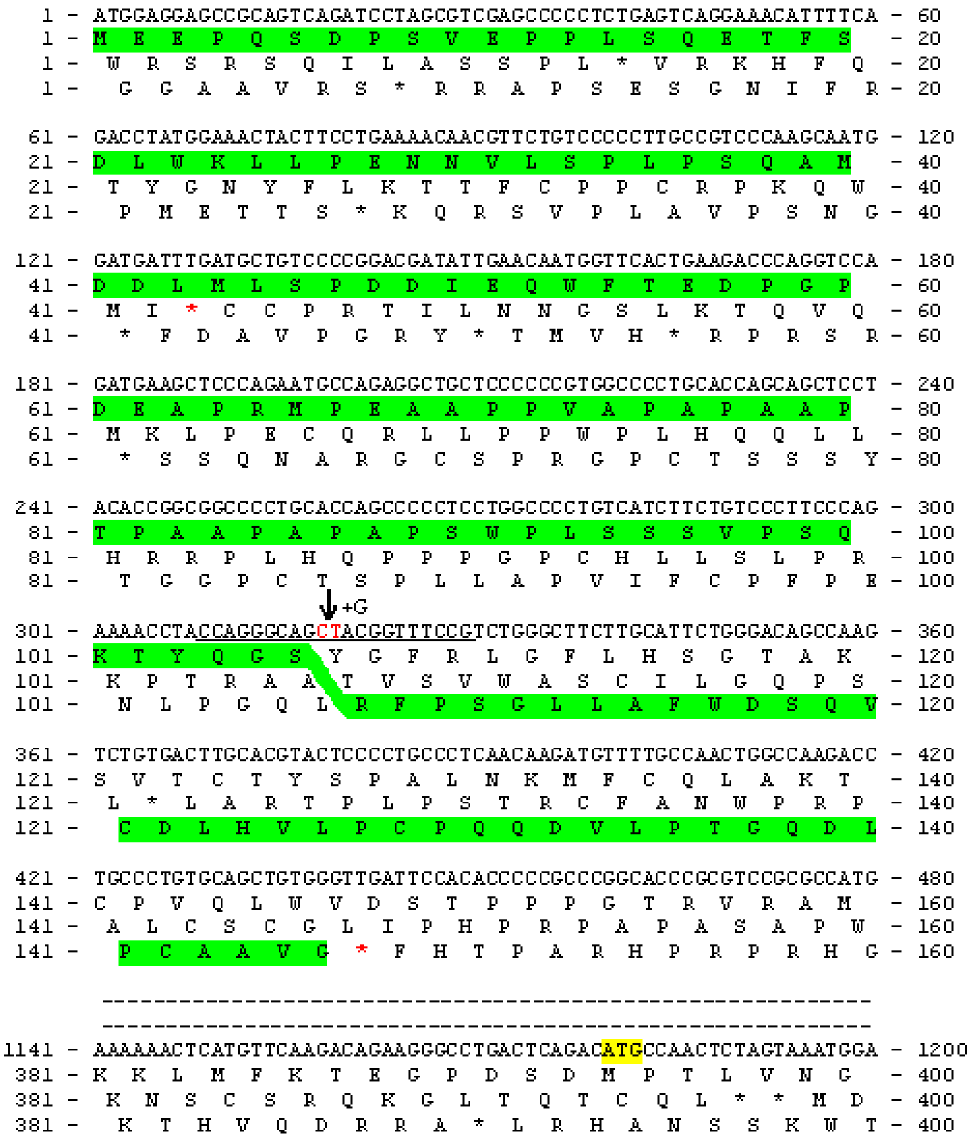

```
   1 - ATGGAGGAGCCGCAGTCAGATCCTAGCGTCGAGCCCCCTCTGAGTCAGGAAACATTTTCA - 60
   1 - M  E  E  P  Q  S  D  P  S  V  E  P  P  L  S  Q  E  T  F  S   - 20
   1 -  W  R  S  R  S  Q  I  L  A  S  S  P  L  *  V  R  K  H  F  Q  - 20
   1 -   G  G  A  A  V  R  S  *  R  R  A  P  S  E  S  G  N  I  F  R - 20

  61 - GACCTATGGAAACTACTTCCTGAAAACAACGTTCTGTCCCCCTTGCCGTCCCAAGCAATG - 120
  21 - D  L  W  K  L  L  P  E  N  N  V  L  S  P  L  P  S  Q  A  M   - 40
  21 -  T  Y  G  N  Y  F  L  K  T  T  F  C  P  P  C  R  P  K  Q  W  - 40
  21 -   P  M  E  T  T  S  *  K  Q  R  S  V  P  L  A  V  P  S  N  G - 40

 121 - GATGATTTGATGCTGTCCCCGGACGATATTGAACAATGGTTCACTGAAGACCCAGGTCCA - 180
  41 - D  D  L  M  L  S  P  D  D  I  E  Q  W  F  T  E  D  P  G  P   - 60
  41 -  M  I  *  C  C  P  R  T  I  L  N  N  G  S  L  K  T  Q  V  Q  - 60
  41 -   *  F  D  A  V  P  G  R  Y  *  T  M  V  H  *  R  P  R  S  R - 60

 181 - GATGAAGCTCCCAGAATGCCAGAGGCTGCTCCCCCCGTGGCCCCTGCACCAGCAGCTCCT - 240
  61 - D  E  A  P  R  M  P  E  A  A  P  P  V  A  P  A  P  A  A  P   - 80
  61 -  M  K  L  P  E  C  Q  R  L  L  P  P  W  P  L  H  Q  Q  L  L  - 80
  61 -   *  S  S  Q  N  A  R  G  C  S  P  R  G  P  C  T  S  S  S  Y - 80

 241 - ACACCGGCGGCCCCTGCACCAGCCCCCTCCTGGCCCCTGTCATCTTCTGTCCCTTCCCAG - 300
  81 - T  P  A  A  P  A  P  A  P  S  W  P  L  S  S  S  V  P  S  Q   - 100
  81 -  H  R  R  P  L  H  Q  P  P  P  G  P  C  H  L  L  S  L  P  R  - 100
  81 -   T  G  G  P  C  T  S  P  L  L  A  P  V  I  F  C  P  F  P  E - 100
                        ↓+G
 301 - AAAACCTACCAGGGCAGCTACGGTTTCCGTCTGGGCTTCTTGCATTCTGGGACAGCCAAG - 360
 101 - K  T  Y  Q  G  S  Y  G  F  R  L  G  F  L  H  S  G  T  A  K   - 120
 101 -  K  P  T  R  A  A  T  V  S  V  W  A  S  C  I  L  G  Q  P  S  - 120
 101 -   N  L  P  G  Q  L  R  F  P  S  G  L  L  A  F  W  D  S  Q  V - 120

 361 - TCTGTGACTTGCACGTACTCCCCTGCCCTCAACAAGATGTTTTGCCAACTGGCCAAGACC - 420
 121 - S  V  T  C  T  Y  S  P  A  L  N  K  M  F  C  Q  L  A  K  T   - 140
 121 -  L  *  L  A  R  T  P  L  P  S  T  R  C  F  A  N  W  P  R  P  - 140
 121 -   C  D  L  H  V  L  P  C  P  Q  Q  D  V  L  P  T  G  Q  D  L - 140

 421 - TGCCCTGTGCAGCTGTGGGTTGATTCCACACCCCCGCCCGGCACCCGCGTCCGCGCCATG - 480
 141 - C  P  V  Q  L  W  V  D  S  T  P  P  P  G  T  R  V  R  A  M   - 160
 141 -  A  L  C  S  C  G  L  I  P  H  P  R  P  A  P  A  S  A  P  W  - 160
 141 -   P  C  A  A  V  G  *  F  H  T  P  A  R  H  P  R  P  R  H  G - 160

        ------------------------------------------------------------
        ------------------------------------------------------------
1141 - AAAAAACTCATGTTCAAGACAGAAGGGCCTGACTCAGACATGCCAACTCTAGTAAATGGA - 1200
 381 - K  K  L  M  F  K  T  E  G  P  D  S  D  M  P  T  L  V  N  G   - 400
 381 -  K  N  S  C  S  R  Q  K  G  L  T  Q  T  C  Q  L  *  *  M  D  - 400
 381 -   K  T  H  V  Q  D  R  R  A  *  L  R  H  A  N  S  S  K  W  T - 400
```

Fig. 77. Relevant part of the wt *hTP53* ORF; nucleotides 481-1140 are not shown (indicated by dashed lines). Last nucleotides of *hTP53* from 1141-1179 are shown with the in-frame-fusion to wt *FBP1* ORF. Yellow ATG represents start codon of *FBP1* gene. Stars indicate stopcodons in the reading frames. Red stars define the reversion window. Underlined sequence corresponds to primer p53ins1 that introduces the frameshift mutation. Red CT at position 319 and 320 is the position where one G is inserted for the +1 frameshift. Green bold line indicates the truncated reading frame of the resulting frameshift allele.

3.5.2. Construction of YPFA

The principle how the mutation was inserted into the *hTP53* is based on the mutagenesis PCR in two steps, which was described in detail in 2.2.1.9.

As a template, the previously constructed plasmid pORFhTP53wt was used to insert the frameshift.

The primer p53ins1 includes the +1 insertion. The primer pUCPD, situated external of p53 was used as the second primer. Conditions for the first PCR of the mutagenesis are indicated below. Expected fragment length was 715 bp as shown in Fig. 78.

step	**Time [seconds]**	**Temperature °C**
Initial denaturation	30	98
30 cycles of next 2 steps:		
Denaturation	*10*	*98*
Annealing + Extension	*28*	*72*
Final extension	300	72

50 µl reaction:
1 µl pORFhTP53wt 1:1000
10 µl 5x HF buffer
1 µl dNTPs
2.5 µl p53ins1
2.5 µl pUCPD
33 µl ddH_2O
0.5 µl Phusion Polymerase (Finnzymes)

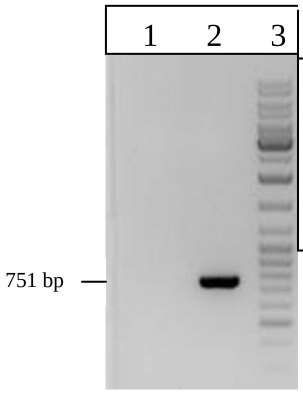

1 → negative control insertion (5 µl)

2 → PCR product 1 insertion (5 µl)

3→ O'Gene Ruler DNA Ladder Mix (5 µl)

Fig. 78. PCR product 1 of first mutagenesis PCR step for insertion in *hTP53*.

The PCR product was purified with GFX columns and prepared for the second PCR. The purified product was used as one primer in the second PCR together with the primer p53UTRrev.

step	**Time [seconds]**	**Temperature °C**
Initial denaturation	30	98
30 cycles of next 2 steps:		
Denaturation	*10*	*98*
Annealing + Extension	*33*	*72*
Final extension	300	72

50 µl reaction:
1 µl pORFhTP53wt 1:10, 000
10 µl 5x HF buffer
1 µl dNTPs
1.6 µl PCR product 1 (insertion)
1.26 µl p53UTRrev
33.14 µl ddH$_2$O
0.5 µl Phusion Polymerase (Finnzymes)

Two “negative” controls were prepared. Since it could not be avoided that the first PCR product still contains remaining template, it will be inevitably present at the second PCR. Consequently, the classical negative control will also result in two PCR products like the sample reaction itself. Therefore, an additional negative control without the primer pUCPD was performed. This reaction should result in no amplification but only the band from the first PCR product, which is included as only primer.

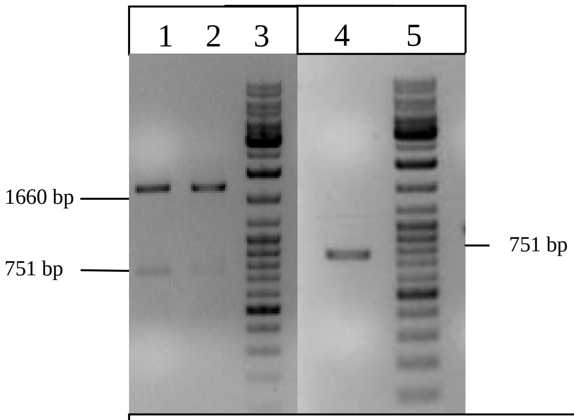

1 → negative control (5 µl)
2 → PCR product 2 (5 µl)
3 → O’Gene Ruler DNA Ladder Mix (5 µl)
4→ neg. control w/o second primer (5 µl)
5 → O’Gene Ruler DNA Ladder Mix (5 µl)

Fig. 79. Second mutagenesis PCR products of insertion in *hTP53*.

As evident from Fig. 79, the mutagenesis PCR to introduce a +1 frameshift produced the correct fragment of 1660 bp. The controls showed the expected bands from the first PCR product as well as the second PCR product from remaining template in the case of the variant with both primers. The PCR product 2 was clearly dominant compared to the band resulting from PCR product 1.

The 1660 bp fragment was purified by precipitating the DNA as described in Materials and Methods 2.2.1.11. The precipitated DNA of the PCR product was digested with two enzymes in order to reduce the PCR derived product to only 425 bp. Subsequently, this fragment was ligated into the original plasmid to create a plasmid carrying *hTP53* with a frameshift (Fig. 80). The two enzymes used were Bsu36I and SgrAI.

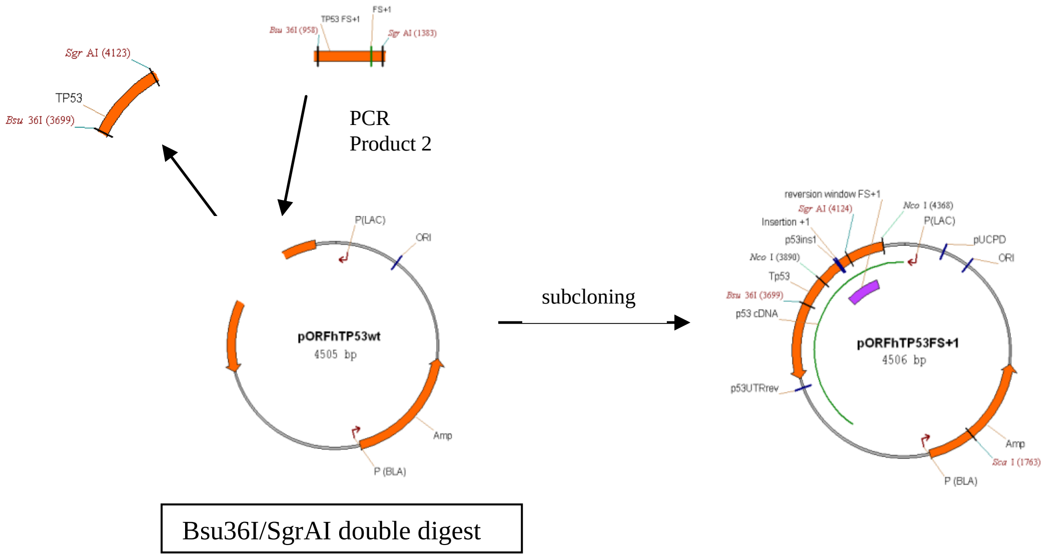
Sgr AI (4123)
TP53
Bsu 36I (3699)
FS+1
TP53 FS+1
Bsu 36I (958)
Sgr AI (1383)
PCR
Product 2
P(LAC)
ORI
pORFhTP53wt
4505 bp
Amp
P (BLA)
Bsu36I/SgrAI double digest
subcloning
reversion window FS+1
Sgr AI (4124)
Insertion +1
p53ins1
Nco I (3890)
Tp53
Bsu 36I (3699)
p53 cDNA
p53UTRrev
Nco I (4368)
P(LAC)
pUCPD
ORI
pORFhTP53FS+1
4506 bp
Amp
Sca I (1763)
P (BLA)

Fig. 80. Construction of pORFhTP53FS+1 from wt plasmid and PCR product 2

After transformation and selecting transformants on LB_{amp} plates, their plasmid DNA was verified with restriction site analysis with the enzymes NcoI and ScaI. Since NcoI cleaved within the sequence that was derived from PCR product 2, concatemeres could be excluded. The restriction site of ScaI was situated in the vector backbone. Correct clones showed a pattern of 2127 bp, 1901 bp and 478 bp as shown in Fig. 81. The double digest was performed with Promega enzymes o/n at 37°C.

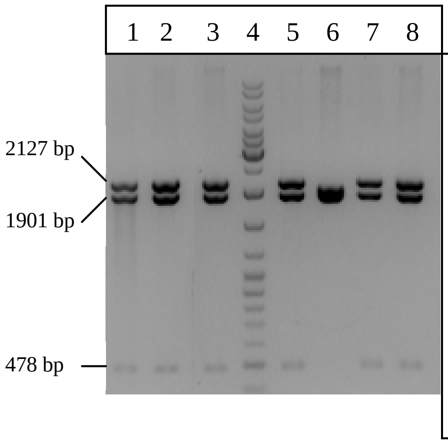
1
2
3
4
5
6
7
8
2127 bp
1901 bp
478 bp

1 → clone 1(6 µl)
2 → clone 2 (6 µl)
3 → clone 4 (6 µl)
4→ O’Gene Ruler DNA Ladder Mix (5 µl)
5 → clone 6 (6 µl)
6 → clone 7 (6 µl)
7 → clone 9 (6 µl)
8 → clone 10 (6 µl)

Fig. 81. Control digest of pORFhTP53FS+1 with NcoI and ScaI as double digest.

According to the control digest, clone 7 was the only one that did not show the correct two bands. Rest of candidates obtained the correct fragments. Clones 2 and 6 were sequenced at VBC Genomics and had to be discarded due to a mutation in the SgrAI recognition site. A following restriction reaction with SgrAI confirmed the sequencing result, that the site could not be recognized. Consequently, no cleavage occurred. Subsequently, the rest of the clones were analyzed for their recognition sites of SgrAI and Bsu36I, respectively in a single digest, since they were not active in the same buffer. Plasmid DNA of correct clones was linearized in both cases to obtain a band at 4506 bp.

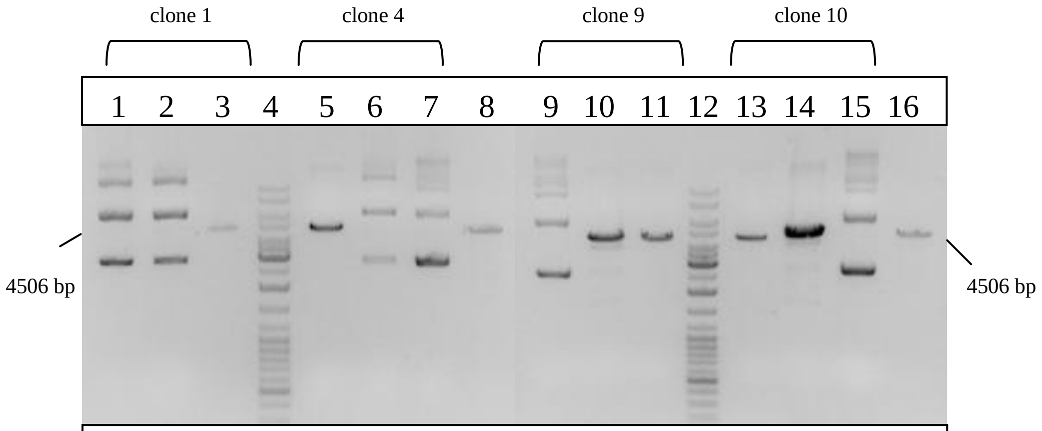

lanes 4 and 12 → O’Gene Ruler DNA Ladder Mix (5 µl)
control (undigested DNA of clones in SgrAI buffer) → lanes 1, 7, 9, 15
positive control: pORFhHTP53wt digested with SgrAI → lanes 8 and 16
SgrAI digest → lanes 2, 6, 10, 14
Bsu36I digest → lanes 3, 5, 11, 13

Fig. 82. Verification of intact subcloning sites in candidates for pORFhTP53FS+1

Fig. 82 shows that the SgrAI digest of clones 1 and 4 result in the same pattern as their undigested DNA, meaning that the restriction site was destroyed. Clones 9 and 10 are the only ones with both intact sites of the subcloning enzymes SgrAI and Bsu36I. From both plasmids the relevant part of the DNA was sequenced and verified. Clone 9 was defined as the new plasmid. The new vector pORFhTP53FS+1 was successfully constructed.

In the next steps the ORF of *hTP53* without stopcodon carrying the frameshift mutation was amplified with megaprimers and transformed in the URA^+ strain YUF (Fig. 83) to create the new frameshift strain YPFA (Fig. 84).

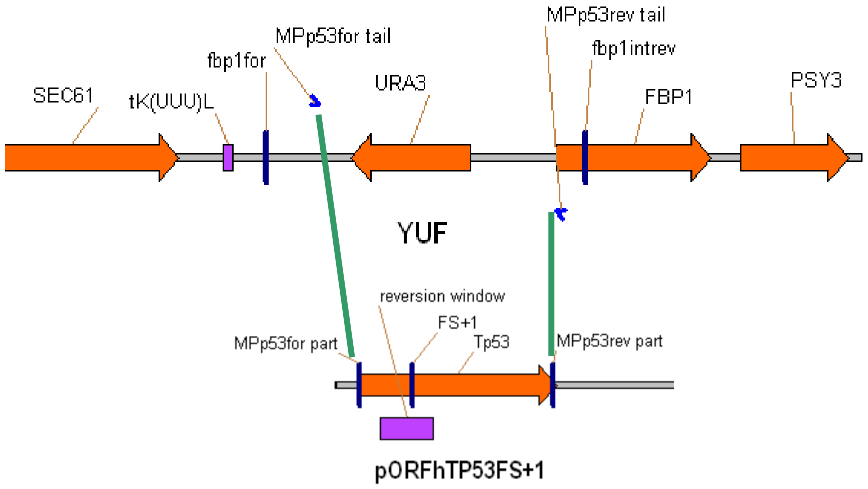
MPp53for tail
MPp53rev tail
fbp1for
fbp1intrev
SEC61
tK(UUU)L
URA3
FBP1
PSY3
YUF
reversion window
FS+1
MPp53for part
Tp53
MPp53rev part
pORFhTP53FS+1

Fig. 83. Gene replacement of *hTP53* FS+1 with *URA3*. Green bold lines indicate sites of homologous recombination

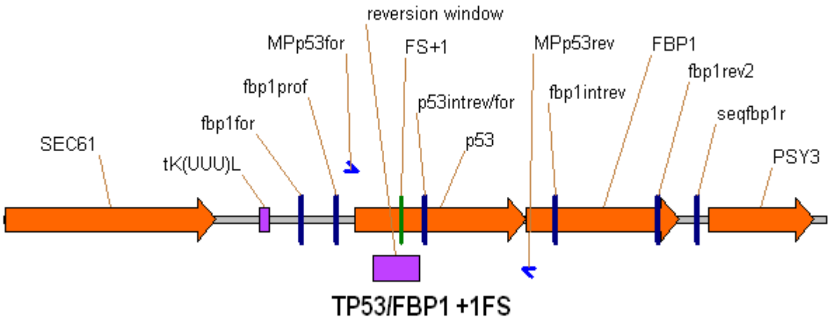
reversion window
MPp53for
FS+1
MPp53rev
FBP1
fbp1prof
p53intrev/for
fbp1intrev
fbp1rev2
fbp1for
p53
seqfbp1r
SEC61
tK(UUU)L
PSY3
TP53/FBP1 +1FS

Fig. 84. New genomic situation of strain YPFA

The settings for PCR and the reaction mix are described below. The PCR Product was loaded on a 1% agarose gel and the 1296 bp band cut from the gel (Fig. 85) for following DNA purification with GFX columns.

step	Time [seconds]	Temperature °C
Initial denaturation	30	98
3 cycles of next 3 steps:		
Denaturation	*10*	*98*
Annealing	*30*	*68*
Extension	*39*	*72*
30 cycles of next 2 steps		
Denaturation	*20*	*98*
Extension	*80*	*72*
Final extension	480	72

50 µl reaction:
1 µl pORFhTP53FS+1 1:100
10µl 5x HF buffer
1 µl dNTPs
2.5 µl MPp53for
2.5 µl MPp53rev
33 µl ddH$_2$O
0.5 µl Phusion Polymerase (Finnzymes)

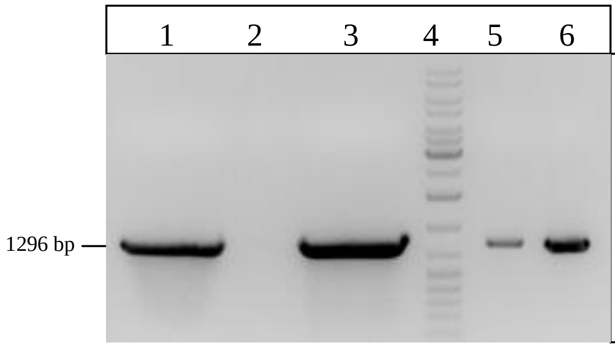

1 → PCR product (22 µl)
2 → neagtive control (6 µl)
3 → PCR product (22 µl)
4→ O'Gene Ruler DNA Ladder Mix (5 µl)
5 → PCR product (1 µl)
6 → PCR product (5 µl)

Fig. 85. Preparative gel of *hTP53* FS+1 amplification

After LiAc-transformation in the host strain YUF, cells were selected on 5-FOA to obtain clones that replaced the *URA3* gene with the *hTP53* frameshift gene. Genomic DNA was isolated and control PCRs performed. The first PCR was performed for multiple clones with two external primers fbp1for and fbp1intrev to distinguish positive clones in their length (Fig. 86).

step	Time [seconds]	Temperature °C
Initial denaturation	300	95
30 cycles of next 3 steps:		
Denaturation	*30*	*95*
Annealing	*30*	*56*
Extension	*80*	*72*
Final extension	300	72

25 µl reaction:
1 µl DNA
2.5 µl 10x buffer
1 µl dNTPs
1.5 µl fbp1for
1.5 µl fbp1intrev
0.5 µl $MgCl_2$
17 µl ddH_2O
0.15 µl Taq Polymerase (Qiagen)

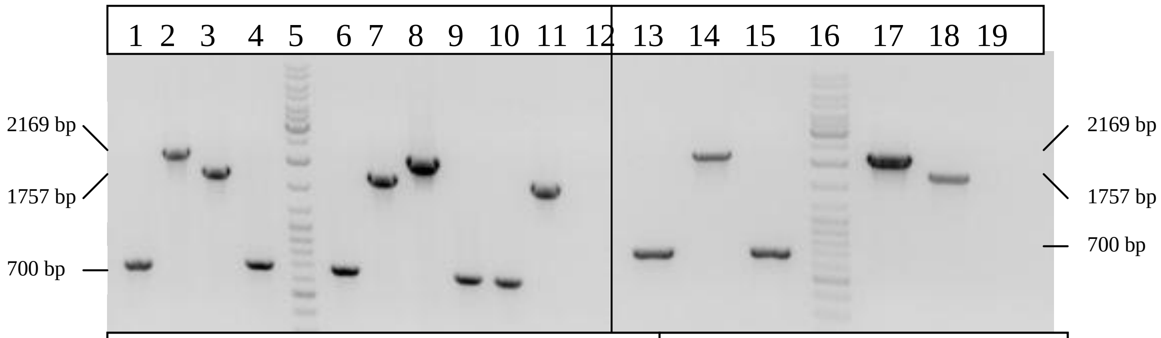

1 → clone 1(5 µl)	10 → clone 8 (5 µl)
2 → clone 2 (5 µl)	11 → clone 9 (5µl)
3 → clone 3 (5µl)	12 → negative control (5 µl)
4 → clone 4 (5 µl)	13 → clone 10
5/16 → O'Gene Ruler DNA Ladder Mix (5 µl)	14 → clone 11 (5 µl)
6 → clone 5 (5 µl)	15 → clone 13 (5 µl)
7 → clone 6 (5 µl)	17 → positive control YUF (5 µl)
8 → positive control YUF (5 µl)	18 → clone 14 (5 µl)
9 → clone 7 (5 µl)	19 → negative control (5 µl)

Fig. 86. Control PCR with two external primers fbp1for and fbp1intrev

Two clones (2 and 11) showed the same length as the positive control YUF, meaning that *URA3* was not replaced by *hTP53*. Seven transformants produced a PCR product at 700 bp, which corresponds to loxP-artifacts mentioned in section 3.4.1. Four positive clones (3, 6, 9, 14) could be obtained with a band at 1757 bp. Those were further analyzed with two PCRs with the combination of one internal and one external primer.

For the control PCR with the primer pair of a p53 internal primer and one external, the only alterations for the PCR program was a decrease in extension time to 39 seconds. The reaction mix varied in the primer pair combination, which were p53intfor + fbp1intrev as well as fbp1for + p53intrev, respectively. In this case a positive control could be used since the DNA of the previously constructed fusion strain YPF63 yielded the same fragments. All four clones obtained PCR products, meaning that *hTP53* is present in the DNA. Furthermore they resulted in the same length of 864 bp and 916 bp respectively as their positive control YPF63 (Fig.87).

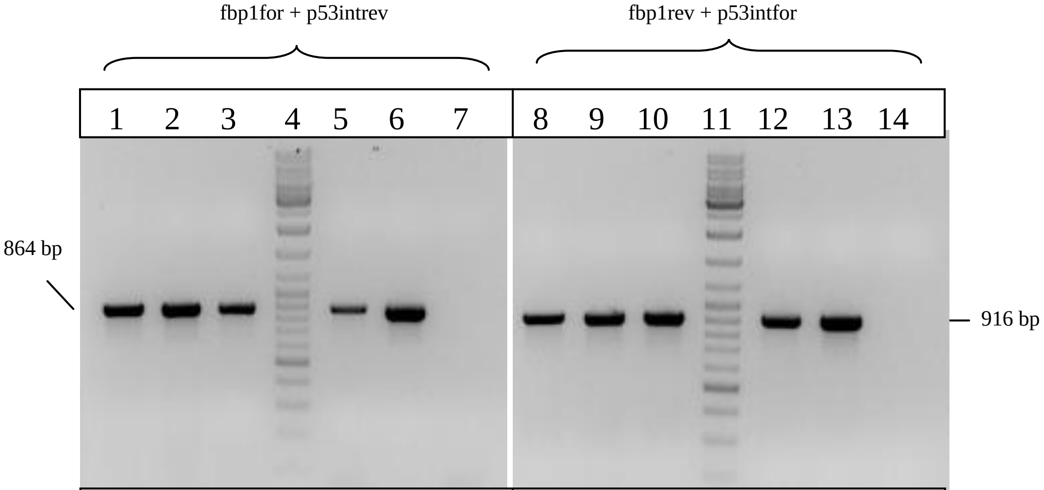

1 → clone 3 (5 µl)
2 → clone 6 (5 µl)
3 → clone 9 (5µl)
4 → O'Gene Ruler DNA Ladder Mix (5 µl)
5 → clone 14 (5 µl)
6 → positive control YPF63 (5 µl)
7 → negative control (5 µl)

8 → clone 3 (5 µl)
9 → clone 6 (5 µl)
10 → clone 9 (5µl)
11 → O'Gene Ruler DNA Ladder Mix (5 µl)
12 → clone 14 (5 µl)
13 → positive control YPF63 (5 µl)
14 → negative control (5 µl)

Fig. 87. Control PCR with combination of internal and external primer.

Clone 6 was sequenced and its sequence with the inserted frameshift verified.

However, further analysis showed that -for unknown reasons- this clone did not revert on SC-Lactate plates. Due to the inserted frameshift, reversion events, which allow the clone to form colonies on SC-Lactate, should occur. Different cell densities were plated onto SC-Lactate plates but no colonies arose over a time course of 12 days. Consequently, the three remaining clones were analyzed for their ability to revert on SC-Lactate. Interestingly, only one clone (clone 3) produced revertants. Thus, this exact clone was sequenced, confirmed and defined as the new frameshift strain YPFA.

Additionally, marker tests by replica plating were performed, confirming following phenotype:

YPFA: MATa *trp1-Δ his3-Δ200 ura3-52 lys2ΔBgl ade2-1o gal mal* CUP^r
fbp1::hTP53FS-320

3.5.3. Adaptive mutation assay with YPFA

Before the adaptive mutation assay was performed, some pilot-experiments were done to characterize the strain YPFA better since only one out of four positive clones reverted on SC-Lactate. The tests performed on SC-Lactate at the end of the strain construction to verify if the clone was able to revert, revealed slightly smaller colonies than revertants of the non-fusion strain YFAM. Even though SC-Lactate was defined as the media of choice, the strain was tested on a combination of lactate with pyruvate and glycerol, respectively.

The setup of the pilot-experiment resembled the starvation assay described in 3.1.2. Two individual experiments were performed. An isolated colony of YPFA was inoculated in 150 ml YPD liquid and incubated o/n at 30°C in an incubator shaker. 19 plates per medium were streaked with 1 x 10^8 cells, whereas 6 plates were used for the determination of residual proliferation, 5 plates were used to check on colony formation each day and the remaining plates were reserved for the determination of survival. Residual proliferation was determined for days 0-3 by rinsing cells from two plates per media per point of time. However, this was not possible for the second series, since on day 3 colonies smaller than 0.5 mm appeared already. Therefore, the plates could not be rinsed for the determination of cells/plate due to the colonies and residual proliferation was only indicated for day 0-2 in Fig. 88A). Curves are similar to the previously determined residual proliferation of the *FBP1* knock out strain YΔF1. Cells entered the cell cycle arrest as expected and residual proliferation was absent in all media types. The determined survival showed that the arrested cells stayed reasonably viable throughout the experiment (Fig. 88B).

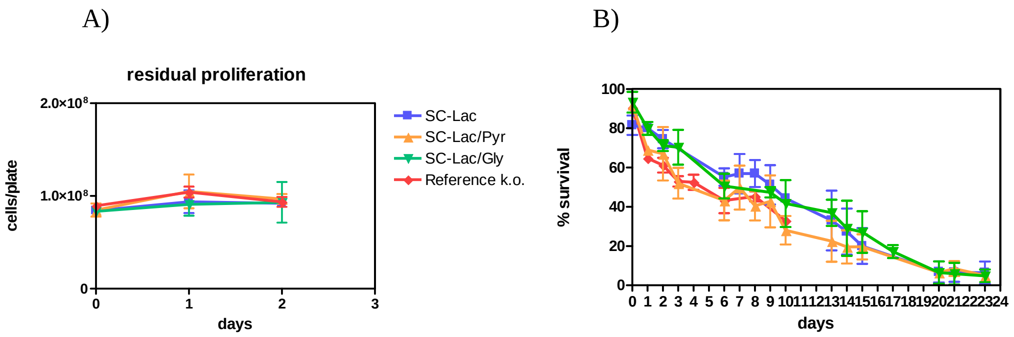

Fig. 88. Residual proliferation of YPFA on different media (A) and survival of arrested cells (B). Red curve represents a reference of YΔF1 on SC-Lactate. For YΔF1 only days 0-10 were monitored.

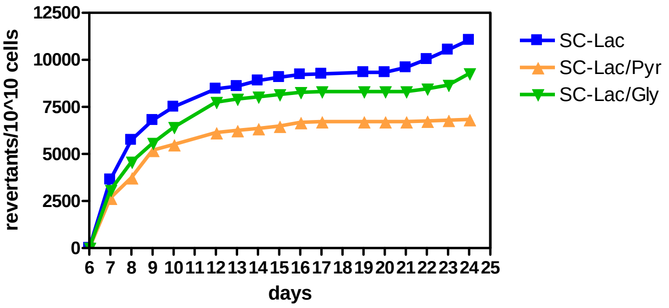

Fig. 89. Frequencies of newly arising colonies of YPFA on different carbon sources.

Mutation frequencies as evident from Fig. 89 are definitely higher than with the *FBP1* FS+1 strain. It was observed that colonies appear with a delay of one day in case of the mixture of lactate and pyruvate, therefore this type of nutrient is no option. If lactate as a single nutrient resource is compared to the mixture with glycerol, no significant differences appeared. Residual proliferation and survival are equal. The phenotype of colonies was comparable as well. A slight increase in mutation frequency was observed for starvation on SC-Lactate when offered as a single carbon source.

To be able to compare data of adaptive mutation frequencies with the results of YFAM and YFA27, it was decided that the carbon source was not altered for adaptive mutation assays for YPFA. Due to the data of the pilot project, a high number of newly arising colonies was expected. Thus, the experimental setup of the adaptive mutation assay as described in 2.2.2.4. was changed for the plated cell density. Inoculation of colonies occurred in 1 ml YPD instead of 4 ml, in order to be able to plate a cell density of approximately 2.5 x 10^7 cells/plate.

As described in the adaptive mutation assay with *FBP1* (3.3.3.) two models for when to draw a line between replication-dependent and replication-independent revertants are offered. In one case day 5 was supposed to include all early arising colonies whereas in the second version also colonies developed on day 6 are included.

Mutation rates were determined for day 5 and day 6 with the method of the median (Lea and Coulson, 1949; Rosche and Foster, 2000). For day 5 mutation rates reached 1.01 x 10^{-7} and for day 6 1.7 x 10^{-7}.

Furthermore, mutation frequencies were also determined starting with day 5 or 6. If day 6 was considered the first day for the appearance of adaptive mutations, then an accumulation of 5.5 x 10^{4} out of 10^{10} cells was observed on SC-Lactate over a time course of 24 days. If day 7 was considered the starting day for adaptive revertants, mutation frequencies of 5 x 10^{4} /10^{10} cells were reached after 24 days (Fig. 90).

Compared to mutation frequencies obtained with the *FBP1* frameshift strain YFAM, the *hTP53* FS+1 fusion with *FBP1* achieves approximately 3500 times higher frequencies. Furthermore, the data can be compared with the derived data from the pilot experiment, where approximately 10000 revertants/10^{10} cells appeared. However, since the experimental setup was not the same (in regard to culture volume, cell density and scale), the comparison is not valid and can only indicate an idea of how many colonies should be expected. The adaptive mutation assay derived 5 times higher frequency than in the starvation pilot experiment.

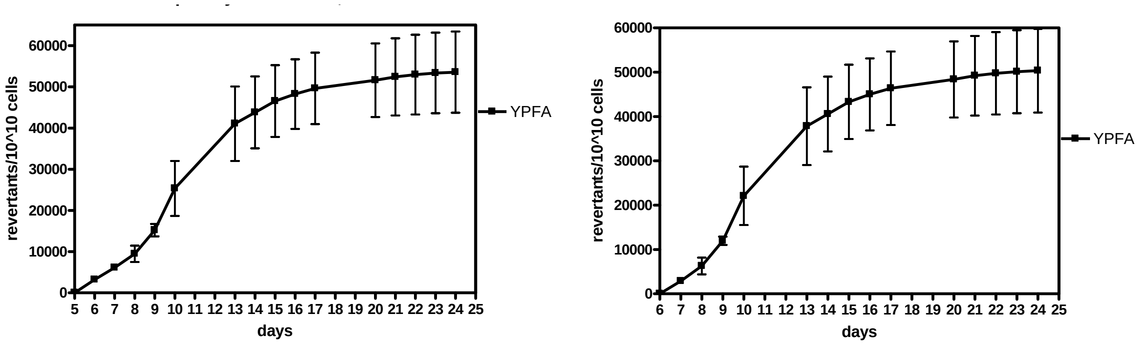

Fig. 90. Time course of the accumulation of adaptive revertants of YPFA starting day 6 (on the left) or day 7 (on the right). Average of 4 independent experiments is shown.

The determined survival curve showed that the arrested cells stayed viable throughout the experiment (Fig. 91). Approximately 50% survived until day 10 and 10% of the cells were still viable at the end of the experiment.

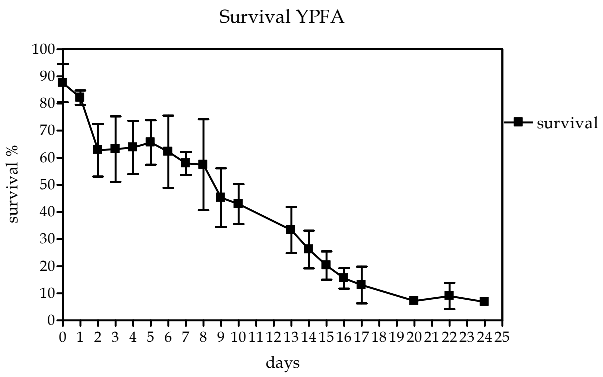

Fig. 91. Survival of arrested YPFA cells.

During the pilot-experiments and the adaptive mutation assay with YPFA I observed differences in the phenotype of colonies. In some cases colonies remained smaller than usual.

Newly arising colonies after day 6 sometimes only reached a diameter of 1 mm, whereas colonies from the *FBP1* FS+1 strain YFAM reached a diameter of approximately 3 mm. Furthermore, these colonies turned brown after 18 days on SC-Lactate plates. This phenomenon was not observed with revertants from the frameshift strains YFAM or YFA27. It was also interesting that the phenotype was not uniform in all experiments. Compared to the pilot-experiments, colonies grew bigger in some series of the adaptive mutation assay.

3.5.4. Endeavors to optimize *hTP53-FBP1* fusion strain

Due to the phenotype problems described above, I tried to optimize the strain to achieve an improved growth in regard to size and color of colonies as well as a uniform phenotype in general.

The idea was to change the so called Kozak consensus sequence, which is a nucleotide sequence of the 5’ translation initiation region and is recognized by ribosomes as the translational start. Studies showed that the sequence affects the translation efficiency. Therefore, the amount of protein synthesized depends on the sequence of the Kozak sequence. The sequence defines strong vs. weak consensus, according to six nucleotides upstream of the start codon of a ORF and three nucleotides downstream of the start codon (Kozak, 1987).

It was found that the optimal consensus sequence in *Saccharomyces cerevisiae* is rich in A-residues compared to mammalian Kozak consensus sequence. The Kozak consensus sequence in budding yeast is the following (Hamilton et al., 1987):

-6	-5	-4	-3	-2	-1	+1	+2	+3	+4	+5	+6
A	A	A	A	A	A	A	T	G	T	C	T
C		C		C							C

+1 corresponds to the first nucleotide of the start codon. Adenin at positions -6, -4 and -2 as well as the thymine at +6 can be replaced by a C in order to still have strong translational efficiency.

In comparison, the Kozak consensus sequence in the fusion strain YPFA is a combination of the *FBP1* promotor sequence and the start codon and the next codon of *hTP53*, resulting in the following sequence:

-6	-5	-4	-3	-2	-1	+1	+2	+3	+4	+5	+6
A	**C**	A	**C**	A	**T**	A	T	G	**G**	**A**	**G**

-6 through -1 correspond to the *FBP1* promotor sequence and +1 through +6 to the *hTP53* sequence. Bold nucleotides are the ones that need to be changed to obtain an optimal sequence. The cytosine on position -3 is thought to reduce mRNA translation efficiency about 20-fold (Kozak, 1986). Therefore, the hope was, to improve protein synthesis of the fusion protein and increase revertant colony size and fitness, once the optimal Kozak sequence was introduced into the genome.

3.5.4.1. Construction of improved URA$^+$ strain without loxP sites (YUFΔlP)

All strain constructions to introduce the optimal Kozak sequence require the URA$^+$ strain YUF as host. Since there were complications with loxP artifacts (compare section 3.4.1.), an improved strain of YUF should be constructed first.

The plan was to amplify *URA3* from the plasmid pUG72 without loxP sites, so that *URA3* (*K.l.*) can be integrated into the yeast genome without those sites (Fig. 93). The new primer sequence was selected as close as possible to the loxP sites in order to avoid truncating essential sequences of the *URA3* promoter or terminator. The location of primers to exclude loxP sites are shown in Fig. 92.

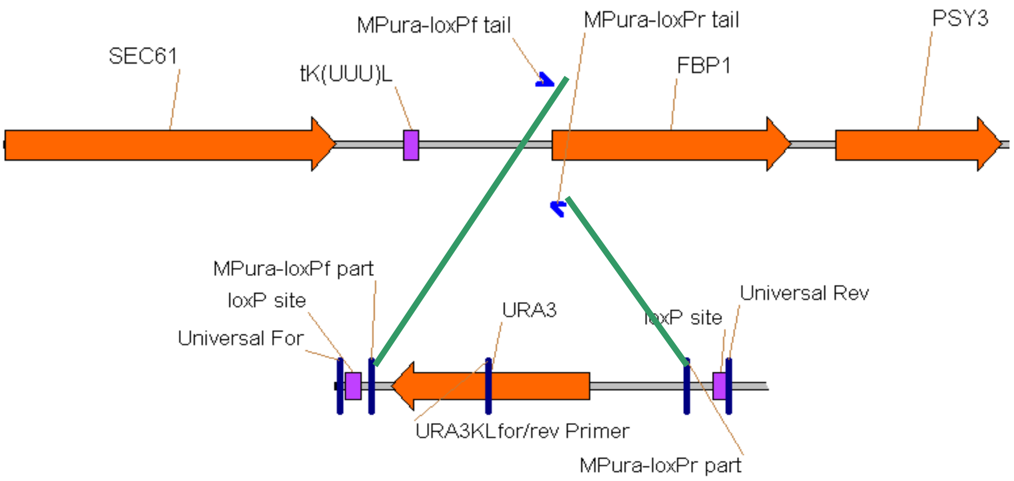
MPura-loxPf tail
MPura-loxPr tail
PSY3
SEC61
tK(UUU)L
FBP1
MPura-loxPf part
loxP site
Universal For
URA3
loxP site
Universal Rev
URA3KLfor/rev Primer
MPura-loxPr part

Fig. 92. Integration of *URA3* without loxP sites into the yeast genome between the promoter and starting sequence of *FBP1* ORF. Green bold lines indicate homologous recombination.

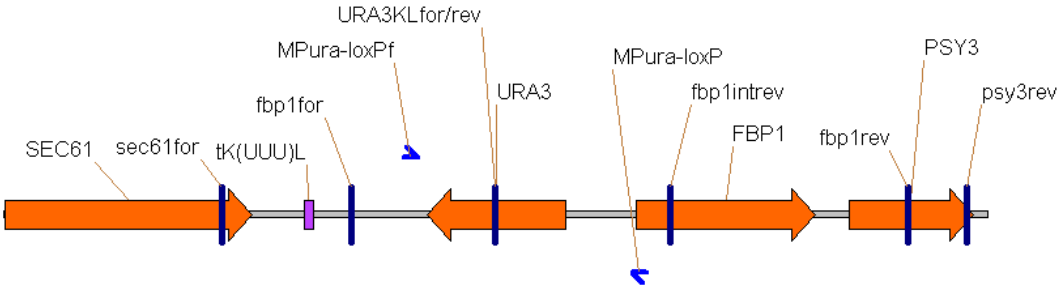
URA3KLfor/rev
MPura-loxPf
fbp1for
SEC61
sec61for
tK(UUU)L
URA3
MPura-loxP
fbp1intrev
FBP1
fbp1rev
PSY3
psy3rev

Fig. 93. New genomic situation for strain YUFΔlP.

The *URA3* ORF with its promoter and terminator but without loxP sites was amplified with the megaprimers MPura-loxPf and MPura-loxPr resulting in a fragment of 1417 bp as seen in Fig. 94.

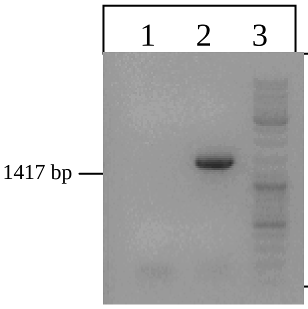

1 → neagative control (5 µl)

2 → PCR product (5 µl)

3→ O'Gene Ruler DNA Ladder Mix (5 µl)

Fig. 94. Gel of megaprimer-PCR amplification of *URA3* from pUG72.

step	Time [seconds]	Temperature °C
Initial denaturation	30	98
3 cycles of next 3 steps:		
Denaturation	*10*	*98*
Annealing	*30*	*68*
Extension	*39*	*72*
30 cycles of next 2 steps		
Denaturation	*20*	*98*
Extension	*80*	*72*
Final extension	480	72

50 µl reaction:
1 µl pORFhTP53FS+1 1:100
10µl 5x HF buffer
1 µl dNTPs
2.5 µl MPura-loxPf
2.5 µl MPura-loxPr
33 µl ddH$_2$O
0.5 µl Phusion Polymerase (Finnzymes)

The PCR product was purified with GFX columns and transformed into the strain YLBM with electroporation. The selection for positive transformants occurred on SC-ura plates. Nine transformants were isolated and tested in three PCRs for the correct length.

The first control PCR was performed with two external primers fbp1for and fbp1intrev. PCR program and conditions are indicted below.

step	Time [seconds]	Temperature °C
Initial denaturation	300	95
30 cycles of next 3 steps:		
Denaturation	*30*	*95*
Annealing	*30*	*55*
Extension	*120*	*72*
Final extension	300	72

25 µl reaction:
0.5 µl DNA
2.5µl 10x BD buffer
0.3 µl dNTPs
0.5 µl fbp1for
0.5 µl fbp1intrev
0.5 µl MgCl$_2$
19 µl ddH$_2$O
0.1 µl FIREPol (Solis BioDyne)

From nine tested transformants all, without the exception of clone 3, showed the expected band at 1877 bp. Clone 3 showed the same fragment length as the host strain YLBM with 577 bp. An additional control proposed PCR products of the strain YPF63 and YUF yielding fragment lengths of 1755 bp and 2169 bp, respectively as shown in Fig. 95.

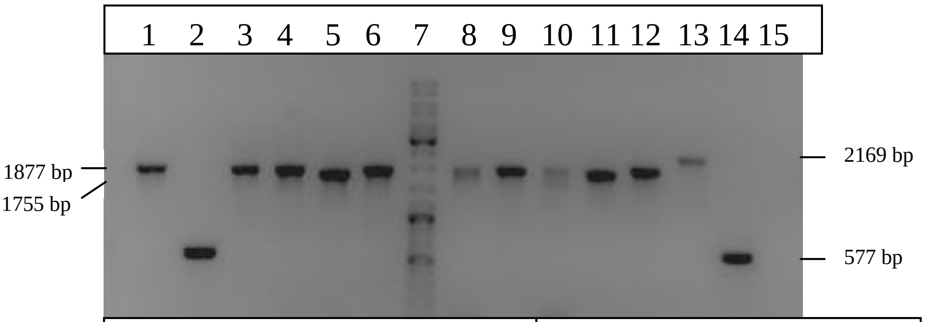
1 2 3 4 5 6 7 8 9 10 11 12 13 14 15
1877 bp
1755 bp
2169 bp
577 bp

1 → clone 1(8 µl)
2 → clone 3 (8 µl)
3 → clone 4 (8µl)
4 → clone 5 (8 µl)
5 → control YPF63 (8 µl)
6 → clone 6 (8 µl)
7 → O'Gene Ruler DNA Ladder Mix (5 µl)

8 → clone 8 (8 µl)
9 → clone 10 (8 µl)
10 → clone 11 (8 µl)
11 → control YPF63 (8 µl)
12 → clone 12 (8µl)
13 → control YUF (8 µl)
14 → control YLBM (8 µl)
15 → negative control (8 µl)

Fig. 95. Control PCR for YUFΔlP candidates with external primers

Clones 5 and 6 were selected for further two control PCRs with the combination of one external and one internal primer. The PCR reaction was only altered in regard to the primer pair. The altered PCR settings are indicated below.

Primer pair	Annealing temperature	Extension time	Expected lengths
fbp1intrev + URA3Klrev	55°C	60 s	1044 bp
fbp1for + URA3Klfor	57°C	50 s	857 bp

For both PCRs, DNA from the strain YUF was used as positive control yielding the fragment lengths 1208 bp in the case of the primer pair fbp1intrev and URA3KLrev and 985 bp with the second primer pair.

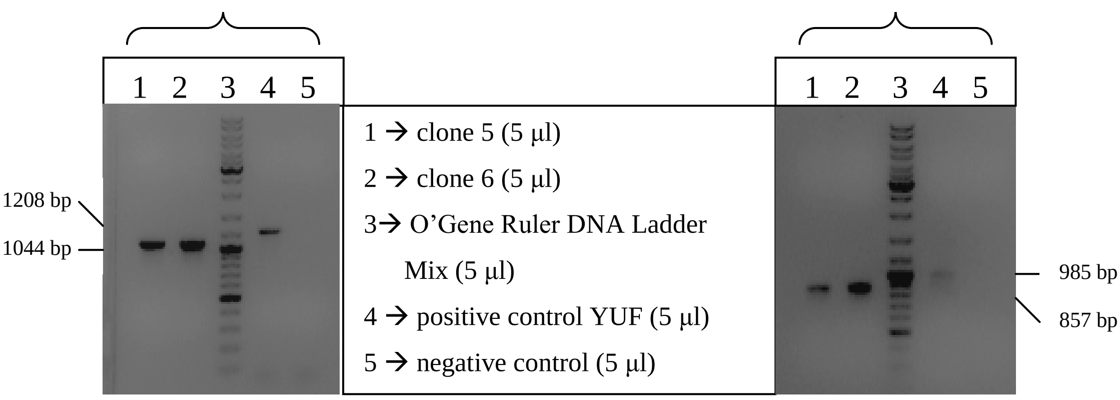
fbp1intrev + URA3Klrev
fbp1for + URA3Klfor
1 2 3 4 5
1 2 3 4 5
1208 bp
1044 bp
985 bp
857 bp

1 → clone 5 (5 µl)
2 → clone 6 (5 µl)
3→ O'Gene Ruler DNA Ladder Mix (5 µl)
4 → positive control YUF (5 µl)
5 → negative control (5 µl)

Fig. 96. Control PCRs with combination of an external and internal primer for clones 5 and 6.

As evident from Fig. 96, both clones showed the correct length in the control PCRs. Clone 6 was selected to be the new strain YUFΔlP. After testing the clone for its markers with replica plating, following phenotype was confirmed:

YUFΔlP: MATa *trp1-Δ his3-Δ200 ura3-52 lys2ΔBgl ade2-1o gal mal CUP*^{r}
fbp1::URA3 (K.l.)

Due to the improved strain without loxP sites, it should be possible to obtain transformants without false positive clones that correspond to loxP artifacts.

3.5.4.2. Optimal Kozak sequence

To introduce the p53 ORF with an optimal Kozak sequence into the yeast genome at the *FBP1* locus the megaprimer MPp53Kozfor with following sequence was designed.

5’TTTGTATGATAGGCCTAAGAATAACAGTGCGAACATATAAGAAACATCCCTC
ATACTACCAAAAAAATGTCTGAGCCGCAGTCAGATCCTA3’

The yellow block corresponds to the p53 ORF sequence; underlined letters indicate optimal Kozak consensus sequence. The upstream sequence is homologous to promoter sequence of *FBP1* and represents the 5’ tail of the megaprimer.

Furthermore, another consideration to improve the phenotype of the YPFA revertants was to truncate the *hTP53* ORF. Possibly, the length difference might propose a problem in the strain since the *FBP1* ORF has a size of 1044 bp and after the fusion with *hTP53*, the obtained ORF is 2223 bp long. Therefore, a further approach was to truncate the *hTP53* ORF 61 nucleotides after the end of the reversion window, retaining only the first 505 bp of the *hTP53* ORF. The in-frame fusion to the *FBP1* ORF was not affected. The truncated version of *hTP53* was used in combination with the optimal Kozak sequence.
Furthermore, special megaprimers with an elongated tail were designed to assure long homologous ends for recombination. First, only the upstream megaprimer was elongated and in a second step the downstream megaprimer was elongated as well. Both primers were designed 120 nt long, since this is the maximum of correctly synthesized nucleotides guaranteed.

Therefore, following variants to construct a new *hTP53-FBP1* fusion frameshift strain were set up (Table 13).

Variants for optimization of *hTP53-FBP1* fusion strain	**Primer pair**
optimal Kozak sequence	MPp53Kozfor + MPp53rev
optimal Kozak sequence + truncated *hTP53*	MPp53Kozfor + MPp53rev2
optimal Kozak sequence + truncated *hTP53* + one elongated megaprimer	MPp53KozF2 + MPp53rev2
optimal Kozak sequence + truncated *hTP53* + two elongated megaprimer	MPp53KozF2 + MPp53R3

Table 13. Overview of optimized construction attempts

For all strategies, the *hTP53* ORF or part of it was amplified from the plasmid pORFhTP53FS+1 and the linear DNA fragment transformed into the newly constructed strain YUFΔlP. Selection of transformants occurred on 5-FOA plates, based on the negative selection of the replaced *URA3*. Selected clones were tested in a control PCR with external primers for their length difference.

Unfortunately, there was not sufficient time left at the end of my thesis to construct the new strains successfully. Even though the new host strain without loxP sites helped to get rid of "loxP artifacts" completely, there seemed to be a problem with the integration of *hTP53* into the yeast genome. To make sure that the competent yeast cells worked well, a custom made positive control with megaprimer disruption of a different gene instead of transforming a plasmid, was created. Since this control with the linear DNA fragment showed efficient transformation rates, it could be ruled out that the transformation worked inefficiently in general.

3.5.5. Complications encountered with YPFA

3.5.5.1. Reconstruction Assays

Some of the revertants from the mutation assay were picked and a reconstruction assay was performed as described in Materials and Methods (2.2.2.5.). 40 CFU's of the revertant were mixed with 2.5 x 10^7 cells of YΔF1 and plated on SC-Lactate.

In some cases (revertants from day 6, 7, 8 and 10) the revertants were also plated on SC-Lactate without competition of YΔF1 to analyze any differences in colony appearance. YPF63 was used as a positive control.

Furthermore, 40 CFU of all revertants were streaked on YPD to be able to calculate the exact number of expected colonies in the reconstruction assay. If 40 colonies were formed on YPD, then 40 colonies are expected on SC-Lactate with or without background cells. According to the colonies on YPD plates, survival rates can be determined for the revertants in the reconstruction assay and the control plates where they were plated on SC-Lactate without YΔF1.

Generally, it was expected that colonies appear with a peak on day 4. However, this was not the case. Another possibility would be that colony formation in the reconstruction assay takes place at the same day as in the adaptive mutation assay. In this case, a revertant from day 9 would have to appear on day 9 in the reconstruction assay as well. That would indicate that the revertant from the mutation assay had developed due to a replication-dependent reversion event, producing a slow growth phenotype. Interestingly, the second possibility was not observed either, as evident from Fig. 97. Instead, very different results were obtained from each individual revertant.

In detail, results obtained with the individual revertants were the following and are shown in Fig. 97 and Fig. 98.

Of the three day 5 revertants one showed the expected peak at day 4 but the second and third revertant had the peak on day 6. As shown in the survival graph (Fig. 98A) 70-90% of the expected colonies appeared on the SC-Lactate plates.

Only one out of the three revertants from day 9 formed colonies at all with a peak on day 7. The survival of this revertant reached approximately 80% as shown in Fig. 98B).

Colony formation was observed in case of all three revertants from day 13. However, only 10, 30 or 40% of the expected colonies appeared. The peak for newly arising colonies was observed on day 9 for revertant III and day 10 for the others.

One tested revertant that appeared on day 20 in the mutation assay, showed a peak on day 6 in the reconstruction assay. The second analyzed revertant from day 20 showed no sharp peak, instead it split up on the days 10 and 11. The survival of the expected colonies reached 70 and 80%.

Analyses of further revertants coming from the same series of mutation assay, were performed with an additional control on SC-Lactate plates without the non-reverting background. The fusion strain YPF63 served as reference. A peak of newly arising colonies was observed at day 4 on the reconstruction plates as well as on the control plates. This presented an expected result. On the contrary, the revertants showed no uniform patterns. Interestingly, colonies of revertants d7 II, d8II and d10II appeared on SC-Lactate plates with non-reverting background but not on control plates lacking the background cells. In all three cases, colonies appeared with a peak on day 7 in the reconstruction assay. Some revertants lacked colony formation on both, reconstruction plates and control plates. Those were the revertants d7I, d8I and d10II.

Only one revertant (d6) produced colonies on control plates and reconstruction plates. However, the appearance on the control plates occurred one day delayed. The peak of newly arising colonies formed on day 5 on the reconstruction plates and day 6 on control plates without competitive background.

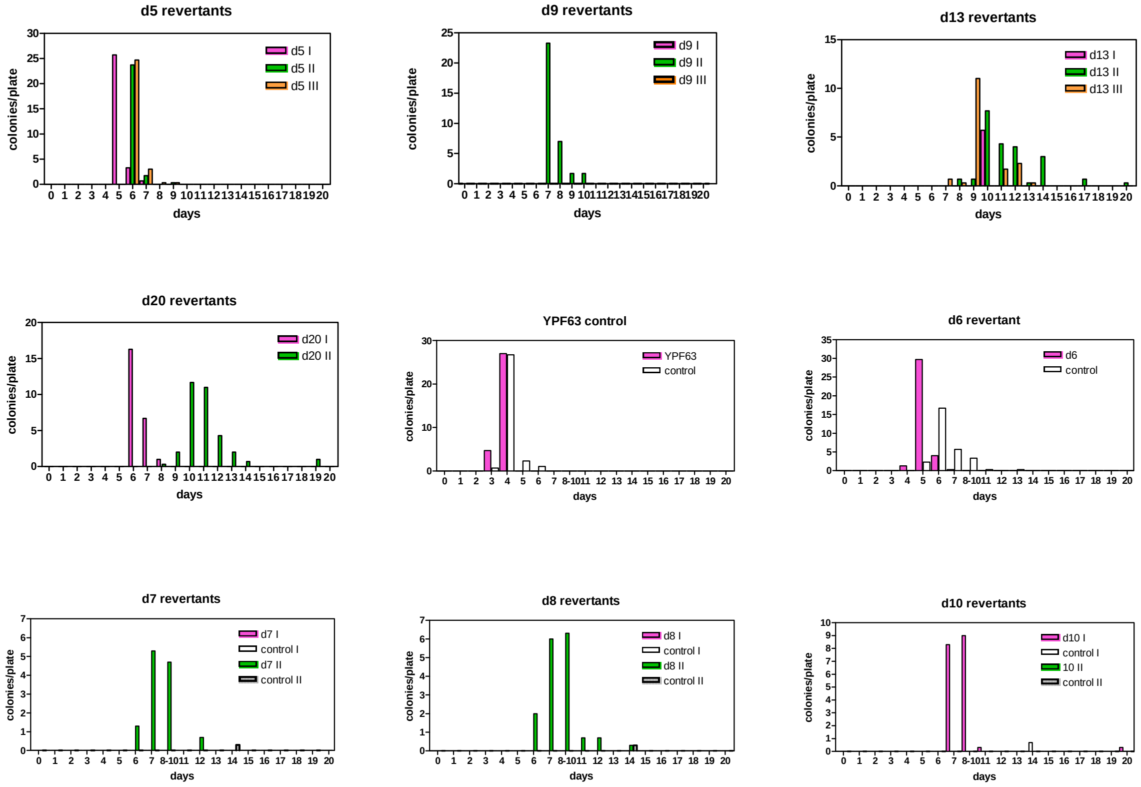

Fig. 97. Colony appearance of YPFA revertants in the reconstruction assay. Control represents plates without background strain. YPF63 indicates the positive control.

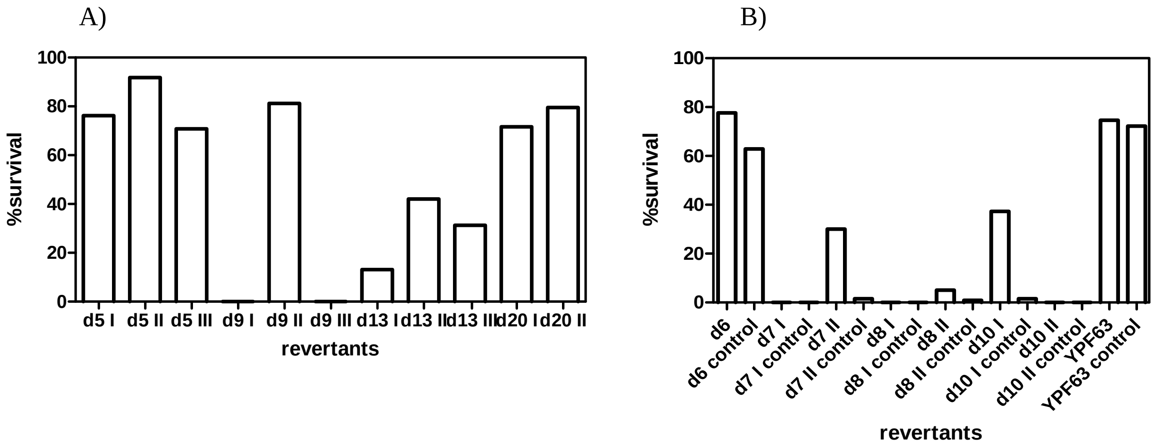

Fig. 98. A) Normalized survival of revertants analyzed in the reconstruction assay. B) Normalized survival of revertants tested in the reconstruction assay and parallel on SC-Lactate plates without background strain, as a control. 100% is normalized to plating efficiency, which was obtained with YPD plates.

Since the results of the first revertants from the reconstruction assay were unexpected, another reconstruction assay was performed with revertants from another series of the adaptive mutation assay. The setup was the same as described above, i.e. with control plates without background cells on SC-Lactate.

Following results of the reconstruction assay are shown in Fig. 99 and the survival in Fig. 100.

The control strain YPF63 showed the expected peak at day 4 on the reconstruction plates as well as on the control plates. Approximately 100% of the expected colonies appeared on both types of plates. The early revertant from day 4 appeared with a peak on day 4 in the reconstruction assay and on the control plates. As evident from Fig. 100, there was a difference in survival. On SC-Lactate plates with background cells, 90% of the expected colonies appeared, whereas only 60% on control plates were observed.

The day 5 revertant has its peak on day 5 and reaches a survival of approximately 80%. However, the control plates showed no homogenous appearance of colonies. Instead, colony formation took place within days 5 through 9, resulting in no sharp peak. Moreover, only 40% survival was obtained.

For the first day 7 revertant the peak of newly arising colonies fell on day 7 with a survival of 70%. The second day 7 revertant had its peak on day 5 and total colony appearance was almost 90%. Both revertants showed a one-day delay with the peak of newly arising colonies on the control plates. Compared to the survival in the reconstruction assay, fewer colonies appeared in both cases on the control plates, reaching 50% for the first revertant and 70% for the second.

Interestingly, the revertant from day 8 showed no colonies at all, neither in the reconstruction assay, nor on the control plates. Therefore, the graph for this revertant is not represented in Fig. 99.

Day 9 revertant showed a sharp peak on day 5 and a survival of 85% was observed. On control plates only 55% of the expected colonies appeared with a peak on day 6.

The first analyzed revertant from day 13 showed low survival of 30% and 10% respectively, on reconstruction plates as well as on control plates. Consequently, only a few colonies appeared on the plates, so that a peak formation was not observed. However, first colonies appeared on day 8 on reconstruction plates and on day 10 on the control plates. The second day 13 revertant showed different characteristics compared to the first one. A survival of 80% was observed on reconstruction plates and control plates. First colonies appeared on day 9 and a peak was formed on day 10. Newly arising colonies on control plates showed a delayed peak of at least one day. Since days 11 through 13 were not counted individually, the peak on the control plates corresponds to the accumulation of colonies from three days.

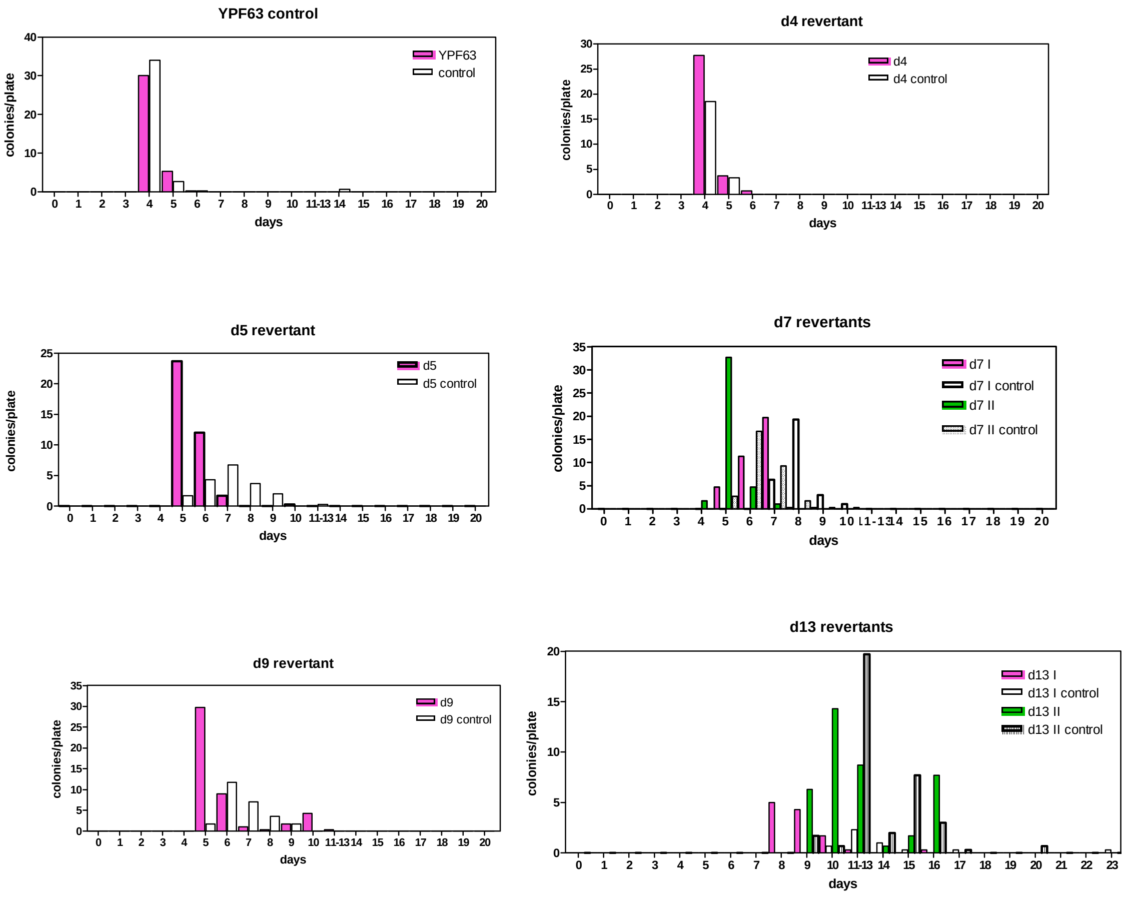

Fig. 99. Colony appearance of YPFA revertants in the second reconstruction assay. Control represents plates without background strain. YPF63 indicates the positive control.

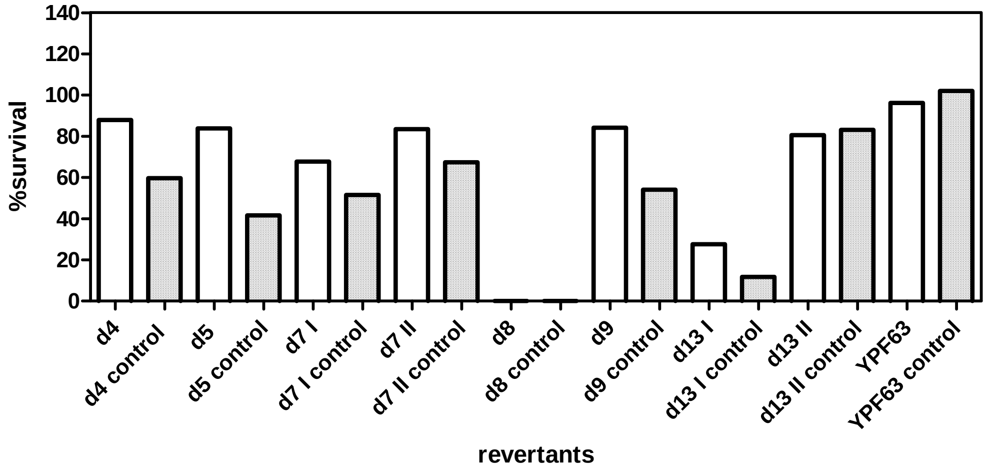

Fig. 100. Normalized survival of revertants tested in the reconstruction assay and parallel on SC-Lactate plates without background strain, as a control. 100% is normalized to plating efficiency, which was obtained with YPD plates.

In general, none of the revertants showed the same characteristics as the control strain YPF63 although their phenotype should be identical. Additionally, there should be no difference in colony appearance when plated with or without background cells, as evident from the YPF63 strain. However, all revertants that produced colonies on either plates, showed a delayed appearance of one day on plates lacking competition. Furthermore, in all cases that survival on control plates was considerably lower with the exception of revertant d13 II.

Since the analysis of 26 revertants in a reconstruction assay yielded suspicious results, I decided to do sequence analysis of some representative revertants to achieve more information about the reversion event.

3.5.5.2. Sequence analysis

Six revertants, which were analyzed in the first reconstruction assay, were chosen for sequence analysis. According to the reconstruction assay results, revertants with three different characteristics were chosen. The first characteristic was, that no colonies were observed in the reconstruction assay. For this phenomenon, revertants d7I, d8I and d10II were selected for sequence analysis.

The second case corresponds to revertants which produced colonies on the reconstruction plates but not on the control plates, lacking the non-reverting background strain YΔF1. Revertants d8II and d10I were chosen.

As a third option, revertant d6 was chosen, which was the only revertant in the first reconstruction assay that showed colonies on plates with and without competition of a background.

DNA of all 6 revertants was isolated and a PCR was performed with the primers fbp1for and fbp1intrev. The PCR products were sent to sequence analysis with p53intrev as sequencing primer. The primer is situated at the end of the reversion window and therefore sequencing will include the whole reversion window of *hTP53*.

Unfortunately, sequencing yielded a completely unexpected result. In all six putative revertants no frameshift-reverting mutation was found in the reversion window. Instead, the sequence analysis of all six revertants showed the same sequence as the original strain YPFA.

Therefore, they cannot be regarded as true revertants and it is unclear how they manage to form colonies in the adaptive mutation assay.

However, the appearance of such artifacts might explain the extremely high frequencies of colonies which were obtained for YPFA in the adaptive mutation assay. Obviously, newly arising colonies did not derive from replication-independent reversion events. Furthermore, this might also be the reason why no uniform results were obtained in the reconstruction assay. Unfortunately, it must be concluded that the *hTP53* frameshift strain YPFA is not suitable for the newly developed model system to study adaptive mutation frequencies.

4. Discussion

4.1. Cell cycle arrest mediated by a block in gluconeogenesis

The major aim of this study was to develop a glucose-limited system to study mutation frequencies in quiescent yeast cells. The well established *lys2ΔBgl* system (Heidenreich and Eisler, 2004; Heidenreich et al., 2006; 2004; 2003; Heidenreich and Wintersberger, 1998, 2001) bears some disadvantages which should be abolished with the new system. The one-sided amino acid starvation for lysine should be replaced by a carbohydrate starvation. So far adaptive mutations selected by carbon source starvation have only been studied in *E. coli* but not in yeast. In those systems lactose was offered as alternative carbon source to glucose (Foster, 1999; Hall, 1998; Rosenberg, 2001). Here, I tried to establish a similar system to avoid amino acid starvation. According to literature, a block in gluconeogenesis provokes that cells enter a cell cycle arrest. Glucose is known to be a signal molecule for growth (Granot and Snyder, 1991), which is a disadvantage when studying resting cells. With the offer of the alternative carbon source, glucose is no longer mandatory in selection medium.

In this study, I showed that cells which cannot undergo gluconeogenesis really enter a quiescent state. A block in gluconeogenesis was triggered by disrupting two genes involved in gluconeogenesis but not in glycolysis. The candidate genes were *PCK1* (encoding phosphoenolpyruvate carboxykinase) and *FBP1* (encoding fructose-1,6-bisphosphatase). A strict cell cycle arrest occurred from the beginning of selection. No residual growth was observed, which is an advantage compared to lysine starvation, where residual proliferation is evident by a doubling of cell count from day 0 to day 1 (Heidenreich and Wintersberger, 1997). This strict arrest indicates that cells enter a more relevant stationary phase when blocked in gluconeogenesis, since starvation is regulated via a canonical pathway.

Three non-fermentable carbon sources (lactate, pyruvate and glycerol) were analyzed for the most favorable effects with regard to strictness of cell cycle arrest, viability and colony formation. No differences in cell cycle arrest were observed with the different types of media or between the two disruption strains *FBP1* and *PCK1*. Once more this proves that the system with regulated gluconeogenesis block is very efficient and leads to a strict cell cycle arrest, where no leakiness is tolerated. Furthermore, the lack of glucose might also have an effect on the strictness of arrest.

However, viability of arrested cells of the Pck1-deficient strain was decreased drastically within the first three days. Thus, the target gene *FBP1*, which showed reasonable viability of arrested cells, was chosen for all further studies. The low viability was an unexpected effect, since alternative carbon sources can be utilized by arrested cells for energy flux and can serve as precursor for other pathways. The mechanisms how the three non-fermentable carbon sources enter the yeast cells are different and might therefore also have an effect on viability. For example, it is known that glycerol enters the cells very slowly and consequently is a poor nutrient source for *Saccharomyces cerevisiae* (Gancedo et al., 1968). Lactate and pyruvate are both transported into the cell by the Jen1 permease and thus share the same initial step of mechanism (Casal et al., 1999; Makuc et al., 2001). Consequently, I expected a similarity of growth on lactate and pyruvate. However, viability on pyruvate showed the same curve like glycerol. Hence, I observed rather a strain-specific dependency than carbon-source dependent effect on viability of cells. One possibility might be that loss of Pck1-activity might lead to a reduced viability, since gluconeogenesis is blocked rather in the upstream part of the pathway and no downstream products can be generated. When *FBP1* is disrupted, the pathway is active with exception of the last three steps. It could be that the intermediates of gluconeogenesis are used for other pathways and therefore benefit a better survival.

In reconstruction assays the *fbp1*-deficient strain was tested if it had an effect on growth of fbp1 intact cells. Moreover, the same three carbon sources lactate, pyruvate and glycerol were analyzed. Interestingly, the *fbp1*-deficient background strain seemed to have a negative influence on growth on pyruvate, since colony formation was delayed for one day. Therefore, this non-sugar was not considered a favorable carbon source. The carbon source lactate showed the most homogenous colony formation compared to glycerol and was therefore defined as standard nutrient source.

The hypothesis to block gluconeogenesis and consequently reach cell cycle arrest in yeast cells could be proven with this system. The system fulfilled all criteria to continue with a frameshift insertion in the *FBP1* gene to be able to study mutation frequencies.

4.2. Homology-driven gene replacements

I repeatedly experienced problems when I tried to direct custom-designed DNA fragments to the genome of the host strain YUF. If at all, gene replacement triggered by homologous recombination of the flanking ends worked very inefficiently. I observed that even the process of homologous recombination between the two loxP sites, which are present in the host strain, was more favored. Each loxP site contains two 13 bp inverted repeats and an 8 bp asymmetric core sequence (Carter and Delneri, 2010; Sauer and Henderson, 1989).

The advantage of loxP sites is to be able to excise and subsequently re-use any marker gene, which is flanked by loxP sites, mediated by a cre-recombinase. For our purpose this function is not needed, since the marker gene should be replaced in the course of integrating custom-made DNA fragments by homologous recombination. However, I observed that homologous recombination was favored between the two loxP sites, resulting in excision of the marker gene but lacking the integration of the new gene into the locus. Consequently a high rate of false positive colonies arose, which I referred to as "loxP artifacts".

Even though the loxP sites originally only comprise of 34 homologous bp, an expanded homology of 48 bp is found in the plasmid pUG72 (see Fig. 101), which results from construction of the plasmid (Gueldener et al., 2002). If the second mismatch at the 5' end is not considered, homology is given for 53 bp. In this case, the sequence seems to be long enough to compete with the 60 bp homology at the end of the transformed linear DNA fragment.

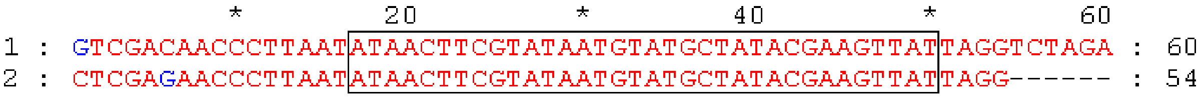

```
             *        20         *        40         *        60
1 : GTCGACAACCCTTAATATAACTTCGTATAATGTATGCTATACGAAGTTATTAGGTCTAGA : 60
2 : CTCGAGAACCCTTAATATAACTTCGTATAATGTATGCTATACGAAGTTATTAGG------ : 54
```

Fig. 101. Homology of loxP sites. Black box indicates original homology of loxP sites.

Certain problems with loxP sites have been reported. The yeast genome consists of cryptic loxP sites on different chromosomes, resembling the original loxP sites. These sites were mapped and shown to rarely trigger chromosomal rearrangement by cre-mediated recombination (Delneri et al., 2000; Sauer, 1992). However, this possibility can be excluded in my case, as control PCRs with external primers yielded products, confirming that rearrangement could not have occurred. Otherwise no PCR products should be obtained as the site of hybridization for the two primers would be present at two different chromosomes.

According to literature, the event of homologous recombination between the loxP sites is estimated to be very low and is over 2000 fold less efficient than cre-mediated recombination (Sauer and Henderson, 1989). On the contrary, I observed a rate of 50% of all transformants undergoing recombination between the two loxP sites.

Due to the high number of clones derived from loxP artifacts, an alternative URA$^+$ strain (YUFΔlP) was constructed, which lacked loxP sites. The marker gene *URA3* was amplified from the plasmid pUG72 excluding loxP sites but as close as possible to them to avoid truncating the promoter and terminator sequence.

The improved URA$^+$ strain was used for the endeavors to introduce the optimal Kozak consensus sequence (Hamilton et al., 1987; Kozak, 1984, 1986, 1987) in the promoter region upstream of the *hTP53/FBP1* fusion gene to improve expression. LoxP artifacts were absent in all cases. Therefore, the strain YUFΔlP fulfilled its purpose.

Unfortunately, the optimal Kozak consensus sequence could not be successfully integrated into the genome. Integration should occur based on homologous recombination triggered by the 60 nt at both ends of the transformed linear DNA fragment. It seemed suspicious that 60 nt would not be sufficient for homologous recombination, especially since it is a commonly used method. Therefore, both megaprimers were elongated, bearing approximately 100 nt complementary to genome sequence. The longer homologous region had no positive effect on the outcome of gene replacement attempts, since it nevertheless failed so far.

Instead, I observed a plethora of Ura3 forward mutants as a result of transformation. Generally, Ura3 forward mutations are thought to happen with a frequency of 10^{-7} (Boeke et al., 1984), however I observed much higher frequencies. These and the loxP artifacts are conspicuous because no real integrations of the DNA into the genome were found. Therefore, I consider the integration into the genome the basic problem and consider loxP artifacts and Ura3 forward mutants as symptoms.

The cause of the problem is unclear. However, low transformation efficiency can be ruled out, since controls (plasmids) were always used. Transformations always work more efficiently for plasmids compared to transformation with linear DNA fragments. Therefore, even linear DNA fragments for gene disruptions were used as positive controls instead of plasmids. This confirmed that the transformation efficiency was given as well when transforming linear fragments.

Consequently, the host strain YUFΔlP cannot be held responsible for the problem and is considered as functional. I assume that the problem of integration underlies the genomic target, which also met difficulties with PCR amplifications (discussed below).

4.3. *FBP1* +1 frameshift strain

4.3.1. Strain construction

In general, it was found that amplifications around the gene *FBP1* were not trivial. Even though optimal primer sequences with regard to melting temperature, GC content, hairpin loops, dimers and duplexes between the primer pair were chosen, PCRs hardly ever worked without optimizations. Many times optimizations with annealing temperature, extension times, $MgCl_2$ concentrations, polymerase buffers, cycles of PCR program and different polymerases had to be performed before a PCR product was obtained.
It was assumed that DNA regions around *FBP1* were especially well packed so that it proposed a problem. The reason for the well packed DNA could be that the *FBP1* gene underlies catabolite repression (Mercado et al., 1991) and consequently is not activated at times of DNA isolation since cells were grown in YPD. *FBP1* is repressed when glucose is present and only gets activated once glucose is limited. Therefore, I hoped that an additional step of a medium switch from YPD to SC-Lactate would derepress *FBP1* and make DNA around *FBP1* regions more accessible. Unfortunately, this hypothesis proved wrong. The same complications in PCR were encountered.

Three approaches for the construction of the *FBP1* frameshift strain were introduced. The strategy with the two-step gene replacement was applied successfully and created the new strain YFAM. The two other methods of the one-step gene replacement and the modified one-step gene replacement posed problems. Even though the marker gene in the host strain could be replaced, the introduced frameshift mutation was not integrated into the genome. It was assumed that the 3'end of homologous sequence was not sufficient since the distance to the frameshift mutation was only 33 nucleotides. Therefore, in a second modified approach the 3'end was elongated. Unfortunately, this was not the solution for the problem since the frameshift still did not integrate into the genome although gene replacement took place. However, the 3' end was excluded as the cause of the problem.
Consequently, I supposed that homologous recombination took place correctly in this case, since clones with correct length verified by PCR were obtained. Another explanation might

be that the transformed linear DNA was degraded either from the 5’ end or the 3’ end due to the mutation. This assumption arises more possibilities. The transformed DNA fragment contained the frameshift mutation and the manipulated stop codon, latter can be detected with restriction site analysis of XhoI. It was assumed, that if the recognition site was active, both mutations would be present in the integrated DNA. In both unsuccessful approaches of the strain construction, the 5’ end was the same, comprising of 60 homologous nucleotides. The mismatch was further 81 nt downstream and the frameshift mutation 127 nt, respectively. If the DNA was degraded from the 5’ end up to the mismatch, this would mean that also the homology in the promoter region of the *FBP1* gene would be gone and with it the replacement of the marker gene *URA3*. Therefore, degradation from 5’ end is very unlikely since selection for URA3$^-$ clones occurred.

If degradation of the linear DNA fragment from the 3’ end is considered, there would still remain about 190 nt or 127 nt, respectively in the two different approaches for homologous recombination. Furthermore, complementary region to the *FBP1* promoter is not affected, so that replacement of the *URA3* gene can take place. If this might be the correct explanation for the problem cannot be proved and remains unresolved.

4.3.2. Adaptive mutation assay

Adaptive mutation assays were performed to obtain a variety of information. First, the threshold between colonies formed by replication-dependent and replication-independent revertants should be defined further with the help of jackpots.

Second, I wanted to know if there were any growth related artifacts. Three types of unwanted artifacts should be excluded. Residual proliferation was determined by washing cells from plates immediately after plating and 24 hours later. The cell count should not differ when no residual growth occurred. Another artifact is crossfeeding, which is a consequence of excreted nutrients from older revertants, which enable proliferation of surrounding cells (Heidenreich, 2007). The third potential artifact is cryptic proliferation, which is triggered by nutrient release of dying or dead cells.

The third information of the adaptive mutation assay is if revertants appear at all and how many of them.

To further define the threshold between early and late arising colonies, the occurrence of jackpots was useful. Unfortunately, jackpots were rarely observed. Only one series presented one jackpot, which formed a high number of colonies on day 4 compared to the other subcultures. According to the appearance of the jackpot, day 5 would be defined as a line to distinguish between early arising replication-dependent colonies and late arising adaptive revertants. However, a second indicator for the threshold is the reconstruction assay, which according to results still includes day 6 for the appearance of replication-dependent colonies. Consequently, mutation rates were defined for day 5 and day 6. Likewise, mutation frequencies were determined starting with day 6 or day 7. Compared to the *FBP1* assay, replication-dependent colonies formed within the first 4 days of adaptive mutation assays with the *lys2ΔBgl* system and colonies appearing from day 5 on were considered as adaptive revertants. This delay corresponds to the different media composition and its utilization of fermentation versus respiration. Since glucose is present in SC-lys plates for the *lys2ΔBgl* selection system, colony formation takes place within the first three days. However, the selective medium SC-Lactate which is required in the *fbp1FS-128* assay is utilized by respiration and shows delayed colony formation of one day. Since fermentation of glucose is faster than respiration of lactate, the delay was expected.

Furthermore, colony formation was monitored over 24 days, whereas revertants in the *lys2ΔBgl* assay were only counted until day 10, since after this day colony formation was rarely observed. Additionally, the monitoring for 24 days in the *fbp1FS-128* assay was possible, since artifacts like crossfeeding and cryptic growth were only observed sporadically starting as late as day 22. Especially crossfeeding seems to be a problem observed in other adaptive mutation systems with *his1-7* allele (Marini et al., 1999; von Borstel et al., 1998) and auxotrophy for tryptophan (Storchova and Vondrejs, 1999). Therefore, the new *fbp1FS-128* system established in this study seems to be superior in regard to growth artifacts, compared to other systems.

The *FBP1* frameshift strain showed a mutation rate 15 times lower compared to mutation rates derived with *lys2ΔBgl* replication-dependent colonies. Interestingly, a similar extent was not observed when mutation frequencies of replication-independent revertants were compared. Instead, only a 3-fold decrease occurred. The unusual difference might correspond to an effect in transcription during inoculation phase. The *FBP1* gene is repressed in the inoculation phase due to the glucose in YPD complete medium. Since cultures are grown until the onset of stationary phase, glucose depletion takes place and the *FBP1* gene is activated, which can already occur during the diauxic shift. Once cells are plated to selective SC-Lactate plates, the gene is already derepressed and transcription can occur promptly. It was shown that highly transcribed genes show elevated levels of spontaneous reversions in yeast (Datta and Jinks-Robertson, 1995). Thus, transcription is considered to be mutagenic.

A reason why the mutation frequency in the *FBP1* assay is lower compared to the *lys2ΔBgl* assay might be an under-representation of hotspots for reversion events within the reversion window (see Fig. 102). Mononucleotide repeats are considered hotspots because they are prone to polymerase slippage errors during synthesis and can lead to so called microsatellite instability (Eckert and Hile, 2009; Sia et al., 1997).
In the reversion window of *FBP1* only 7 mononucleotide runs of triplets are present, whereas the *lys2ΔBgl* window contains 9 triplet runs. Moreover, also mononucleotide runs of 4, 5 and 6 are present, resulting in a total of 13 hotspots for compensating the frameshift mutation. Since the *lys2ΔBgl* reversion window provides almost the double amount of hotspots, this might propose an explanation for the lower mutation frequency of *fbp1FS-128*.

fbp1FS-128 reversion window:

TAAATGGACCAAGAAGAGACTCTACCGAAGGGTTTGATACCGATATCATCACTCTTCCTAGATTCATACTCGAGCACCAGAAGCAATTTAAGAACGCTACTGGTGATTTCACATGTAGTACTGAATGCCTTGCAATTCGCGTTCAAATTTGTATCTCACACCATCAGACGTGCTGA

lys2ΔBgl reversion window:

TAGCTGAAAAAATTCAAAGTTGCCAAGATCGATCTGGAAAGGACCCCTCAGTTGTTCCGTTTGGCCTTTTTGGAAAACCAAGATTTCAAATTAGACGAGTTCAAGCATCATTTAGTGGACTTTGCTTTGAATTTGGATACCAGTAATAA

Fig. 102. Reversion windows of *fbp1FS-128* and *lys2ΔBgl*. Yellow highlighted sequence represent ≥3 mononucleotide repeats. Red highlights indicate position of frameshift.

Nevertheless, the new assay with the *fbp1FS-128* allele to study adaptive mutations was established successfully and could be used for further application as described below.

The low mutation frequency of *FBP1* was used as a chance to study the *rad27* k.o. DNA repair mutant. Effects of the *rad27* k.o. mutant could not be studied in a mutation assay with the *lys2ΔBgl* assay since the high mutation rate resulted in overcrowding of the selective plates within the first three days, so that it was impossible to monitor late arising colonies. Here, in the *FBP1* assay, the mutation rate could be successfully reduced by a factor 55 compared to the *lys2ΔBgl* assay. Therefore, it was possible for the first time to study mutation frequencies with the repair mutant *rad27*. I could observe that the adaptive mutation frequency was increased when compared to the *RAD27* wild type assay, however only 3-fold and not 5.5-fold like the mutation rate.

4.3.3. Reconstruction assay

A total of 17 revertants (6 early arising colonies from days 4-6 and 11 late arising ones from days 7-15) were analyzed in reconstruction assays. All revertants showed the expected growth pattern with a peak of newly arising colonies on either day 3 or 4. One revertant was an exception since the peak was delayed one day to day 5. However, since day 6 was defined as the threshold to distinguish between replication-dependent and replication-independent derived colonies, the appearance on day 5 in the reconstruction assay was still accepted.

The reconstruction assay confirmed that the revertants produced in the adaptive mutation assay are real revertants with replication-independent origin and no slowly growing replication-dependent colonies. Therefore, the *fbp1FS-128* system was established successfully.

4.3.4. Sequence analysis

Four late arising revertants from the days 8 to 11 were sequenced to obtain more information about the position of the reversion event within the reversion window. The sequencing results of all four clones showed a reversion event close to the actual frameshift mutation. Interestingly, the frameshift was not reverted by a deletion in of one of the seven mononucleotide runs. None of the four revertants showed a reversion upstream of the original frameshift. Instead, two revertants obtained a +2 duplication only 5 nucleotides downstream of the frameshift. Another revertant was derived from a +5 duplication 8 nucleotides downstream of the frameshift. In the fourth sequenced clone, the functionality of the *FBP1* gene was restored by deletion of one nucleotide, occurring 14 nucleotides downstream of the frameshift. Although the number of sequenced revertant clones was low, this suggests that reversion events are not tolerated upstream of the frameshift or all over the reversion window, but only in a close region downstream of the frameshift. A reason might be that long stretches of altered amino acid sequence compared to the original ORF of *FBP1* are not tolerated. Therefore, reversion events at sites of mononucleotide runs within the reversion window might not be hotspots as cells might not be viable if the altered amino acid sequence is not accepted. It is assumed that this reason might also correlate with the low mutation frequency observed in the *FBP1* adaptive mutation assay. This would also explain why the mutation frequency is reduced by a factor 3 compared to the *lys2ΔBgl* assay (Heidenreich and Wintersberger, 1998), where studies showed that reversion events take place spread over the whole reversion window, favoring mononucleotide repeats as hot spots for simple deletion to revert the frameshift (Heidenreich and Wintersberger, 2001). Considering the fact, that 13 hot spots in the *lys2ΔBgl* reversion window are actively used for compensating the frameshift and assuming that the hot spots in *FBP1* are not accessible for reversion events, it is remarkable that the mutation frequency is only decreased three times in the *FBP1* frameshift assay.

4.4. *hTP53-FBP1* +1 frameshift fusion strain

The fusion construct of the human tumor suppressor gene *hTP53* and the new mutation detection gene *FBP1* brings many advantages with it. The main reason for a fusion construct was to be able to create a longer reversion window which should result in an increased mutation frequency in adaptive mutation assays. The reversion window within the *hTP53* ORF could be chosen with more freedom due to following reasons.

Since it is an artificially introduced gene, cells do not rely on the function of the p53 protein. The introduction of the frameshift mutation in *hTP53* and its resulting reversion window requires no consideration of interactions with active centers or conserved domains since it has no effect on the downstream fused *FBP1* gene functionality once the frameshift is compensated. This poses a big advantage compared to the frameshift in the *fbp1FS-128* allele. Another benefit is given by the fact that the mutation event to reverse the original frameshift mutation should be tolerated anywhere within the reversion window, even if the amino acid sequence is changed for a large part compared to the p53 wt sequence. A change of amino acids within the *FBP1* ORF clearly has an influence on the functionality of the fbp1 enzyme. On the contrary, a non functional p53 protein in cells with the *fbp1::hTP53FS-320* allele does not interfere with the viability of cells. Therefore, each cell undergoing a reversion event should be viable.

The choice of the gene fell on the human tumor suppressor gene *TP53* because mutations in the gene have a high relevance in cancer development. Mutations in p53 were first described in colon carcinoma and in lung cancer (Baker et al., 1989; Takahashi et al., 1989) and were soon after reported to show increased frequency in various tumors (Nigro et al., 1989). Today, ongoing research reveals that mutations in p53 are found in more than 50% of human cancers (Hadj Amor et al., 2008; Joerger et al., 2006; Pearson and Merrill, 1998; Soussi, 2007). Therefore, research on p53 has a big community and various p53 databases exist by now, for example the “International Agency for Research on Cancer” IARC TP53 database[1] or the p53 Knowledgebase[2] or the TP53 Web Site[3]. The databases provide information about patient’s mutations in p53. Even though early p53 research focused on exons 5-8, it was shown later that 10-15% of mutations are distributed on other exons (Hjortsberg et al., 2008). In general, about 10% of all mutations in p53 correspond to frameshift mutations (Smardova et al., 2005). Distribution analysis shows that hotspots for frameshift mutations within p53 are given in codons 151, 176, 209 and 241, which correspond to exons 5, 6 and 7 (extracted from IARC database). In exons 4, 9 and 10 frameshift mutations were observed with a significant increase (Hjortsberg et al., 2008).

The defined reversion window in the *hTP53* strain YPFA to study mutation frequencies ranges from codon 40 – 147. These codons correspond to exons 4 and 5. The reversion window in upstream located exons was preferred in order to avoid a negative effect on the downstream *FBP1* sequence.

Since a plethora of data about mutations in p53 is available and accessible, this gene was chosen to be able to compare received reversion events with the p53 databases and to be able to compare them with mutations occurring in cancer patients.

Since p53 research sometimes seems to be too complex to study in mammalian cells, researchers antagonize the hurdle by using a simpler model organism. The yeast *Saccharomyces cerevisiae* does not possess an ortholog to the human p53, however it constitutes a suitable system due to its conserved mechanisms. It was shown that human p53 can be expressed in yeast cells and can even function as a transcription factor (Fields and Jang, 1990; Scharer and Iggo, 1992). Furthermore, Schärer and Iggo showed that specific mutations in p53 found in human cancers inhibited transcription activation in yeast (Scharer and Iggo, 1992). A special assay was developed (Flaman et al., 1995) to study transcriptional activity of the p53 protein in yeast. This functional analysis of separated alleles in yeast (FASAY) is an assay based on *ADE2* functioning as reporter gene under the control of the p53 responsive element to be able to distinguish between mutant and wt p53. When wt p53 is expressed, the colonies appear white, whereas expression of mutant p53 leads to accumulation of a red dye in yeast colonies due to lack of *ADE2* expression (Flaman et al., 1995; Smardova et al., 2005).

---

[1] http://www-p53.iarc.fr/ (2011)

[2] http://p53.bii.a-star.edu.sg/ (2011)

[3] http://p53.free.fr/ (2011)

The mechanism behind p53-dependent transcription in yeast was further investigated with aspects of histone-modifying and chromatin-remodeling complex, confirming that there are remarkable similarities in transcription between mammalian cells and yeast cells (Yousef et al., 2008). In order to better understand the relationship between transcriptional function and mutation of p53, 2314 p53 mutants were screened in a yeast-based assay, representing all possibilities of missense mutations within the whole protein (Kato et al., 2003). Del Carratore et al. found evidence that wt p53 can reduce DNA-damage induced homologous recombination in yeast (Del Carratore et al., 2004). In 2008, expression of human wt p53 in yeast was found to have an effect on the transcription of some yeast genes, specifically it downregulates thioredoxin expression, which furthermore leads to increased ROS accumulation. Also, studies suggest that overexpression of human wt p53 protein in yeast might target some genes involved in growth inhibition and apoptotic cell death on minimal medium, whereas mutant p53 showed no effect (Hadj Amor et al., 2008). In contrast, further analysis of hot spot p53 mutants showed reduced growth patterns and induced cell death, comparable to the effects of wt p53 (Yacoubi-Hadj Amor et al., 2009).

Moreover, some studies confirm that expression of p53 in yeast results in smaller colonies and reduced double time in liquid media (Fields and Jang, 1990; Mokdad-Gargouri et al., 2001; Nigro et al., 1992).

Some studies might argue against the use of *TP53* in yeast, especially suggested growth inhibition on minimal medium and the smaller size of colonies. However, in this study only one copy of p53 was present in cells, in contrary to the used overexpression in the corresponding study. Furthermore, the precursor strain YPF63 carrying the intact *hTP53-FBP1* fusion confirmed normal growth on minimal medium. No negative effect due to p53 expression was observed. Additionally, *hTP53* only serves as detection system for colonies that are able to grow on SC-Lactate medium.

4.4.1. Adaptive mutation assay

Additionally to the adaptive mutation assay, pilot-experiments with the only reverting clone were performed to better define its characteristics. Already with the pilot experiments a high number of newly arising colonies was obtained on SC-Lactate plates. Therefore the cell density per plate was reduced from 1 x 10^8 to 2.5 x 10^7 to avoid overcrowding on plates.

This was an essential step, since even more colonies appeared on the plates of the adaptive mutation assay compared to the pilot-experiment. Interestingly, the pilot experiment yielded 5 times lower mutation frequencies. Even though the experimental setup was slightly different, it was suspicious that there would be a 5-fold increase in the adaptive mutation assay. Mutation rates were only defined for the adaptive mutation assay, since the setup of the pilot-experiments did not meet the requirements of a fluctuation assay setup. Mutation rates were 190 fold increased compared to the rates obtained with the *FBP1* frameshift strain YFAM. The mutation rate came close to the border of 1 x 10^{-7}, which was shown in literature to pose a problem regarding overcrowding plates (Babudri et al., 2001). However, it was still possible to count late arising colonies and study the mutation frequency. The frequency of newly arising colonies was 3500-fold increased, which seemed very suspicious. Higher mutation frequencies were expected as a result of the almost twice as big reversion window in *hTP53*. Consequently, more hotspots for reversion events are present. In the *FBP1* reversion window only 7 mononucleotide repeats were present. Here, alone 11 runs of three mononucleotides are present. Moreover, seven runs of 4, one of 5 and another one of six mononucleotides (Fig. 103). This results in 20 hotspots, almost three times as many as in the *FBP1* reversion window.

fbp1::hTP53FS-320 reversion window:

TGATGCTGTCCCCGGACGATATTGAACAATGGTTCACTGAAGACCCAGGTCCAGATGAAGCTCCCAGAATGCCAGAGGCT
GCTCCCCCCGTGGCCCCTGCACCAGCAGCTCCTACACCGGCGGCCCCTGCACCAGCCCCCTCCTGGCCCCTGTCATCTTCT
GTCCCTTCCCAGAAAACCTACCAGGGCAGCGTACGGTTTCCGTCTGGGCTTCTTGCATTCTGGGACAGCCAAGTCTGTGAC
TTGCACGTACTCCCCTGCCCTCAACAAGATGTTTTGCCAACTGGCCAAGACCTGCCCTGTGCAGCTGTGGGTTGA

Fig. 103. Reversion window of *hTP53* frameshift allele. Hotspots for reversion events are highlighted in yellow color. Red highlighted guanine represents inserted frameshift.

Also, according to the sequencing results of the *fbp1FS-128* revertants, it was assumed that mutations in hotspots might have occurred but led to non viable cells, since no long stretches of altered amino acids seem to be tolerated. Therefore, one of the advantages of the *hTP53* frameshift was that the change in amino acids within the full length of the reversion window has no effect on enzyme activity of fbp1. Thus, it was expected that more reversion events would occur in the *hTP53* allele compared to the *FBP1*. However, a 3500-fold increase is suspicious and cannot be sufficiently explained by the number of hotspots.

The phenotype of the newly arising colonies was not uniform within the series. Especially colonies in the pilot-experiment remained small and lost their round shape over the time course. However, this phenotype was not always given. When the actual mutation assays were performed, colony formation was better comparable to revertants of the *FBP1* frameshift strain YFAM. The observation of smaller colonies was also made in other laboratories when p53 was expressed in yeast (Fields and Jang, 1990; Mokdad-Gargouri et al., 2001). However, expression of mutant p53 reduced the negative growth effect dramatically (Nigro et al., 1992).

I considered the inhomogeneity of colony formation suspicious and unfavorable. This led to the approach to positively influence the expression by introducing the optimal Kozak consensus sequence.

4.4.2. Reconstruction assay

All revertants should show the same characteristics in the reconstruction assay. Cells rely on the restored functionality of the *FBP1* gene but not on the functionality of the *hTP53* gene. Since the frameshift is far upstream of the *FBP1* gene, changes of amino acids have no effect on Fbp1.

A total of three reconstruction assays were performed with 26 revertants from the *hTP53* frameshift derived colonies. The first reconstruction assay obtained peculiar results. Colonies did not appear at the expected day 4 which would prove that the isolated colonies were of replication-independent origin. Unfortunately, revertants also could not be defined as slowly growing replication-dependent colonies, since they did not appear on the same day as in the adaptive mutation assay. It seemed that colonies appeared arbitrarily. Therefore, the reconstruction assay was expanded by including SC-Lactate control plates, where revertants were plated without a competitor strain background. A variety of results were obtained, but none showed the expected characteristics. The only pattern that could be observed was that colonies appeared with a delay of one day on control plates compared to the reconstruction plates. However, in other cases colony formation took place on reconstruction plates but not on control plates. The possibility that the background strain is leaky could be ruled out since it was tested for strict cell cycle arrest and no residual proliferation was observed.

In summary, results of all three reconstruction assays were highly suspicious.

4.4.3. Sequence analysis

On account of the outstanding mutation frequency and the unexpected reconstruction assay results, I decided to do sequence analysis of six clones to elucidate the inconsistency of *hTP53* revertants.

Unfortunately, none of the six clones showed a reversion event which compensated the original frameshift mutation. Instead, the sequence within the reversion window remained the same as before the adaptive mutation assay. Since the frameshift mutation was not reverted, cells should not be able to grow on SC-Lactate plates but be arrested in cell cycle. This suggests that these colonies are artifacts. Why growth for these cells was nevertheless possible remains unclear. Further, it is not clear if all newly arising colonies in adaptive mutation assays were artifacts or if a fraction of obtained colonies were actual revertants. However, the striking mutation frequency suggests that a majority of monitored colonies were artifacts.

Retrospectively, when considering the construction of the strain, it was suspicious that only one out of four candidates for the new strain reverted on SC-Lactate. Even though they were verified for the correct length by PCR and one clone was even sequenced, no revertants were produced when they were plated in high density (1 x 10^8 cells) on SC-Lactate plates with the exception of one clone, which was declared the new strain YPFA.

4.4.4. Concluding remarks on the *hTP53/FBP1* fusion

In general it was expected that the functionality of the *fbp1::hTP53FS-320* assay would be somewhere between the *fbp1*-deficient strain YΔF1 and the strain YPF63 which has a fusion of the intact p53 and *FBP1* gene. However, this was not the case since mostly artifacts were observed. The phenotype of YPF63 colonies was not different from the wt strain YLBM, if at all, colonies might have appeared to be slightly flatter without the sharp peak in the inner circle of the colony. However, it was not observed that colonies would stay small or lose their round shape after a course of some days. Thus, it was unexpected that the *fbp1::hTP53FS-320* assay would not function properly and produce artifacts. Nevertheless, the normal colony formation of the strain YPF63 indicates that also the phenotype of colonies in the *hTP53-FBP1* fusion assay should be satisfactory, once it is established successfully.

Consequently, a *TP53* fusion construct with *FBP1* is still desired, to establish an assay with a sufficient mutation frequency. The freedom of the reversion window and its arising advantages with it are of great benefit and could accomplish an increased mutation frequency compared to the *fbp1FS-128* assay.

One possibility is to proceed the strategy to insert the optimal Kozak sequence and truncate the p53 ORF. However, this approach seems challenging due to the observed integration problems. Nevertheless, it would be worthwhile still trying.

Another strategy would be to abandon *TP53* and its cancer relevance and use a custom-designed sequence, which is fused upstream of *FBP1*. The advantage would be that the sequence can be chosen freely. Thus, an optional amount of mononucleotide repeats can be introduced to guarantee hot spots in the reversion window. Furthermore, also the optimal Kozak sequence can be considered and integrated, which would be another bonus for good expression of FBP1. This could serve as a hopeful strategy to construct a new fusion and achieve a desirable mutation frequency to study adaptive mutations with carbohydrate starvation in quiescent yeast cells.

5. References

Babudri, N., Lucaccioni, A., and Achilli, A. (2006). Adaptive mutagenesis in the yeast *Saccharomyces cerevisiae*. Ecol Genet *4*, 20-28.

Babudri, N., Pavlov, Y.I., Matmati, N., Ludovisi, C., and Achilli, A. (2001). Stationary-phase mutations in proofreading exonuclease-deficient strains of the yeast Saccharomyces cerevisiae. Mol Genet Genomics *265*, 362-366.

Baker, S.J., Fearon, E.R., Nigro, J.M., Hamilton, S.R., Preisinger, A.C., Jessup, J.M., vanTuinen, P., Ledbetter, D.H., Barker, D.F., Nakamura, Y., *et al.* (1989). Chromosome 17 deletions and p53 gene mutations in colorectal carcinomas. Science *244*, 217-221.

Baker, S.J., Markowitz, S., Fearon, E.R., Willson, J.K., and Vogelstein, B. (1990). Suppression of human colorectal carcinoma cell growth by wild-type p53. Science *249*, 912-915.

Baranowska, H., Policinska, Z., and Jachymczyk, W.J. (1995). Effects of the CDC2 gene on adaptive mutation in the yeast Saccharomyces cerevisiae. CurrGenet *28*, 521-525.

Boeke, J.D., LaCroute, F., and Fink, G.R. (1984). A positive selection for mutants lacking orotidine-5'-phosphate decarboxylase activity in yeast: 5-fluoro-orotic acid resistance. Mol Gen Genet *197*, 345-346.

Breslauer, K., Frank R, Blöcker H, and LA., M. (1986). Predicting DNA duplex stability from the base sequence. Proc Nat Acad Sci *83*, 3746-3750.

Cairns, J., and Foster, P.L. (1991). Adaptive reversion of a frameshift mutation in Escherichia coli. Genetics *128*, 695-701.

Cairns, J., Overbaugh, J., and Miller, S. (1988). The origin of mutants. Nature *335*, 142-145.

Carter, Z., and Delneri, D. (2010). New generation of loxP-mutated deletion cassettes for the genetic manipulation of yeast natural isolates. Yeast *27*, 765-775.

Casal, M., Paiva, S., Andrade, R.P., Gancedo, C., and Leao, C. (1999). The lactate-proton symport of Saccharomyces cerevisiae is encoded by JEN1. J Bacteriol *181*, 2620-2623.

Cejka, P., Vondrejs, V., and Storchova, Z. (2001). Dissection of the functions of the Saccharomyces cerevisiae RAD6 postreplicative repair group in mutagenesis and UV sensitivity. Genetics *159*, 953-963.

Cui, D.Y., Brown, C.R., and Chiang, H.L. (2004). The type 1 phosphatase Reg1p-Glc7p is required for the glucose-induced degradation of fructose-1,6-bisphosphatase in the vacuole. J Biol Chem *279*, 9713-9724.

Datta, A., and Jinks-Robertson, S. (1995). Association of increased spontaneous mutation rates with high levels of transcription in yeast. Science *268*, 1616-1619.

Del Carratore, R., Petrucci, A., Simili, M., Fronza, G., and Galli, A. (2004). Involvement of human p53 in induced intrachromosomal recombination in Saccharomyces cerevisiae. Mutagenesis *19*, 333-339.

Delneri, D., Tomlin, G.C., Wixon, J.L., Hutter, A., Sefton, M., Louis, E.J., and Oliver, S.G. (2000). Exploring redundancy in the yeast genome: an improved strategy for use of the cre-loxP system. Gene *252*, 127-135.

DeRisi, J.L., Iyer, V.R., and Brown, P.O. (1997). Exploring the metabolic and genetic control of gene expression on a genomic scale. Science *278*, 680-686.

Dujon, B. (1996). The yeast genome project: what did we learn? Trends Genet *12*, 263-270.

Eckert, K.A., and Hile, S.E. (2009). Every microsatellite is different: Intrinsic DNA features dictate mutagenesis of common microsatellites present in the human genome. Mol Carcinog *48*, 379-388.

Eisler, H., Frohlich, K.U., and Heidenreich, E. (2004). Starvation for an essential amino acid induces apoptosis and oxidative stress in yeast. Exp Cell Res *300*, 345-353.

Entian, K.D., Vogel, R.F., Rose, M., Hofmann, L., and Mecke, D. (1988). Isolation and primary structure of the gene encoding fructose-1,6-bisphosphatase from Saccharomyces cerevisiae. FEBS Lett *236*, 195-200.

Fearon, E.R., and Vogelstein, B. (1990). A genetic model for colorectal tumorigenesis. Cell *61*, 759-767.

Fields, S., and Jang, S.K. (1990). Presence of a potent transcription activating sequence in the p53 protein. Science *249*, 1046-1049.

Flaman, J.M., Frebourg, T., Moreau, V., Charbonnier, F., Martin, C., Chappuis, P., Sappino, A.P., Limacher, I.M., Bron, L., Benhattar, J., *et al.* (1995). A simple p53 functional assay for screening cell lines, blood, and tumors. Proc Natl Acad Sci U S A *92*, 3963-3967.

Foster, P.L. (1993). Adaptive mutation: the uses of adversity. AnnuRevMicrobiol *47*, 467-504.

Foster, P.L. (1999). Mechanisms of stationary phase mutation: a decade of adaptive mutation. Annu Rev Genet *33*, 57-88.

Galdieri, L., Mehrotra, S., Yu, S., and Vancura, A. (2010). Transcriptional regulation in yeast during diauxic shift and stationary phase. Omics : a journal of integrative biology *14*, 629-638.

Gancedo, C., and Delgado, M.A. (1984). Isolation and characterization of a mutant from Saccharomyces cerevisiae lacking fructose 1,6-bisphosphatase. Eur J Biochem *139*, 651-655.

Gancedo, C., Gancedo, J.M., and Sols, A. (1968). Glycerol metabolism in yeasts. Pathways of utilization and production. Eur J Biochem *5*, 165-172.

Gancedo, J.M. (1998). Yeast carbon catabolite repression. Microbiol Mol Biol Rev *62*, 334-361.

Gietz RD, S.R. (2007). High-efficiency yeast transformation using the LiAc/SS carrier DNA/PEG method. Nat Protoc *2(1)*.

Goffeau, A. (2000). Four years of post-genomic life with 6,000 yeast genes. FEBS Lett *480*, 37-41.

Granot, D., and Snyder, M. (1991). Glucose induces cAMP-independent growth-related changes in stationary-phase cells of Saccharomyces cerevisiae. Proc Natl Acad Sci USA *88*, 5724-5728.

Gueldener, U., Heinisch, J., Koehler, G.J., Voss, D., and Hegemann, J.H. (2002). A second set of loxP marker cassettes for Cre-mediated multiple gene knockouts in budding yeast. Nucleic Acids Res *30*, e23.

Guldener, U., Heck, S., Fielder, T., Beinhauer, J., and Hegemann, J.H. (1996). A new efficient gene disruption cassette for repeated use in budding yeast. Nucleic Acids Res *24*, 2519-2524.

Hadj Amor, I.Y., Smaoui, K., Chaabene, I., Mabrouk, I., Djemal, L., Elleuch, H., Allouche, M., Mokdad-Gargouri, R., and Gargouri, A. (2008). Human p53 induces cell death and downregulates thioredoxin expression in Saccharomyces cerevisiae. FEMS Yeast Res *8*, 1254-1262.

Halas, A., Baranowska, H., Podlaska, A., and Sledziewska-Gojska, E. (2009). Evaluation of the roles of Pol zeta and NHEJ in starvation-associated spontaneous mutagenesis in the yeast Saccharomyces cerevisiae. Curr Genet *55*, 245-251.

Halas, A., Baranowska, H., and Policinska, Z. (2002). The influence of the mismatch-repair system on stationary-phase mutagenesis in the yeast Saccharomyces cerevisiae. Curr Genet *42*, 140-146.

Hall, B.G. (1990). Spontaneous point mutations that occur more often when advantageous than when neutral. Genetics *126*, 5-16.

Hall, B.G. (1992). Selection-induced mutations occur in yeast. Proc Natl Acad Sci USA *89*, 4300-4303.

Hall, B.G. (1998). Adaptive mutagenesis: a process that generates almost exclusively beneficial mutations. Genetica *102-103*, 109-125.

Hamilton, R., Watanabe, C.K., and de Boer, H.A. (1987). Compilation and comparison of the sequence context around the AUG startcodons in Saccharomyces cerevisiae mRNAs. Nucleic Acids Res *15*, 3581-3593.

Hanahan, D., and Weinberg, R.A. (2000). The hallmarks of cancer. Cell *100*, 57-70.

Hanahan, D., and Weinberg, R.A. (2011). Hallmarks of cancer: the next generation. Cell *144*, 646-674.

Hartwell, L.H. (2002). Nobel Lecture. Yeast and cancer. Biosci Rep *22*, 373-394.

Haurie, V., Perrot, M., Mini, T., Jeno, P., Sagliocco, F., and Boucherie, H. (2001). The transcriptional activator Cat8p provides a major contribution to the reprogramming of carbon metabolism during the diauxic shift in Saccharomyces cerevisiae. J Biol Chem *276*, 76-85.

Heidenreich, E. (2007). Adaptive mutation in *Saccharomyces cerevisiae*. Crit Rev Biochem Mol Biol *42*, 285-311.

Heidenreich, E., and Eisler, H. (2004). Non-homologous end joining dependency of gamma-irradiation-induced adaptive frameshift mutation formation in cell cycle-arrested yeast cells. Mutat Res *556*, 201-208.

Heidenreich, E., Eisler, H., and Steinboeck, F. (2006). Epistatic participation of *REV1* and *REV3* in the formation of UV-induced frameshift mutations in cell cycle-arrested yeast cells. Mutat Res *593*, 187-195.

Heidenreich, E., Holzmann, V., and Eisler, H. (2004). Polymerase zeta dependency of increased adaptive mutation frequencies in nucleotide excision repair-deficient yeast strains. DNA Repair *3*, 395-402.

Heidenreich, E., Novotny, R., Kneidinger, B., Holzmann, V., and Wintersberger, U. (2003). Non-homologous end joining as an important mutagenic process in cell cycle-arrested cells. EMBO J *22*, 2274-2283.

Heidenreich, E., and Wintersberger, U. (1997). Starvation for a specific amino acid induces high frequencies of rho- mutants in *Saccharomyces cerevisiae*. Curr Genet *31*, 408-413.

Heidenreich, E., and Wintersberger, U. (1998). Replication-dependent and selection-induced mutations in respiration-competent and respiration-deficient strains of *Saccharomyces cerevisiae*. Mol Gen Genet *260*, 395-400.

Heidenreich, E., and Wintersberger, U. (2001). Adaptive reversions of a frameshift mutation in arrested *Saccharomyces cerevisiae* cells by simple deletions in mononucleotide repeats. Mutat Res *473*, 101-107.

Hjortsberg, L., Rubio-Nevado, J.M., Hamroun, D., Claustre, M., Béroud, C., and Soussi, T. (2008). The p53 Mutation HandBook. *2.0*.

Horak, J., Regelmann, J., and Wolf, D.H. (2002). Two distinct proteolytic systems responsible for glucose-induced degradation of fructose-1,6-bisphosphatase and the Gal2p transporter in the yeast Saccharomyces cerevisiae share the same protein components of the glucose signaling pathway. J Biol Chem *277*, 8248-8254.

Hung, G.C., Brown, C.R., Wolfe, A.B., Liu, J., and Chiang, H.L. (2004). Degradation of the gluconeogenic enzymes fructose-1,6-bisphosphatase and malate dehydrogenase is mediated by distinct proteolytic pathways and signaling events. J Biol Chem *279*, 49138-49150.

Joerger, A.C., Ang, H.C., and Fersht, A.R. (2006). Structural basis for understanding oncogenic p53 mutations and designing rescue drugs. Proc Natl Acad Sci U S A *103*, 15056-15061.

Kato, S., Han, S.Y., Liu, W., Otsuka, K., Shibata, H., Kanamaru, R., and Ishioka, C. (2003). Understanding the function-structure and function-mutation relationships of p53 tumor suppressor protein by high-resolution missense mutation analysis. Proc Natl Acad Sci U S A *100*, 8424-8429.

Kozak, M. (1984). Point mutations close to the AUG initiator codon affect the efficiency of translation of rat preproinsulin in vivo. Nature *308*, 241-246.

Kozak, M. (1986). Point mutations define a sequence flanking the AUG initiator codon that modulates translation by eukaryotic ribosomes. Cell *44*, 283-292.

Kozak, M. (1987). An analysis of 5'-noncoding sequences from 699 vertebrate messenger RNAs. Nucleic Acids Res *15*, 8125-8148.

Lea, D., and Coulson, C. (1949). The distribution of the numbers of mutants in bacterial populations. JGenetics *49*, 264–285.

Loeb, L.A. (1991). Mutator phenotype may be required for multistage carcinogenesis. Cancer Res *51*, 3075-3079.

Loeb, L.A., Loeb, K.R., and Anderson, J.P. (2003). Multiple mutations and cancer. Proc Natl Acad Sci U S A *100*, 776-781.

Luria, S.E., and Delbruck, M. (1943). Mutations of Bacteria from Virus Sensitivity to Virus Resistance. Genetics *28,* 491-511.

Makuc, J., Paiva, S., Schauen, M., Kramer, R., Andre, B., Casal, M., Leao, C., and Boles, E. (2001). The putative monocarboxylate permeases of the yeast Saccharomyces cerevisiae do not transport monocarboxylic acids across the plasma membrane. Yeast *18*, 1131-1143.

Marini, A., Matmati, N., and Morpurgo, G. (1999). Starvation in yeast increases non-adaptive mutation. Curr Genet *35*, 77-81.

Mercado, J.J., and Gancedo, J.M. (1992). Regulatory regions in the yeast FBP1 and PCK1 genes. FEBS Lett *311,* 110-114.

Mercado, J.J., Vincent, O., and Gancedo, J.M. (1991). Regions in the promoter of the yeast FBP1 gene implicated in catabolite repression may bind the product of the regulatory gene MIG1. FEBS Lett *291*, 97-100.

Mokdad-Gargouri, R., Belhadj, K., and Gargouri, A. (2001). Translational control of human p53 expression in yeast mediated by 5'-UTR-ORF structural interaction. Nucleic Acids Res *29*, 1222-1227.

Muller, M., Muller, H., and Holzer, H. (1981). Immunochemical studies on catabolite inactivation of phosphoenolpyruvate carboxykinase in Saccharomyces cerevisiae. J Biol Chem *256*, 723-727.

Nigro, J.M., Baker, S.J., Preisinger, A.C., Jessup, J.M., Hostetter, R., Cleary, K., Bigner, S.H., Davidson, N., Baylin, S., Devilee, P., *et al.* (1989). Mutations in the p53 gene occur in diverse human tumour types. Nature *342*, 705-708.

Nigro, J.M., Sikorski, R., Reed, S.I., and Vogelstein, B. (1992). Human p53 and CDC2Hs genes combine to inhibit the proliferation of Saccharomyces cerevisiae. Mol Cell Biol *12*, 1357-1365.

Oliver, S.G., van der Aart, Q.J., Agostoni-Carbone, M.L., Aigle, M., Alberghina, L., Alexandraki, D., Antoine, G., Anwar, R., Ballesta, J.P., Benit, P., *et al.* (1992). The complete DNA sequence of yeast chromosome III. Nature *357*, 38-46.

Olivier, M., and Taniere, P. (2011). Somatic mutations in cancer prognosis and prediction: lessons from TP53 and EGFR genes. Curr Opin Oncol *23,* 88-92.

Pearson, G.D., and Merrill, G.F. (1998). Deletion of the Saccharomyces cerevisiae TRR1 gene encoding thioredoxin reductase inhibits p53-dependent reporter gene expression. J Biol Chem *273*, 5431-5434.

Pedruzzi, I., Burckert, N., Egger, P., and De Virgilio, C. (2000). Saccharomyces cerevisiae Ras/cAMP pathway controls post-diauxic shift element-dependent transcription through the zinc finger protein Gis1. Embo J *19*, 2569-2579.

Reagan, M.S., Pittenger, C., Siede, W., and Friedberg, E.C. (1995). Characterization of a mutant strain of Saccharomyces cerevisiae with a deletion of the RAD27 gene, a structural homolog of the RAD2 nucleotide excision repair gene. J Bacteriol *177*, 364-371.

Rojas Gil, A.P., and Vondrejs, V. (1999). Development of papillae on colonies of two isopolyauxotrophic strains of Saccharomyces cerevisiae allelic in RAD6 during adenine starvation. Folia Microbiol *44*, 299-305.

Rosche, W.A., and Foster, P.L. (2000). Determining mutation rates in bacterial populations. Methods *20*, 4-17.

Rosenberg, S.M. (2001). Evolving responsively: adaptive mutation. Nat Rev Genet *2*, 504-515.

Rothstein, R. (1991). Targeting, disruption, replacement, and allele rescue: integrative DNA transformation in yeast. Methods Enzymol *194*, 281-301.

Ryan, F.J. (1955). Spontaneous mutation in non-dividing bacteria. Genetics *40*, 726-738.

Sambrook J, R.D. (1992). Molecular Cloning: A Laboratory Manual.

Sambrook J., F.E.F., Maniatis T. (1989). Molecular Cloning: A Loboratory Manual, Vol second edition.

Sauer, B. (1992). Identification of cryptic lox sites in the yeast genome by selection for Cre-mediated chromosome translocations that confer multiple drug resistance. J Mol Biol *223*, 911-928.

Sauer, B., and Henderson, N. (1989). Cre-stimulated recombination at loxP-containing DNA sequences placed into the mammalian genome. Nucleic Acids Res *17*, 147-161.

Scharer, E., and Iggo, R. (1992). Mammalian p53 can function as a transcription factor in yeast. Nucleic Acids Res *20*, 1539-1545.

Schuller, H.J. (2003). Transcriptional control of nonfermentative metabolism in the yeast Saccharomyces cerevisiae. Curr Genet *43*, 139-160.

Sia, E.A., Kokoska, R.J., Dominska, M., Greenwell, P., and Petes, T.D. (1997). Microsatellite instability in yeast: dependence on repeat unit size and DNA mismatch repair genes. Mol Cell Biol *17*, 2851-2858.

Smardova, J., Smarda, J., and Koptikova, J. (2005). Functional analysis of p53 tumor suppressor in yeast. Differentiation *73*, 261-277.

Soussi, T. (2007). p53 alterations in human cancer: more questions than answers. Oncogene *26*, 2145-2156.

Steele, D.F., and Jinks-Robertson, S. (1992). An examination of adaptive reversion in Saccharomyces cerevisiae. Genetics *132*, 9-21.

Steinboeck, F., Hubmann, M., Bogusch, A., Dorninger, P., Lengheimer, T., and Heidenreich, E. (2010). The relevance of oxidative stress and cytotoxic DNA lesions for spontaneous mutagenesis in non-replicating yeast cells. Mutat Res *688*, 47-52.

Storchova, Z., Rojas Gil, A.P., Janderova, B., and Vondrejs, V. (1998). The involvement of the RAD6 gene in starvation-induced reverse mutation in Saccharomyces cerevisiae. Mol Gen Genet *258*, 546-552.

Storchova, Z., and Vondrejs, V. (1999). Starvation-associated mutagenesis in yeast Saccharomyces cerevisiae is affected by Ras2/cAMP signaling pathway. Mutat Res *431*, 59-67.

Strauss, B.S. (1992). The origin of point mutations in human tumor cells. Cancer Res *52*, 249-253.

Takahashi, T., Nau, M.M., Chiba, I., Birrer, M.J., Rosenberg, R.K., Vinocour, M., Levitt, M., Pass, H., Gazdar, A.F., and Minna, J.D. (1989). p53: a frequent target for genetic abnormalities in lung cancer. Science *246*, 491-494.

Thomas, K. (1996). Yeasties and beasties: 7 years of genome sequencing. FEBS Lett *396*, 1-6.

Tishkoff, D.X., Filosi, N., Gaida, G.M., and Kolodner, R.D. (1997). A novel mutation avoidance mechanism dependent on S. cerevisiae RAD27 is distinct from DNA mismatch repair. Cell *88*, 253-263.

Torkelson, J., Harris, R.S., Lombardo, M.J., Nagendran, J., Thulin, C., and Rosenberg, S.M. (1997). Genome-wide hypermutation in a subpopulation of stationary-phase cells underlies recombination-dependent adaptive mutation. Embo J *16*, 3303-3311.

von Borstel, R.C., Savage, E.A., Wang, Q., Hennig, U.G., Ritzel, R.G., Lee, G.S., Hamilton, M.D., Chrenek, M.A., Tomaszewski, R.W., Higgins, J.A., *et al.* (1998). Topical reversion at the HIS1 locus of Saccharomyces cerevisiae. A tale of three mutants. Genetics *148*, 1647-1654.

Warburg, O. (1956a). On respiratory impairment in cancer cells. Science *124*, 269-270.

Warburg, O. (1956b). On the origin of cancer cells. Science *123*, 309-314.

Yacoubi-Hadj Amor, I., Smaoui, K., Belguith, H., Djemal, L., Dardouri, M., Mokdad-Gargouri, R., and Gargouri, A. (2009). Selection of cell death-deficient p53 mutants in Saccharomyces cerevisiae. Yeast *26*, 441-450.

Yousef, A.F., Xu, G.W., Mendez, M., Brandl, C.J., and Mymryk, J.S. (2008). Coactivator requirements for p53-dependent transcription in the yeast Saccharomyces cerevisiae. Int J Cancer *122*, 942-946.

Curriculum Vitae

Petra Dorninger

Wurmserg. 15/33
1150 Vienna
mobile: 0676-3471144
e-mail: petra.dorninger@yahoo.com

Date of birth: January 25th 1982 in St. Pölten, Austria

Nationality: Austria

Education:

Jan 2008 – Apr 2011: PhD thesis at the Institute of Cancer Research

Oct 2006 – Sep 2011: prolonged PhD studies at the University of Technology in Vienna for graduates of a "Fachhochschule"
Technical Chemistry (Biotechnology und Bioanalytics)

2004 – 2006: Studies at the „Europa-Fachhochschule Fresenius" in Vienna
Major: Bioanalysis und Biotechnology as well as Marketing

Diploma thesis:
„Establishment of a bead based assay for the quantification of Aβ40 and Aβ42" at the Research Institute of Molecular Pathology (IMP) 01.02. – 31.07.2006 in cooperation with Affiris GmbH
Graduation: 12.07.2006

2002 – 2004: Secondary technical college of chemistry at „Rosensteingasse" in Vienna
(Major: Biochemistry and Gene Technology)

Internships:

Aug. 2006: Affiris GmbH (continuing my diploma thesis project)

July 2005: Belimo Automation Österreich HandelsgesmbH
in the field of economies (marketing and management)

Oct 2004 – Feb 2005: Boehringer Ingelheim Austria subdevision FEC
(Project: Automated aliquotation of analysis compounds in chemical research)

Aug 2003 und 2004: Glanzstoff Austria GmbH (lab: analysis of cellulose)

Experience abroad:

June 2010: Cancer Research Institute Bratislava, Slovak Republic
Cooperation in the course of my PhD thesis

Sep 2000 – 2001: Aupair in Bolingbrook, IL (suburb of Chicago)
College-course at Joliet Junior College: „Biology 103- Health“ (3 credits)

Languages: German (mother tongue)
English (fluent in speech and writing)
French (basics)

EDV: Word, Excel, PowerPoint, GraphPad Prism, Vector NTI

List of publications:

Heidenreich, E., Eisler, H., Lengheimer, T., **Dorninger, P.**, and Steinboeck, F. (2010). A mutation-promotive role of nucleotide excision repair in cell cycle-arrested cell populations following UV irradiation. DNA Repair *9*, 96-100.

Steinboeck, F., Hubmann, M., Bogusch, A., **Dorninger, P.**, Lengheimer, T., and Heidenreich, E. (2010). The relevance of oxidative stress and cytotoxic DNA lesions for spontaneous mutagenesis in non-replicating yeast cells. Mutat Res *688*, 47-52.